

AD-A164 305

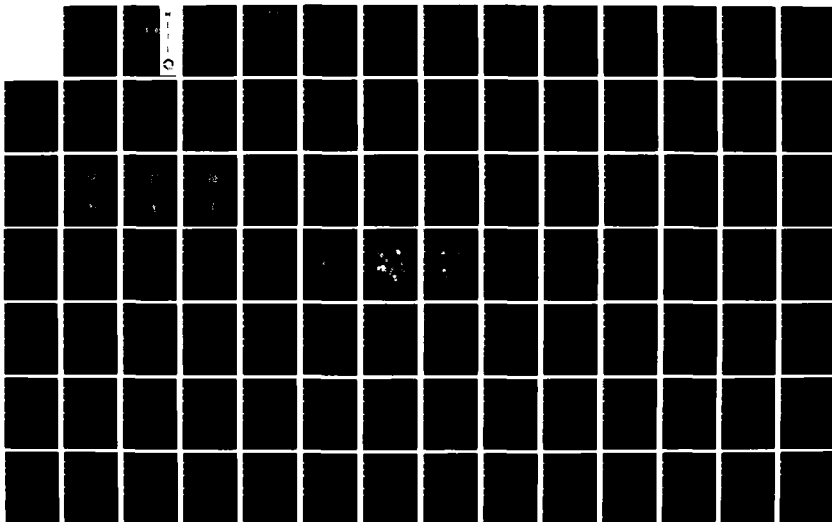
DIGITAL TERRAIN ELEVATION MODEL ANALYSIS(U) OHIO STATE
UNIV RESEARCH FOUNDATION COLUMBUS J C LOON ET AL
JUL 85 OSURF-716042 ETL-0393 DARG29-81-D-0100

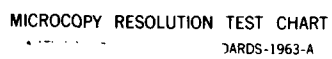
1/2

UNCLASSIFIED

F/G 8/6

NL

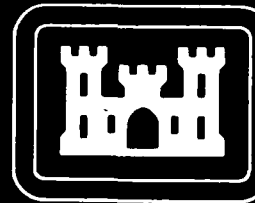




MICROCOPY RESOLUTION TEST CHART
NBS-1963-A

2

ETL - 0393



Digital terrain elevation model analysis

Joseph C. Loon
Petros G. Patias



AD-A164 305

The Ohio State University Research
Foundation
1314 Kinnear Road
Columbus, Ohio 73212

July 1985

DTIC FILE COPY

APPROVED FOR PUBLIC RELEASE; DISTRIBUTION IS UNLIMITED.

Prepared for
U.S. ARMY CORPS OF ENGINEERS
ENGINEER TOPOGRAPHIC LABORATORIES
FORT BELVOIR, VIRGINIA 22060 - 5546

Monitored by
U.S. Army Research Office
Research Triangle Park, N.C. 27709



E
T
L

86 2 14 082

Destroy this report when no longer needed.
Do not return it to the originator.

The findings in this report are not to be construed as an official
Department of the Army position unless so designated by other
authorized documents.

The citation in this report of trade names of commercially available
products does not constitute official endorsement or approval of the
use of such products.

UNCLASSIFIED

SECURITY CLASSIFICATION OF THIS PAGE (When Data Entered)

REPORT DOCUMENTATION PAGE		READ INSTRUCTIONS BEFORE COMPLETING FORM
1. REPORT NUMBER ETL-0393	2. GOVT ACCESSION NO. AD-A164305	3. RECIPIENT'S CATALOG NUMBER
4. TITLE (and Subtitle) DIGITAL TERRAIN ELEVATION MODEL ANALYSIS		5. TYPE OF REPORT & PERIOD COVERED Final Report
		6. PERFORMING ORG. REPORT NUMBER Project No. 716042
7. AUTHOR(s) Joseph C. Loon Petros G. Patias		8. CONTRACT OR GRANT NUMBER(s) DAAG29-81-D-0100
9. PERFORMING ORGANIZATION NAME AND ADDRESS The Ohio State University Research Foundation 1314 Kinnear Road Columbus, Ohio 43212		10. PROGRAM ELEMENT, PROJECT, TASK AREA & WORK UNIT NUMBERS
11. CONTROLLING OFFICE NAME AND ADDRESS U.S. Army Engineer Topographic Laboratories Fort Belvoir, Virginia 22060-5546		12. REPORT DATE July 1985
		13. NUMBER OF PAGES 108
14. MONITORING AGENCY NAME & ADDRESS (if different from Controlling Office) U.S. Army Research Office P.O. Box 12211 Research Triangle Park, N.C. 27709		15. SECURITY CLASS. (of this report) Unclassified
		15a. DECLASSIFICATION/DOWNGRADING SCHEDULE
16. DISTRIBUTION STATEMENT (of this Report) Approved for public release; distribution is unlimited.		
17. DISTRIBUTION STATEMENT (of the abstract entered in Block 20, if different from Report)		
18. SUPPLEMENTARY NOTES		
19. KEY WORDS (Continue on reverse side if necessary and identify by block number) Cartography Contour to Grid Algorithms Digital Elevation Model Digital Terrain Elevation Data Fourier Series Surface Interpolation Synthetic Surface		
20. ABSTRACT (Continue on reverse side if necessary and identify by block number) An effort to develop techniques to evaluate contour-to-grid interpolation algorithms. The use of synthetic surfaces as a tool is explored. A set of synthetic surfaces is generated using Fourier Series to represent terrain with different degrees of ruggedness; each surface represented by an equation of the form: $Z=F(X,Y)$. The results of a contour-to-grid interpolation can then be evaluated by comparison with the "true elevations", the elevations calculated from the synthetic surfaces..		

DD FORM 1 JAN 73 1473

EDITION OF 1 NOV 65 IS OBSOLETE

UNCLASSIFIED

PREFACE

This document was prepared under the U.S. Army Research Office's contract DAAG29-81-D-0100 for the U.S. Army Engineer Topographic Laboratories, Fort Belvoir, Virginia. The work was performed by the Ohio State University Research Foundation, Columbus, Ohio. The Contracting Officer's Representative was Ms. Betty Mandel.

INDEX

	Page
1. Introduction	1
2. Review of Literature	2
3. Synthetic Surfaces	2
3.1 What is a Synthetic Surface	2
3.2 A Method of Generating Synthetic Surfaces	3
3.3 Generation of Synthetic Surfaces Used in This Study	8
3.4 Generation of Synthetic Surfaces up to 3 rd Harmonic Surface	18
3.5 Generation of Synthetic Surface Contours in Raster Mode	26
3.6 Complexity of the 3 rd Harmonic Surfaces	26
4. Interpolation Methods	28
4.1 Interpolation from Contours to Grid	28
4.2 Contour Specific Algorithms	28
4.2.1 Input Data	29
4.2.2 LIXY: Linear Interpolation Along X and Y Axes	29
4.2.3 LISS: Linear Interpolation the Direction of the Steepest Slope	30
4.2.4 CISS: Cubic Interpolation Along the Direction of the Steepest Slope	30
5. Accuracy Evaluation Techniques	33
6. Results Using Small Datasets	34
6.1 Numerical Evaluation Results	34
6.2 Non-numerical Evaluation	39
7. Conclusions	78
7.1 Method for Evaluation	78
7.2 Future Work	79
APPENDIX A: Bibliography of selected references	81
APPENDIX B: Description of selected programs used in this study	91
APPENDIX C: Equations for the six synthetic surfaces	99

1. Introduction

The research covered by this report is part of an effort to develop techniques for the evaluation of interpolation methods in Digital Elevation Models (DEM's).

In order to evaluate the fidelity of an interpolation method, one needs to know true heights in an area. These true heights can then serve as the basis for a comparison with height obtained by some interpolation method.

In practice, one deals with varying types of terrain. To try to simulate conditions encountered in practice, one therefore needs true heights for a group of surfaces. These surfaces should represent a selection of the types of surfaces which may be encountered in practice.

In order to obtain a true height at any point on a surface, we need a synthetic surface. That is, a surface defined by a mathematical equation where height (or elevation) is a function of position (x and y coordinates).

This report deals with methods for the evaluation of contour-to-grid interpolation methods in a DEM. It is in essence a feasibility analysis and should be considered as an effort to develop an initial plan for the evaluation of DEM interpolation techniques.

This research was done in the framework of the Scientific Services Program - STAS and the specified objectives and specific tasks are given below.

Objective:

The objective of this short term analysis is to develop evaluation tools and methodologies to evaluate contour-to-grid interpolation algorithms.

Specific Tasks:

- a. Review literature regarding relevant research in the area of contour-to-grid interpolation evaluation using analytical approximations.
- b. Evaluate techniques for generating synthetic surfaces to approximate Digital Terrain Elevation Data (DTED).
- c. Develop numerical and non-numerical techniques for evaluating the accuracy of contour-to-grid interpolation algorithms.
- d. Demonstrate the methodology for creating synthetic surfaces approximating DTED and evaluating the interpolation techniques. This will be done on a small sample data set.



Accession For	
NTIS	<input checked="checked" type="checkbox"/>
CRA&I	<input type="checkbox"/>
DTIC	<input type="checkbox"/>
TAB	<input type="checkbox"/>
Unannounced	<input type="checkbox"/>
Justification	
By	
Distribution /	
Availability Codes	
Dist	Avail and/or Special
A-1	

2. Review of Literature

Relevant literature was reviewed in journals, conference proceedings, reports, etc. References related to the research topic were selected and are given in Appendix A. Each reference is accompanied by a brief description of the main topics dealt with.

Nothing specific was found in the literature dealing with interpolation methods in a DEM where the DEM may represent varying types of terrain.

3. Synthetic Surfaces

3.1 What is a Synthetic Surface?

Unlike original topographic surfaces, synthetic surfaces are those surfaces, that can be fully described by an analytical function of the form:

$$z = f(x, y) \quad (3-1)$$

Depending on the mathematical formulation, synthetic surfaces vary in complexity. Such equations may be in the form of a series of polynomials:

$$z = ax + by + cx^2 + dy^2 + exy + \dots \quad (3-2)$$

or a series of trigonometric functions:

$$z = \sin \frac{2\pi ix}{Tx} \cdot \sin \frac{2\pi iy}{Ty} \quad (3-3)$$

with cosines instead of sines or combinations of them. On the other hand covariance functions can be explicitly formulated (Loon, 1982) and from these synthetic surfaces can be generated.

All these methodologies are not unknown in Cartography. Morrison (1971) has generated four synthetic surfaces for cartographic use.

The way in which the synthetic surfaces are generated, provides them with some characteristics which do not always exist in topographic surfaces. They may be smooth, continuous (no breaklines), or periodic and always free of measurement errors. This makes the synthetic surface easier to handle than an original topographic surface.

The usefulness of synthetic surfaces, however, lies on the fact that since they are strictly defined, they can provide absolute measures. For example, the analytical functions used in this study produce surfaces which are smooth and continuous and, being free of any measurement error, can provide an absolute error of point accuracy, simply by comparing the height value at the interpolated point to its true value as obtained by the analytical function. This big advantage makes the use of synthetic surfaces a necessary tool in this study.

3.2 A Method of Generating Synthetic Surfaces

Given a DEM, where the heights of the points are given in a rectangular grid pattern, a way to construct a synthetic surface, that simulates the original terrain, is a Fourier series expansion of the given DEM. The Fourier series expansion is used for generating synthetic surfaces in this project because it is useful for collecting information relating to the characteristics of the surface. Future studies will indicate how useful this method will be for definitive synthetic surfaces, but other methods for generating synthetic surfaces could be used. An in-depth evaluation of all the possible techniques for generating synthetic surfaces is a project on its own. The time constraints in this project have not allowed us to concentrate exclusively on this aspect. The synthetic surfaces generated for this project by the Fourier method have been adequate for demonstrating the evaluation of interpolation techniques. This is a method widely used (in Geology, and Gravity field studies, for example) and is also demonstrated in Morrison's surface III. (Morrison 1971).

The basic assumptions underlying the Fourier expansion of a function $f(t)$, are given by the Dirichlet conditions (M. Bath, 1974):

1. $f(t)$ should be periodic, i.e. $f(t) = f(t + 2n)$, where $2n$ is the period. If $f(t)$ is not periodic, but defined over a finite range, the sum of the sinusoidal terms will still converge to $f(t)$ over the defined range. Outside the range, the sum will represent repetition of $f(t)$.
2. $f(t)$ should be at least sectionally continuous, with at most a finite number of discontinuities and finite jumps.
3. $f(t)$ should possess a finite number of maxima and minima.
4. The integral $\int_{-n}^n f(t) dt$ should be convergent.

According to Fourier's theorem, any function $f(t)$ satisfying these conditions, can be expressed as a sum of a finite number of sinusoidal terms. However, it must be noted that the Dirichlet conditions are sufficient, but not all of them are necessary. This means that the Fourier theorem is valid for a much wider class of functions.

In the two-dimensional case of the Fourier expansion - in which we are interested in Cartography - a function $z(x, y)$ can be expressed as follows (Davis, 1973):

$$\begin{aligned}
 z_{ij}(x, y) = & \sum_{i=1}^{\cdot} \sum_{j=1}^{\cdot} a_{nm} \cdot \cos \frac{2n\pi xi}{\lambda_1} \cdot \cos \frac{2m\pi yj}{\lambda_2} + \\
 & \sum_{i=1}^{\cdot} \sum_{j=1}^{\cdot} b_{nm} \cdot \cos \frac{2n\pi xi}{\lambda_1} \cdot \sin \frac{2m\pi yj}{\lambda_2} + \\
 & \sum_{i=1}^{\cdot} \sum_{j=1}^{\cdot} c_{nm} \cdot \sin \frac{2n\pi xi}{\lambda_1} \cdot \cos \frac{2m\pi yj}{\lambda_2} + \\
 & \sum_{i=1}^{\cdot} \sum_{j=1}^{\cdot} d_{nm} \cdot \sin \frac{2n\pi xi}{\lambda_1} \cdot \sin \frac{2m\pi yj}{\lambda_2} \quad (3-4)
 \end{aligned}$$

where we assume discrete ($n \times m$) data and λ_1, λ_2 refer to the fundamental wavelengths along the two mutual perpendicular axes x and y .

Another useful representation of the Fourier series is in complex form. Assuming again two-dimensional discrete data, the representation of the Fourier series in the data domain is:

$$Z = f(x, y) = \sum_{n=0}^{N-1} \sum_{m=0}^{M-1} F(n, m) e^{i2\pi \left(\frac{nx}{N} + \frac{my}{M} \right)} \quad (3-5)$$

where: N = number of samples along x -direction

M = number of samples along y -direction

and the complex Fourier coefficients $F(n, m)$ are orthogonal.

Another important notion is the Fourier Transform defined as:

$$F(n, m) = \frac{1}{NM} \sum_{n=0}^{N-1} \sum_{m=0}^{M-1} f(x, y) e^{-i2\pi \left(\frac{nx}{N} + \frac{my}{M} \right)} \quad (3-6)$$

The term spectrum is often used as a synonym for the Fourier Transform.

Using Fourier analysis methods, we are transforming data from the space domain (X, Y, Z coordinates) to the frequency domain (ranking of frequencies present in the surface). In the space domain, we can calculate the autocorrelation (or covariance) function of points in a DEM. This function tells us something about the correlation of the heights.

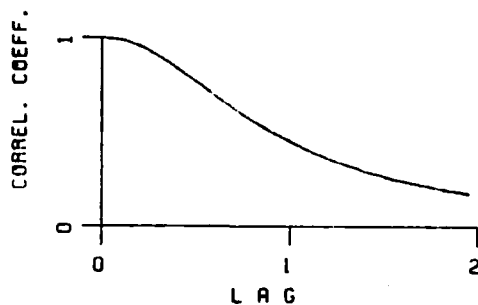


Figure 1

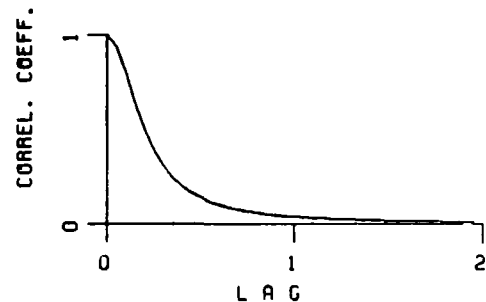


Figure 2

Autocorrelation Curves

For example, in Figure 1, the autocorrelation curve indicates that the heights of adjacent points tend to be the same - that is, we have a fairly smooth terrain. On the other hand, in Figure 2, the autocorrelation curve indicates that height of adjacent points differ greatly - that is, they have a low correlation and therefore the surface described by this curve is rough or complex. The autocorrelation curve deals with the space domain and the equivalent concept in the frequency domain is the power spectrum or the power density. Power spectra are frequently used in geophysics and they may be calculated in two ways:

1. First calculate the autocorrelation function and then take the Fourier transform of this function.
2. Calculate the Fourier transform of the original surface and then take the square of its absolute value.

The power spectrum gives us information about the contribution of the high and low frequency components as a function of, in our case, the elevation. Surfaces with strong low frequencies and relatively unimportant high frequencies tend to be smooth with small local fluctuation. On the other hand,

surfaces whose high frequencies contribute most of the total power tend to have extreme local fluctuations.

Other researchers (Frederiksen, et al., 1984) have used the (2-D) power spectrum of profiles for terrain classification. There may be much scope for using the (3-D) power spectrum of surfaces for the classification or matching of terrain regions. This is an area that still needs investigating.

Therefore from the Fourier transform, the power densities are: (Engelis, 1983)

$$P_{nm} = \begin{cases} |F(0, 0)|^2 & : \text{ for } n=m=0 \\ 4|F(n, m)|^2 & : \text{ for } n=1, \dots, L_1-1, \quad m=1, \dots, L_2-1 \\ 4|F(L_1, L_2)|^2 & : \text{ for } n=L_1, \quad m=L_2, \quad N, M=\text{odd} \\ 2|F(L_1, L_2)|^2 & : \text{ for } n=L_1, \quad m=L_2, \quad N, M=\text{even} \end{cases} \quad (3-7)$$

The total power is given by:

$$P = \sum_{n=0}^{L_1} \sum_{m=0}^{L_2} P_{n, m} \quad (3-8)$$

Two considerations at this point are very important:

1. Depending on the data sampling, the highest recoverable frequency in each direction, is called the Nyquist frequency (denoted by L_1 for x and L_2 for y axis) given by:

$$L = \begin{cases} \frac{N+1}{2} & : \text{ for } N:\text{odd} \\ \frac{N}{2} & : \text{ for } N:\text{even} \end{cases} \quad (3-9)$$

2. "At least theoretically, the mean value of the original data is not affected by the filtering operation. Indeed, since the filter coefficients add up to unity, and in theory the sampled data are of infinite extent, the mean value of the input data is the same as the one of the output results. This is not the case though, for the actual filtering of finite samples, where the mean is also subject to the occurring distortions. So, in order to reduce as much as possible the effect of these distortions, the mean value of the data should be subtracted before the filtering process and then added back to the filtered values." (Engelis, 1983).

Since the Fourier transform is computed for the DEM using the Fast Fourier Transform Method, the power spectrum and the percentile contribution of each frequency component to the overall power can be obtained. A kind of low-pass filtering can then be applied, only the significant frequencies are retained. Their significance is actually tested against a tolerance value, as described below.

Assuming that $Z(x, y)$ is a sequence of normal, independent (μ, σ^2) variables, the Fourier coefficients a, b, c, d being linear combinations of $Z(x, y)$ will be normally distributed. These coefficients are also independent, since the sine and cosine functions are orthogonal in the basic interval.

Assume that $|F(n, m)|$ is the amplitude of the frequency $f_{n, m}$ with power $P(n, m)$ or variance σ_{nm}^2 . The significance of this frequency can be tested with a t-test as:

$$P(t > t_{DF, \alpha}) = 1 - \alpha \quad (3-10)$$

where

$t_{DF, \alpha}$: critical value as obtained from t-distribution tables

α : type I error

DF: degrees of freedom

$$t: \frac{(|F(n, m)| - 0) \cdot \sqrt{n \cdot m}}{\sigma_{nm}}$$

and the null hypothesis to be tested is:

$$H_0 = F(n, m) = 0$$

with the alternative:

$$H_1 = F(n, m) \neq 0$$

If (3-10) holds we reject H_0 , which means that the frequency $f_{n, m}$ should be retained as significant at $(1-\alpha)\%$ significance level.

An important point, here, would be the determination of the degrees of freedom. Each frequency corresponds to 4 degrees of freedom ($v_1=4$, in the two-dimensional case), as by virtue of the Fourier theorem there are four constants (a, b, c, d) needed to characterize each frequency component in a waveform. (Bath, 1974). On the other hand, when spectra are calculated directly by the Fast Fourier Transform method, each raw estimate has 2 degrees of freedom (in the two-dimensional case). Averaging over N estimates (when taking the transforms with respect to one of the variables) yields new

estimates with $2N$ degrees of freedom. Then, the transforms are taken with respect to the second variable, and finally we have $2N \times 2M$ ($v_2=4NM$) degrees of freedom.

After retaining only the significant frequencies, the Inverse Fourier Transform can be used to obtain the filtered surface in the data domain. This surface is now strictly known, since the complex Fourier coefficients are determined, and can serve as a synthetic surface

3.3 Generation of Synthetic Surfaces Used in This Study

The synthetic surfaces used in this study have been generated using Fourier series expansion of six original topographic surfaces. As explained previously, the density of the data prohibit the recovery of terms with frequency higher than a boundary value (Nyquist frequency). This means that the Fourier series are not of infinite length. Moreover, not all the frequencies are significant and contribute the same way in the given surface. Therefore performing a t-test of significance, we can furthermore truncate the Fourier series retaining only the significant terms. This can provide us with the formulation of a Fourier series in exponential form which keeps the characteristic of the original terrain and, mathematically generates a synthetic surface.

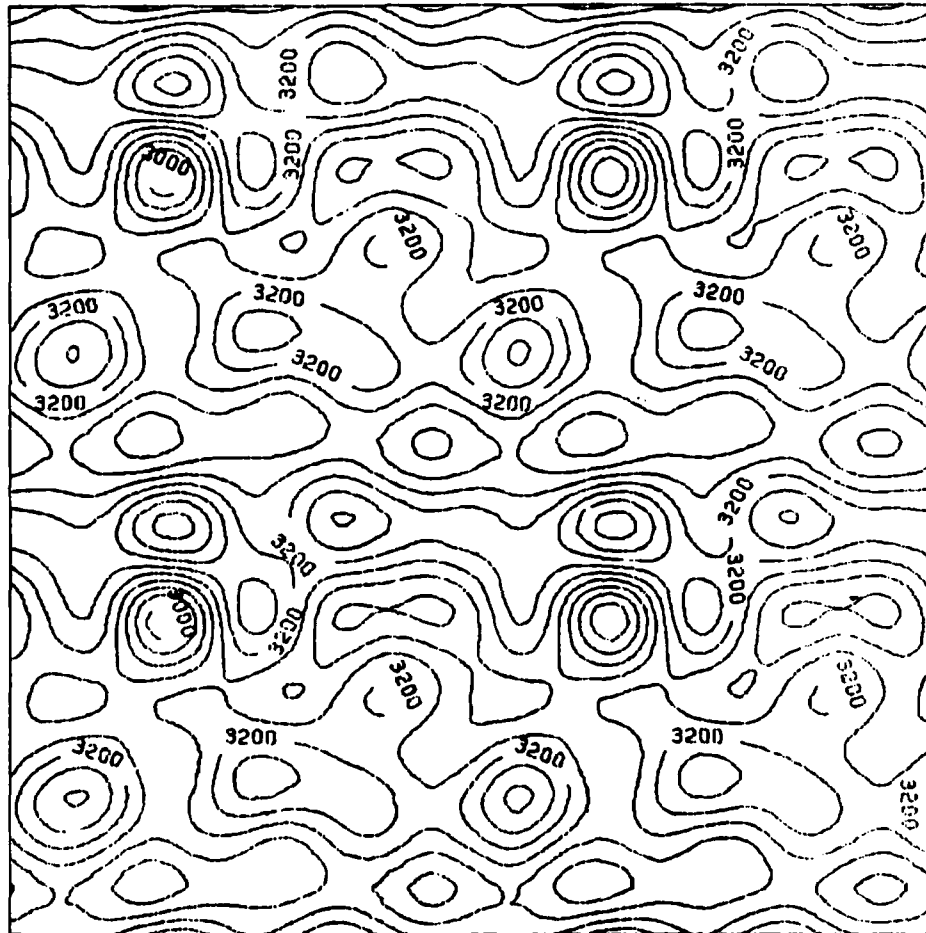
For this project, we chose to generate synthetic surfaces which can be described by a Fourier series up to the third harmonic surface. The third harmonic surface gives 49 terms in the equation for the synthetic surface. Higher order harmonic surfaces would greatly increase the complex mathematical manipulation. Time did not allow us to include these higher order harmonic surfaces. Spectrum analysis has shown that, in the majority of cases, most of the power of the original surface is contained in the harmonic terms up to the third harmonic surface. Comparing the power in the first three harmonic surfaces with the power in the first nine harmonic surfaces in Table 1 will confirm the previous statement.

The synthetic surfaces, as can be seen in the figures below, do not look like "terrain types" which one would expect in mapped topography. If the aim of this project was to classify terrain types, then this would be a serious fault. In terrain type classification we would expect to find areas with breaklines and varying degrees of surface complexity. In this project, however, we restrict ourselves to "interpolation regions", that is, regions where interpolation algorithms will be applied. The boundaries of these interpolation regions are the breaklines because a basic assumption in interpolation (especially in cartography) is that one never crosses a breakline. Therefore, the fact that the interpolation region does not look like terrain or the fact that the interpolation region show some periodic pattern will not invalidate our suggested evaluation methods. In Clarke (1982) it is shown that when one applies an interpolation algorithm to topographic surfaces the results are better than what one gets from synthetic surfaces. This could possibly be due to the fact that topographic surfaces carry more information in the form of

Figure 1

Surface 1

Scale 1:20,000 C.I. = 40 ft.



Surface 2

Scale 1:20,000

C.I. = 100 ft.

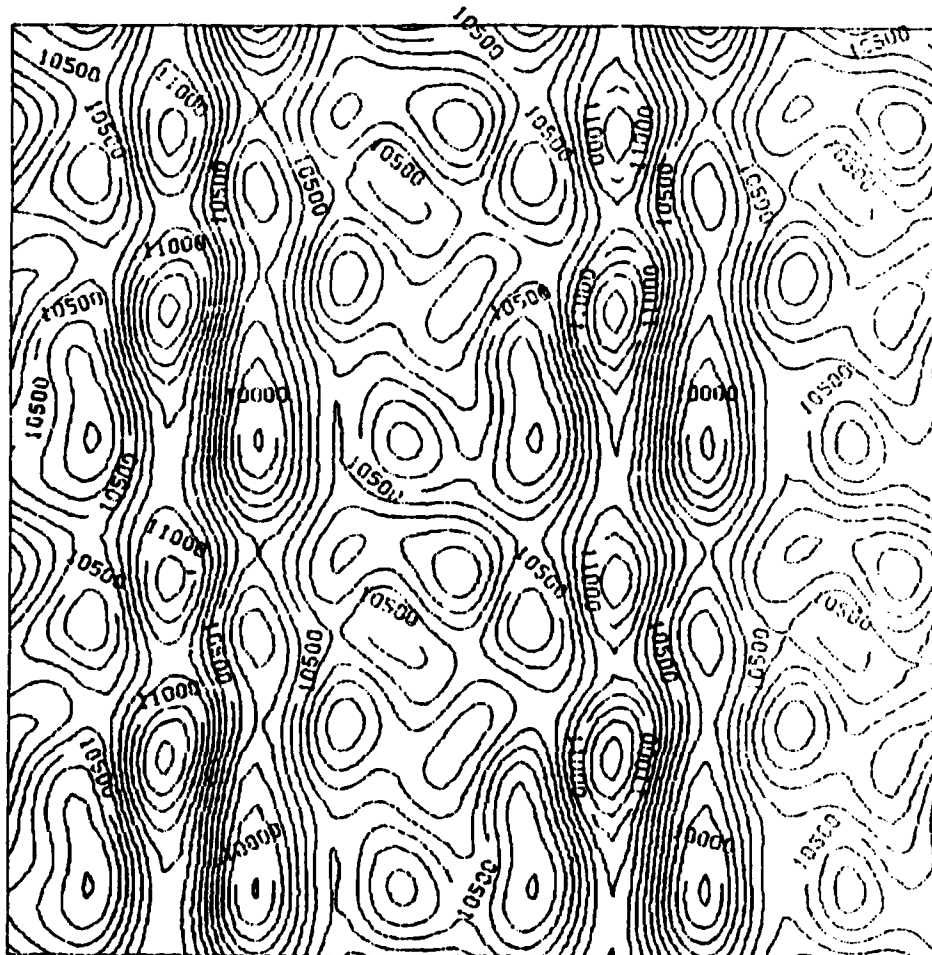


Figure 3

Surface 3

Scale 1:20,000 C.I. = 30 ft.

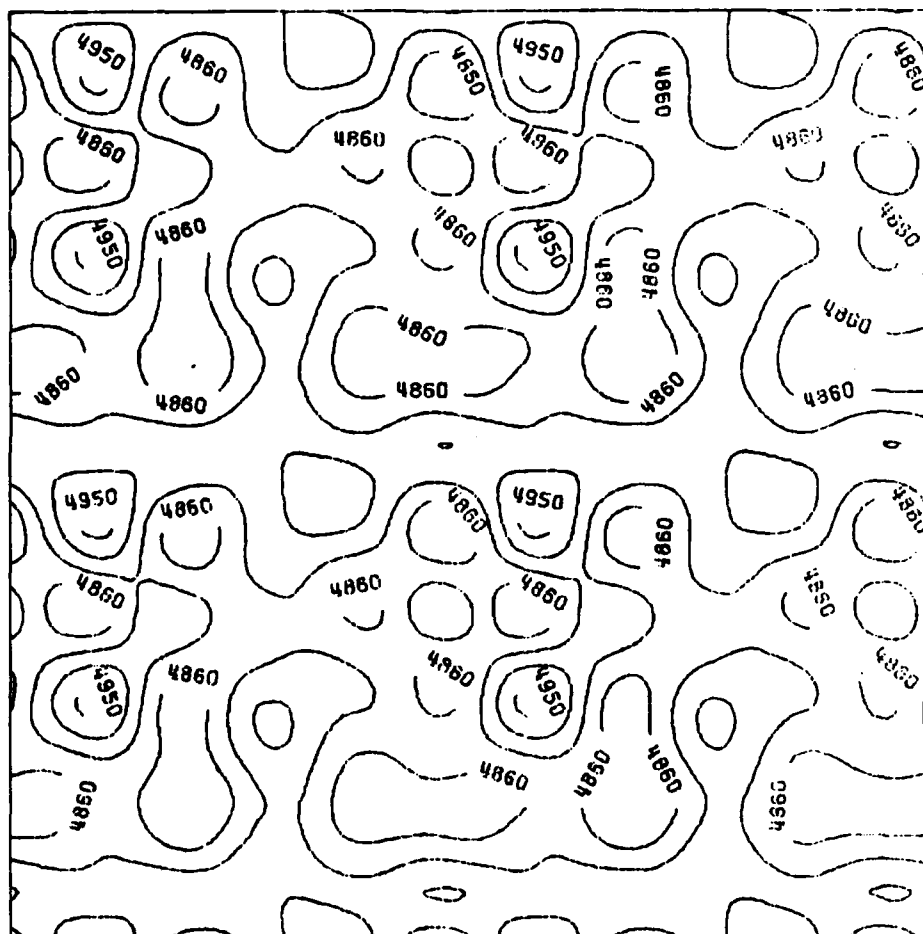


Figure 4

Surface 4

Scale 1:20,000 C.I. = 80 ft.

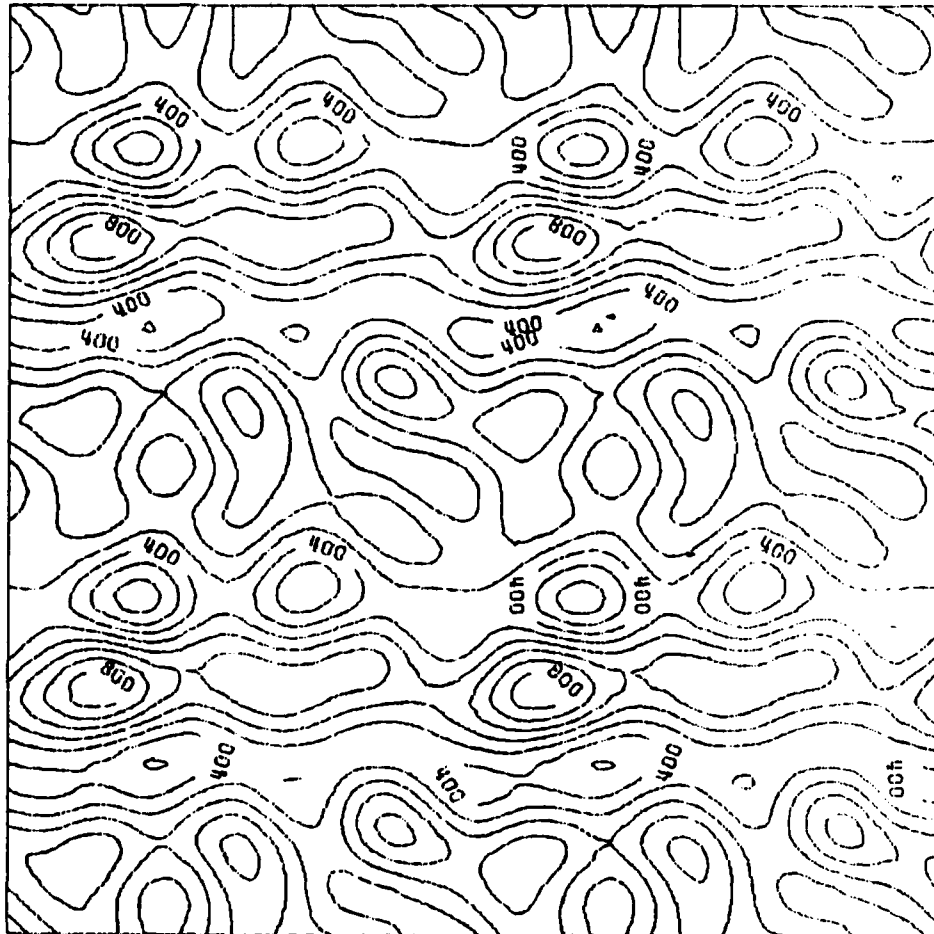


Figure 5

Surface 5

Scale 1:20,000 C.I. = 9 ft.

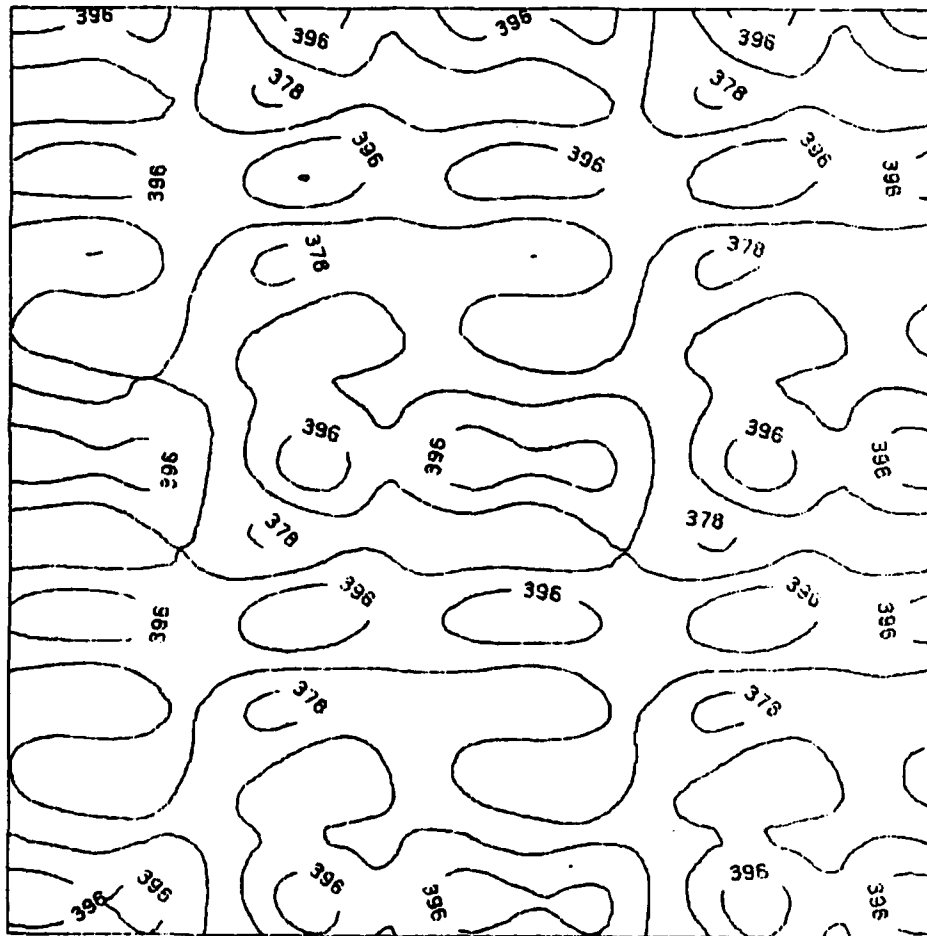
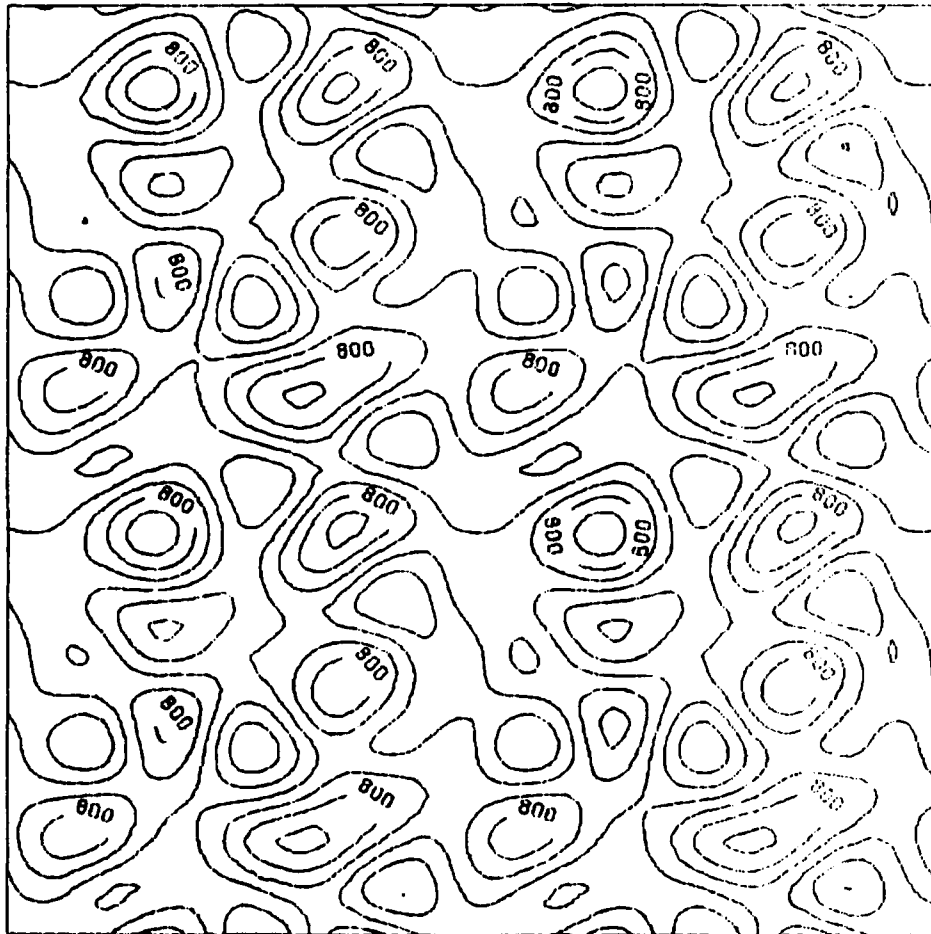


Figure 6

Surface 6

Scale 1:20,000 C.I. = 20 ft.



additional height values at critical points.

Throughout this project one needs to bear in mind that interpolation regions are being discussed and not terrain types.

The first five surfaces have been based on the 15' topographic series, scale 1:62,500, and cover areas of 9.5 km x 9.5 km. A DEM has been constructed (by estimation) from countours for each one of them, consisting of 20 x 20 points 500 m apart.

The sixth surface has been based on the 7½' topographic series, scale 1:24,000 and covers an area of 4.75 x 4.75 km. The DEM which has been constructed consists of 20 x 20 points 250 m apart.

The surfaces based on the above maps are given below. The name of the sheet is given together with the U.T.M. coordinates of the South-West corner of the square from which the elevations were taken.

These synthetic surfaces do not resemble the original surfaces (as represented on the topographic maps). The reasons are given above and we need to add that relatively few points were used to sample the original surfaces - points 500 m apart for the first five surfaces and 250 m apart for the sixth surface. This means that wavelengths smaller than 1000 m (twice the sampling distance) in the first five surfaces and smaller than 500 m in the sixth surface cannot be represented. The topographic map surfaces were used as a basis for generating synthetic surfaces of varying complexities. This complexity is defined by the power spectra of the surfaces (see Table 1).

SURFACE 1: Mineral King, CALIF., Quadrangle
x = 355,000 m E
y = 4,026,560 m N

SURFACE 2: Georgetown, COLO., Quadrangle
x = 447,550 m E
y = 4,374,800 m N

SURFACE 3: Sundance, WYO., Quadrangle
x = 540,000 m E
y = 4,899,600 m N

SURFACE 4: Reedsport, OREG., Quadrangle
x = 409,800 m E
y = 4,816,900 m N

SURFACE 5: New Haven, ILL-IND-KY, Quadrangle
x = 399,000 m E
y = 4,188,800 m N

SURFACE 6: Horse Cave, KY., Quadrangle
x = 589,000 m E
y = 4,114,000 m N

The synthetic surfaces (that is, as defined by an equation) are numbered 1 to 6. The "surfaces" as defined by the 20x20 array of sampled points (as described above) are numbered 1A to 6A.

The program FFTANAL (see Appendix B) was used to transform the data to the frequency domain and perform a spectrum analysis.

Table 1 shows the power spectrum of each DEM and the contribution of each harmonic surface to the total power.

Table 1
Power Spectra for Surfaces

Terrain Harmonic Surface	SURFACE 1A	SURFACE 2A	SURFACE 3A	SURFACE 4A	SURFACE 5A	SURFACE 6A
1	748,888.62	1,274,028.00	11,045.83	46,150.52	360.93	757.20
2	864,992.69	1,541,718.00	13,771.84	66,141.75	429.87	1,749.58
3	954,735.37	1,663,460.00	15,842.46	81,075.62	483.34	2,741.20
4	1,014,243.00	1,725,843.00	16,684.37	90,158.56	519.15	3,880.22
5	1,055,326.00	1,765,785.00	17,192.65	105,619.06	558.24	4,716.52
6	1,080,899.00	1,799,287.00	18,161.14	112,990.56	581.96	5,015.91
7	1,093,569.00	1,820,198.00	18,948.91	116,617.37	601.14	5,388.87
8	1,109,376.00	1,850,144.00	19,489.89	124,812.44	617.94	5,647.41
9	1,127,147.00	1,870,697.00	19,860.60	132,066.87	629.57	5,795.30

The six surfaces used are of differing complexities. This can be seen by visual inspection (that is, do the contours, in a general sense, show complex or simple form) or by analysing their spectra. A general ranking of the order of complexity is as follows:

Surface 2A
Surface 1A
Surface 4A
Surface 3A
Surface 6A
Surface 5A

The complexity will be defined by the power spectrum. An examination of Table 1 shows that the above ranking holds true when one examines the first three harmonic surfaces or when one examines the first nine harmonic surfaces.

As we will note below, the complexity of the surface will affect the accuracy of the interpolation.

3.4 Generation of Synthetic Surfaces up to 3rd Harmonic Surface

As described in previously, a Fourier series expansion up to the third harmonic surface follows equation (3-4) where $n=m=0, 3$, and this gives 49 non-zero harmonic coefficients. These unknown coefficients have been found for each surface using the least squares adjustment program FOURIER. (See Appendix B). The equations of all surfaces were obtained and are included in Appendix C.

The contouring algorithm used for all the output in this project is the Geodetic Science Plotting Package (GSPP) as described in Sunkel (1980).

The following figures show the power spectra of the six surfaces. The 3-D representations show only one quarter of each spectrum - the other three quarters are symmetric.

In some of the related references (for example Bath 1974, Jacobi 1980) the spectrum is given in graphs of $\log P$ vs $\log 1/\lambda$, where P is the power of each frequency, t , and λ is the corresponding wavelength. This is mainly used to find the slope of the spectrum which is a characteristic of different terrain types. The following logarithmic scales show the plots of $\log P$ vs f . This exaggerates the high frequencies which normally have low amplitudes.

An examination of the following figures shows that when the power spectrum is plotted at a logarithmic scale then more details of the spectrum become visible. For future research this could make it easier to classify terrain or interpolation regions. It may also be easier to match existing terrain spectra with previously defined criteria spectra. For this purpose one could fit a plane to the spectrum and examine the slope and direction of this plane. For the 2-D case, logarithmic scales were used by Frederiksen et al. (1984).

The following figures of power spectra give us general impressions of the character of the interpolation regions. For example, comparing figures 7 and 11 we can note that the terrain represented by figure 11 is smoother, less rugged and more homogeneous than the terrain represented by figure 7. The homogeneity of surface 3 is seen from figure 11 where the power spectrum shows that in both the X and Y directions the same frequency components have approximately the same power.

It is clear to us that much work needs to be done in the area of classification of surfaces. For this project, we will classify the complexity of the synthetic surfaces according to the value obtained for the power of the 3rd harmonic surface. Ordering of complexity according to the elements of the spectrum (as shown in the following figures) still needs investigation. Fitting a plane to the 3-D spectrum may be one way of accomplishing this ranking or ordering.

Figure 7

Power Spectrum - Surface 1
Normal Scale

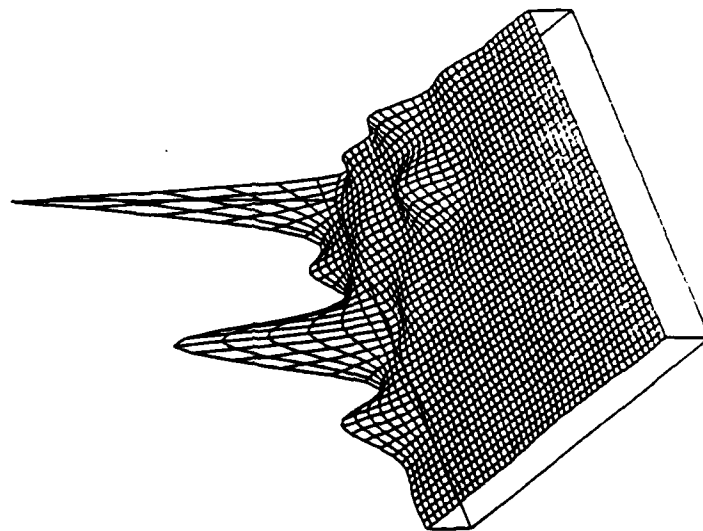


Figure 8

Power Spectrum - Surface 1
Logarithmic Scale

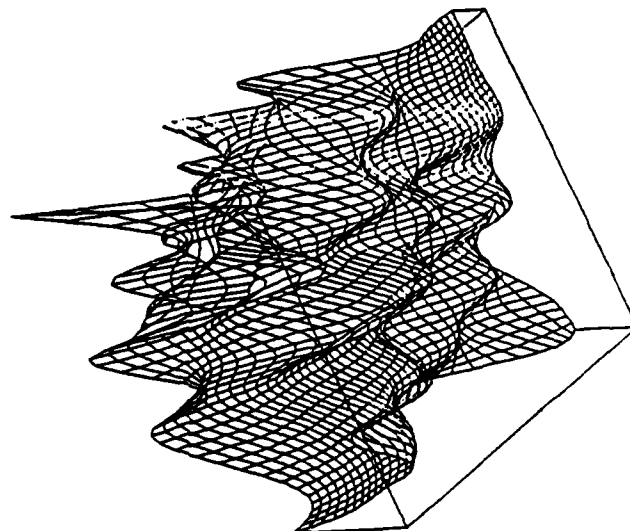


Figure 9

Power Spectrum - Surface 2
Normal Scale

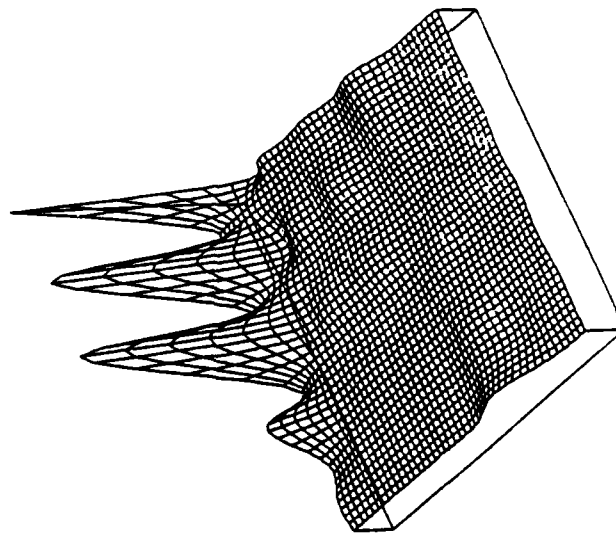


Figure 10

Power Spectrum - Surface 2
Logarithmic Scale

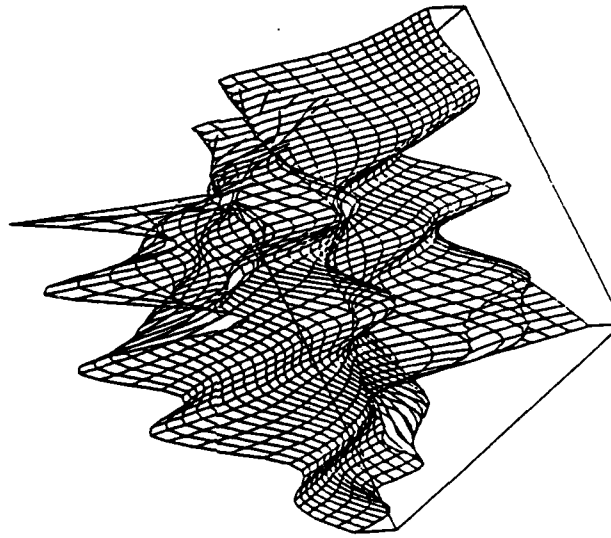


Figure 11

Power Spectrum - Surface 3
Normal Scale

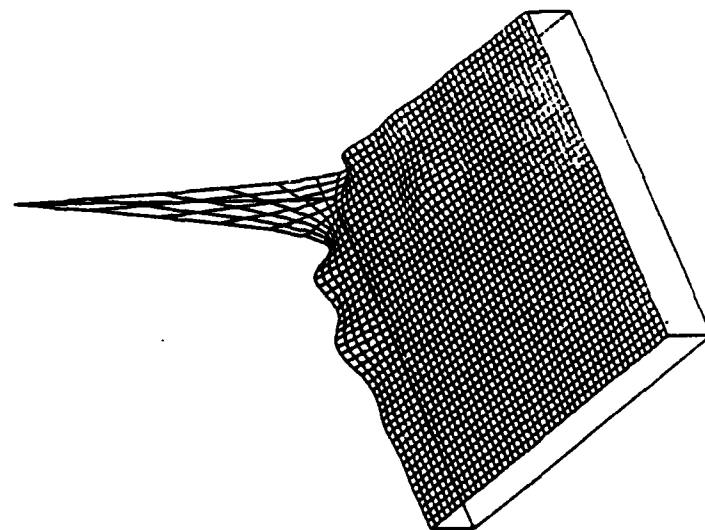


Figure 12

Power Spectrum - Surface 3
Logarithmic Scale

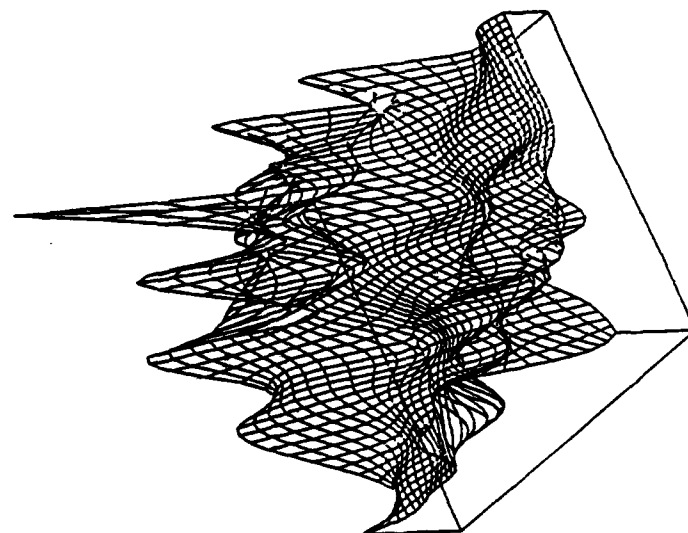


Figure 13

Power Spectrum - Surface 4
Normal Scale

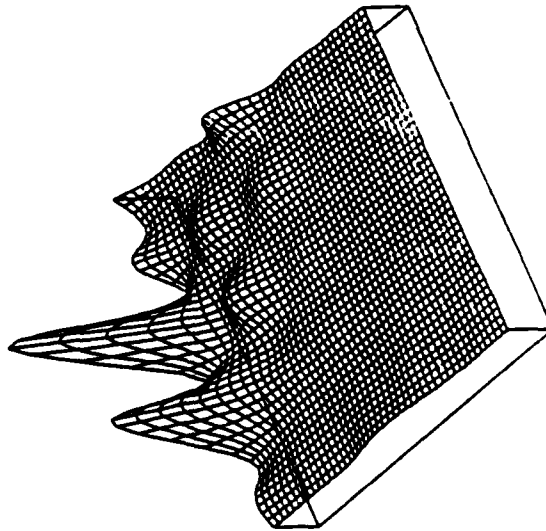


Figure 14

Power Spectrum - Surface 4
Logarithmic Scale

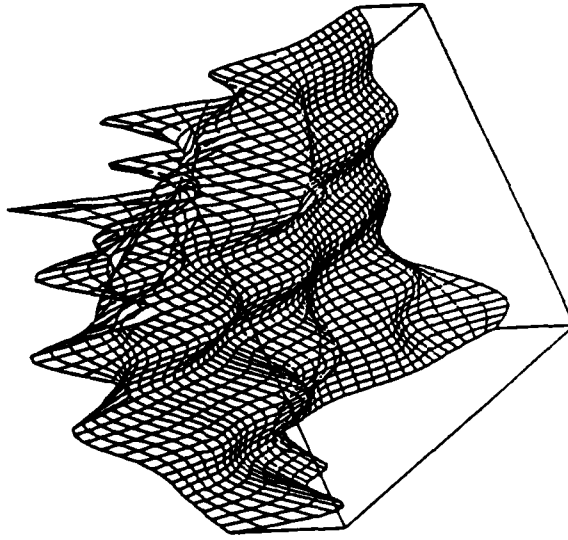


Figure 15

Power Spectrum - Surface 5
Normal Scale

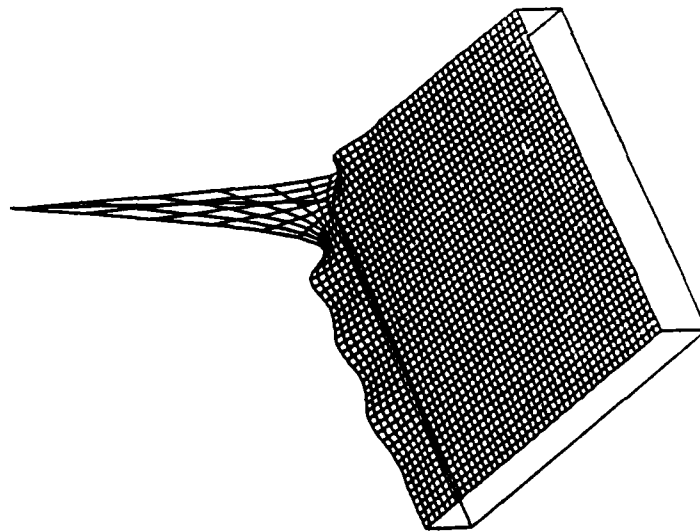


Figure 16

Power Spectrum - Surface 5
Logarithmic Scale

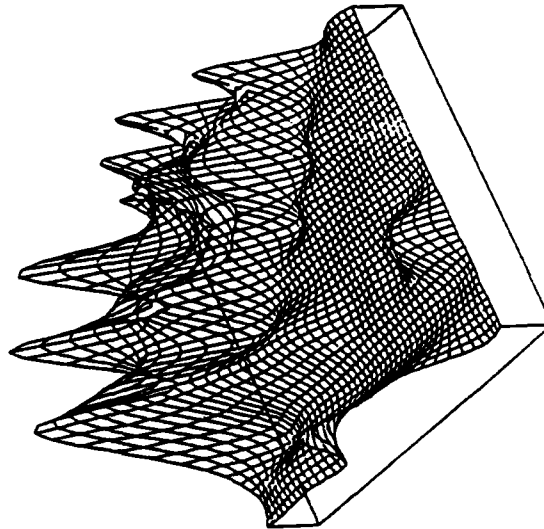


Figure 17

Power Spectrum - Surface 6
Normal Scale

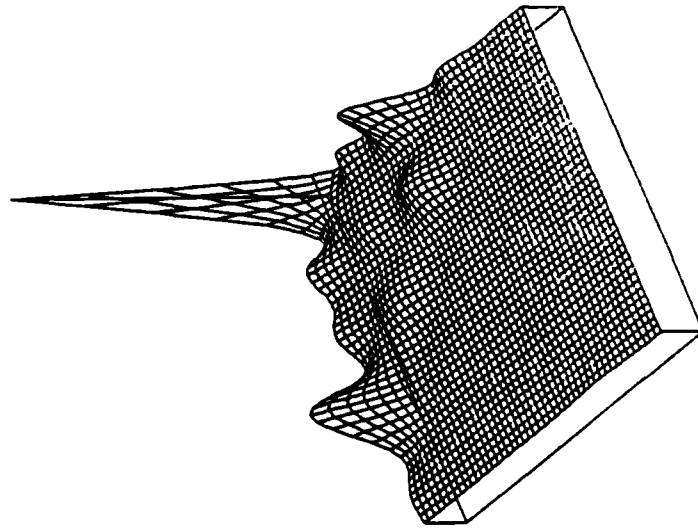
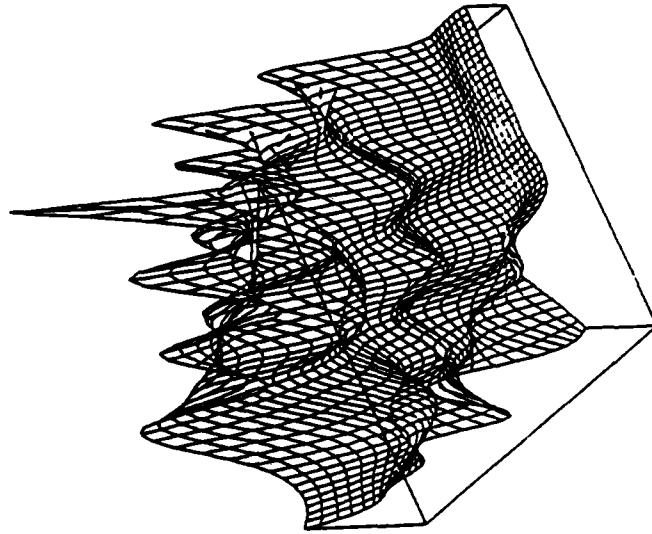


Figure 18

Power Spectrum - Surface 6
Logarithmic Scale



3.5 Generation of Synthetic Surface Contours in Raster Mode

In order to generate a raster image of synthetic surface contours, a blank raster matrix of size 101x101 points 25 m apart is set up. Then for each pixel $(x, y)_i$ the equation of the synthetic surface is solved, obtaining a z_i value for the height. Then setting a contour interval, every z value close to a contour value, within a tolerance limit, takes the value of the contour, the other pixels are zeroed out, and thus a raster image is produced. For example, see figure 19(a).

Some errors produced by this procedure will be added to the errors produced by the interpolation algorithms. Such errors are:

1. In very steep areas gaps may occur in the contour lines.
2. The tolerance values used have already introduced an error in contour line determination.

However, no attempt has been made to correct these errors in contour line determination. The reasons are:

1. They reflect actual situations where a scanner is used to scan an existing contour map. Gaps may be left in contour lines or very thick contours may be produced, depending on the resolution.
2. Depending on the algorithm used to draw, smooth, or generalize the contours on a contour map, errors of different magnitudes are introduced.

3.6 Complexity of the 3rd Harmonic Surfaces

As mentioned previously, the six terrains used in this study are of different complexity. The resulting 3rd harmonic surfaces are also of different complexity as shown in Table 3, where the order of complexity is: SURFACE 2, SURFACE 1, SURFACE 4, SURFACE 3, SURFACE 6 and SURFACE 5 from the most complex to the least complex.

Table 2 below gives the mean height, variance and total power of each surface and Table 3 below shows that most of the power of the original sampled terrain is included in these synthetic surfaces when they are expanded to include all the frequencies existing in the harmonic surfaces up to the third order.

Table 2
Some Surface Attributes
(the array of sampled points)

Surface	Mean Height	Variance	Total Power
1A	10,372.023 ft.	818,611.000	1,127,147.00
2A	10,594.547	995,733.437	1,870,697.00
3A	4,885.422	20,067.152	19,860.60
4A	528.100	87,116.375	132,066.87
5A	389.042	360.502	629.57
6A	765.375	4,935.863	5,795.30

Table 3
Power of the Synthetic Surfaces

Surface	Contribution of 3rd h.s. to the total power	power of 3rd h.s.
1	84%	954,735.37
2	89%	1,663,460.00
3	80%	15,842.46
4	61%	81,075.62
5	77%	483.34
6	47%	2,741.20

The complexity of these surfaces has a direct effect on the definition of the contour lines, as will be discussed below. These errors are therefore added to the actual errors in the interpolation algorithms.

4 Interpolation Methods

4.1 Interpolation from Contours to Grid

It is often desired to estimate the value of a function in locations where it has not been sampled. This process is known as interpolation. The kind of interpolation to be used must be such that takes advantage of all the information contained in the data, while at the same time does not produce artificial results. This means that the design of the method should be closely related to the type and the organization of the input data.

Conversion of contour lines, in digital form, to a rectangular DEM is a problem that cannot be handled by some general interpolation method. The first constraint is the enormous amount of data obtained during digitization or scanning of the contour lines. A study of the published contour-specific algorithms suggests that the most accurate results should be obtained if the actual interpolation takes place along the line of the steepest slope. In the next section three algorithms are presented as examples and an effort to evaluate their performance and efficiency is made.

We need to distinguish between "method" and "algorithm". A method is a manner of procedure, that is, a description of how something could be done. An algorithm translates a method into a set of well-defined processes which leads to the solution of a problem in a finite number of steps. Algorithms can be turned into computer programs but not all methods can be turned into algorithms.

4.2 Contour Specific Algorithms

The problem of interpolation seems to be more peculiar in the case of digitized contours, than in any other general case. There are a number of reasons for that:

1. This field has not been explored in great detail. Algorithms are available in the literature, (Roberts 1980, Leberl et al. 1980, for example), but no evaluation tools are reported in the literature.
2. The data structure of digitized contours has a particular form. That is, the data is in string format and concentrated along lines leaving large areas devoid of data.
3. Besides the height of the points, the contours give additional information, which should be accommodated in the algorithm. The contours describe the structure of the surface.
4. Besides the contours, other lines of special interest (breaklines, ridge lines) and spot heights provide supplementary information, which should not be ignored in the interpolation algorithm.

In this study, three contour-specific interpolation algorithms have been evaluated using synthetic surfaces. In the next sections the form and the

structure of the input data and the logic of interpolation method are explained.

4.2.1 Input Data

Normally, the input data for these algorithms consists of digitized contours, breaklines and spot heights. After the digitization in vector mode all the above information is converted into a raster image of the terrain. In this study, since synthetic surfaces have been used, no breaklines or spot heights have been incorporated. The actual input data consists of a raster image of 101x101 pixels, describing each surface by contours in raster mode. The output is a DEM of 21x21 height points, 125 m apart each other so to comply with DTED specifications used by DMA. (DMA 1979). Other parameters should also be specified in these algorithms, i.e. dimensions of raster image and output DEM, resolution of the raster (pixel size in mm), contour interval, and ground resolution of the pixels. Finally, at least approximate height values for the four corners of the output DEM should be provided by the user. For more information, refer to A.L. Clarke, (1982). Figure 19(b) illustrates the principles of the following algorithms.

4.2.2 LIXY: Linear Interpolation Along X and Y Axes

This method implies linear interpolation along two pre-specified axes. It is computationally efficient, but it is not expected to be very accurate especially in the case of steep terrain. The algorithm is rather simple: the height at the interpolation point is found by linear interpolation between the points on the nearest contours in the X and Y directions. See Appendix B.

The whole procedure includes the following steps:

1. Approximate height values for the four corners of the derived DEM are provided by the user.
2. The interpolated height values, for the points of the DEM along the four edges of the map, are found by linear interpolation between the nearest contours along these edges.
3. The corner and edge values of the DEM are added back to the original contour map, as already gained information.
4. The corresponding row (x-direction) and column (y-direction) is found for the next interpolation point.
5. If the point happens to be on a contour line this contour value is assigned to the point as its elevation. Otherwise the interpolation value is found as the mean of the two values resulting by linear interpolation between the nearest contours along the x and y axes.
6. Finally, the output is a line printer map of the raster data and the DEM point locations, and a listing of the interpolated DEM.

4.2.3 LISS: Linear Interpolation Along the Direction of the Steepest Slope

This algorithm is a variation of the LIXY algorithm and is based in the first place, on the definition of the direction of the steepest slope, and secondly, on the linear interpolation between the two nearest contour points along this profile.

For the definition of the direction of the steepest slope four directions are searched; N-S, W-E, NW-SE, NE-SW. Then the direction of the steepest slope is approximated by one of these directions that show the steepest slope.

The steps of the algorithm are:

1. The user must define the parameters needed in the program and provide approximate height values for the four corner points of the derived DEM.
2. The interpolated values of the DEM points along the edges of the map are found by linear interpolation between the nearest contour points along these edges.
3. The corner and edge points of the derived DEM are added back to the raster image.
4. For every DEM point in the interior, eight data points in the X, Y and diagonal directions are located and the profile with the steepest slope is found. If two or more profiles have the steepest slope, then the profile with the shortest distance is chosen.
5. Along this profile a linear interpolation is performed and the interpolated height value for the DEM is computed.
6. The program output consists of a line printer map of the raster data and the DEM point locations, a listing of the interpolation directions and heights for each DEM point, and a listing of the derived DEM.

This method differs from the previous one in that the interpolation is performed in one profile only. The search for the steepest slope makes the LISS algorithm less efficient, in terms of cost, than the LIXY, but the results obtained by this method are expected to be more accurate.

4.2.4 CISS: Cubic Interpolation Along the Direction of the Steepest Slope

This is the most complex algorithm since, besides the search for the direction of the steepest slope, it requires the location of additional points and performs interpolation based on a cubic polynomial or spline fitting. The computational time is also greater but the results are expected to be even more accurate than the above methods especially in steep terrains.

The proposed model here, is a "moving bicubic spline patch" interpolation algorithm. A bicubic spline surface is local, smooth and exactly fits the input data. Spot heights (local minima and maxima) may be incorporated by setting the first derivative of the surface to zero, where the first and second derivatives (slope and curvature) can be manipulated to accomodate breakline

features. Further approximations make the algorithm more efficient: reduction of the bicubic spline surface to a three-dimensional cubic space curve in the direction of the steepest slope and finally the approximation of the space curve by a two dimensional profile in the direction of the steepest slope containing the interpolation point.

The "minimum norm" and the "best approximation" (Moritz, 1978) properties of the cubic spline are desired in the DEM interpolation. The end conditions for the splines are essentially arbitrary. Natural splines assume second derivatives set to zero at the end points which is equivalent to linearity at the extremities, and so produces flatter curves. Because of this stability, a natural spline with conditions is used by the CISS algorithm. Tests have also shown (A. Clarke, 1982) that "either a cubic polynomial or natural cubic splines may be used for interpolation in the central segment, but only the spline function is suitable in an end segment. The similar results for the central segment allow the choice of an interpolation function for that segment to be based on computational considerations".

The actual steps of the algorithm are:

1. Parameters needed by the program should be defined and approximate values for the DEM corners must be provided by the user.
2. For the edge points the interpolated height value is found using cubic spline interpolation using four data points located on the intersections of the map edge and the four nearest contours.
3. The corner and edge points are added back to the raster data to provide a boundary.
4. As in LISS the direction of the steepest slope is found.
5. Along this profile the interpolated height is computed. The kind of interpolation used depends on the local situation:
 - a) If no breaklines of edges are encountered in the neighborhood, a Newton form cubic polynomial using the four nearest contour points is fitted to the data, two points on each side.
 - b) If a breakline of data edge is located in the steepest slope profile, natural cubic spline interpolation is used.
 - c) If both ends of this profile are on a breakline or data edge, then linear interpolation is used.
6. The interpolated height is compared to the adjacent data point for gross errors detection.
7. The program output consists of the usual line printer map, a listing of the derived DEM and detailed information for each DEM point interpolation (for example, direction of steepest slope, raster and DEM point location, terrain slope, number of points used in the interpolation, flags for blunders).

Example of Line Printer Map from Vector to Raster Conversion
(Extract from Morrison's Surface III)
(from Clarke, 1982)

```

--(NNNN)--2--2--0
--(NNNN)--00000000--22--22--0
--(NNNN)--00000000--2--222--0
--(NN)--00000--2222222222222222222222--0
000--22222222--222--00--
000--2222--2--000--
00--222--2--00000--(N
--22--AA,AAAAAAA--A--000--(N
222--AAA--A--22--000--(NNNNN
--AA--A--22--00--(NNNN
--AA--AA--22--00--(N
--AA--AAA--222--00--(N
AA--AAAAA--222--00--(N
AAAAAAA--222--00--(N
--222--000--(N--66666666
--222--000--(N--66666666
--222--000--(N--66
--222--000--(NNN)
--222--000--(NNN)
--22--00--(NNN)
--222--00--(NNN)

```

**The Principles of the Algorithms LIXY, LISS and CISS
(from Clarke 1982)**

32

5. Accuracy Evaluation Techniques

The basic scenario is as follows. Contours, representing a surface, are digitized. An interpolation method is then used to predict points on a regular grid. As we are using synthetic surfaces, the true values of these predicted points are known.

By comparing the predicted values and the true values, one arrives at a number of measures which indicate the accuracy of the prediction over the surface. These measures are:

mean error;
standard deviation of error;
maximum absolute error

and any of the above as a percentage of the contour interval.

One can obtain added insight into the accuracy of the interpolation method by looking at a map of the residuals (true value minus predicted value) plotted in their correct locations. This visual aid can indicate the existence of systematic error, as well as other isolated errors (or perhaps blunders) in any part of the surface.

To understand what all the above really means in practical terms, we have added maps showing contours produced from grid values which were predicted (by the interpolation method) superimposed on contours produced from true grid values (obtained from the synthetic surface equation). Ideally, the two sets of contours should be plotted in different colors but we did not have the facilities to do this. The difference between the two sets of contours gives an impression of the practical effects of all the interpolation errors.

6. Results Using Small Datasets

6.1 Numerical Evaluation Results

The purpose of obtaining a DEM from digitized contours was to derive a digital form of a surface which complies with the accuracy of the "Digital Terrain Elevation Data" (DTED). The accuracy of the DTED as specified by the Defense Mapping Agency (DMA 1979) is: "DTED accuracy is specified as ± 12 m linear error relative to mean sea level with 90% confidence". What this means statistically is that the probability of an error to be less than -12 m and greater than +12 m is 90%.

Assuming that errors follow a normal distribution, the probability:

$$P\{x_1 \leq e \leq x_2\} = 90\% \quad (6-1)$$

yields:

$$\begin{aligned} F(x_1) &= 0.05 \\ F(x_2) &= 0.95 \end{aligned} \quad (6-2)$$

where $F(x_i)$ is the cumulative probability density function of the normal distribution. Using the tables for the normal distribution we get:

$$\begin{aligned} x_1 &= -1.6449.\sigma \\ x_2 &= 1.6449.\sigma \end{aligned} \quad (6-3)$$

where σ = the standard deviation of the errors.

Therefore (6-1) becomes:

$$P\{-1.6449 \sigma \leq e \leq 1.6449 \sigma\} = 90\% \quad (6-4)$$

The next table (Table 4) gives the confidence intervals of the errors for the six datasets, using the three interpolation algorithms, at 90% significance level.

Table 4
Error Confidence Intervals and Variances
units are in meters

Surface	CISS		LISS		LIXY	
	σ (m)	*1.6449 σ (m)	σ (m)	*1.6449 σ (m)	σ (m)	*1.6449 σ (m)
1	4.29	*7.06	9.64	* 15.85	5.93	*9.74
2	7.22	*11.80	13.43	*22.08	14.15	*23.28
3	1.43	*2.35	1.66	*2.73	1.27	*2.08
4	7.99	*13.14	10.99	*18.09	10.28	*16.92
5	0.90	*1.48	0.67	*1.10	0.69	*1.14
6	1.44	*2.37	1.80	*1.30	1.45	*2.38

Table 5
Errors of Interpolation Methods
units are in meters

Surface	CISS			LISS			LIXY		
	mean	std. dev.	max. absolute	mean	std. dev.	max. absolute	mean	std. dev.	max. absolute
1	-0.23	4.29	20.00	-0.22	9.64	83.00	-0.31	5.93	35.00
2	-0.95	7.22	30.79	-1.62	13.43	61.89	-1.43	14.15	89.33
3	-0.09	1.43	20.43	0.12	1.66	23.47	0.14	1.27	6.10
4	-0.09	7.99	52.13	-1.44	10.99	50.00	-0.56	10.28	46.04
5	0.08	0.90	6.10	-0.06	0.67	3.05	-0.05	0.69	2.18
6	-0.12	1.44	10.67	-0.16	1.80	11.28	0.03	1.45	5.49

The errors mentioned in Tables 4 and 5 are true errors, because the synthetic surface equation gives the true values. That is, the error is the difference between the true value (as obtained from the synthetic surface equation) and the interpolated value (as obtained from the particular algorithm being examined).

We need to bear in mind that the surfaces ranked from the most complex to the least complex (as shown by the power spectra given in Table 1):

Surface 2
Surface 1
Surface 4
Surface 3
Surface 6
Surface 5

An analysis of the results given in Tables 4 and 5 lead us to the following observations:

1. The CISS algorithm performed best (according to the standard deviation of the error) for surface 5 and worst for surface 4. The LISS and LIXY algorithms performed best for surface 5, worst for surface 2 and, for the first four surfaces listed above, the algorithm performed as the CISS algorithm.

The ranking of the surfaces was as follows:

CISS: 5,3,6,1,2,4
LISS: 5,3,6,1,4,2
LIXY: 5,3,6,1,4,2

In other words, all three algorithms performed best for the three least complex surfaces.

2. One can also consider each surface separately and rank the algorithms according to how they performed for the surface. The ranking would then be as follows:

Surface 2: CISS, LISS, LIXY
Surface 1: CISS, LIXY, LISS
Surface 4: CISS, LIXY, LISS
Surface 3: LIXY, CISS, LISS
Surface 6: CISS, LIXY, LISS
Surface 5: LISS, LIXY, CISS

That is, for surface 2 (the most complex), CISS performed better than LISS which performed better than LIXY. For surface 5 (the least complex), LISS performed better than LIXY which performed better than CISS. To put these observations in perspective, one should note that even though LIXY gave the worst results (compared to the other two algorithms) for the most

complex surface, it may have produced a standard deviation of the error which is quite acceptable for some particular purpose.

3. The reason why the three algorithms behaved as they did in the above observation is not within the area of study for this project. (These three algorithms were chosen simply because they were available). To investigate the reasons why the algorithms behaved as they did, would involve an in-depth investigation of the relationships between the theoretical basis of each algorithm and the physical structure of each interpolation region. But from the point of view of evaluating algorithms in a practical way (by using synthetic surfaces), the above observation indicates clearly that an interpolating algorithm should be evaluated against the different complexities of interpolation regions.

The contour interval plays a significant role in filtering out information contained in the actual terrain. When the contour interval is increased, information about the original surface is lost. In order to gain an insight into this aspect of evaluation of interpolation methods, we can express the standard deviation of the residuals as percentages of the contour interval. This is shown in Table 6.

Table 6
Standard Deviation as a Percentage of the Contour Interval

Surface	C.I. (ft)	CISS		LISS		LIXY	
		σ (m)	σ /CI%	σ (m)	σ /CI%	σ (m)	σ /CI%
1	70	4.29	20%	9.64	45%	5.93	28%
2	100	7.22	24%	13.43	44%	14.15	46%
3	20	1.43	23%	1.66	27%	1.27	21%
4	100	7.99	26%	10.99	36%	10.28	34%
5	10	0.90	30%	0.67	22%	0.69	23%
6	20	1.44	24%	1.80	30%	1.45	24%

An examination of Table 6 shows that the accuracies of the three interpolation methods used in the six surfaces range from 20% to 46% of the contour interval. Comparing the results of the three interpolation methods for each surface (that is, reading along the rows of Table 6) we note that for each surface, one of the methods will give an accuracy of between 20% and 30% of

the contour interval. The National Map Accuracy Standards give a limiting value of 50% of the contour interval. Compared to these standards, all three interpolation methods performed well on all six surfaces.

The importance of this research is shown in Table 6 and in the comments made in this section. A particular algorithm does not give the best results for all types of interpolation regions. In evaluating algorithms, an important factor (if not the most important factor) is the type of interpolation region. At present, we do not have a reliable method of classifying interpolation regions. If we had a reliable terrain classification method, and if we could build up experiences of using different interpolation techniques on different types of terrain, we may have the beginnings of an Expert System in this field of computer-assisted mapping.

6.2 Non-Numerical Evaluation

The statistical analysis of the residuals gives a measure of their range of magnitude assuming some probability level. However, what matters from a cartographic point of view is also their locations and their pattern. As mentioned previously, we can extract information concerning the existence of blunders or any kind of systematic errors and draw our conclusions for the performance of the interpolation. For this reason residual maps for all datasets and for all the interpolation methods have been produced and are shown below. A closer look at these maps will help to draw more general conclusions about the performance of the three interpolation methods.

The spatial character of the residual maps will tell us something about the procedures which produced the residuals. "Topography type terrain" on a residual map could indicate the existence of systematic error in the process. Very high "peaks" or very low "depressions" could indicate the presence of blunders. Sparse, low-valued contours could indicate the random nature of the process. If the pattern of the residuals closely resembles the pattern of the original terrain, one would expect to find a systematic error present.

An analysis of the following residual maps, leads us to the following general observations:

SURFACE 1: The best results are given by the CISS residuals, that is, we notice a general random pattern of low-valued contours. The pattern of the residual contours does not resemble the contours of the original surface - this means that generally there is no systematic error in the interpolation. We do notice three areas of dense, relatively high-valued contours. These areas appear to indicate larger errors. Usually blunders would be flagged out by the algorithm. The residuals for LISS and LIXY show larger errors indicating that these two algorithms give worse results than CISS. This is an expected result - linear interpolation is not suitable for complex terrain.

SURFACE 2: The residual (error) pattern for all three algorithms appears to be random. The values for LISS and LIXY are large. (Refer also to Table 5 where the maximum absolute errors are given). The best algorithm is again CISS - an expected result as Surface 2 is a complex surface. None of the

algorithms seem to have any systematic errors in this surface. Again we conclude that linear interpolation is not suitable for this type of interpolation region.

SURFACE 3: This surface ranked fourth in order of complexity of the six surfaces. The residual maps indicate that LIXY performs the best. None of the three algorithms show evidence of systematic error - that is, the contour patterns are of a random nature. Both the CISS and the LISS patterns indicate a large error in about the same position (the dense contours in the lower left of each figure). The size of the error is about 20 m in each case, approximately equal to the contour interval of the original surface. Normally the algorithms would flag these areas for further investigation. Our concern in this project is not with the actual reason for these discrepancies, we are rather drawing attention to the method for evaluating. An important point to note is this: Table 5 indicates that the maximum absolute error for CISS for surface 3 is 20.43 m and the residual map shows that this size of error occurred in only one place - the dense contours in the lower left of the CISS residual map for surface 3. This fact draws attention to the value of having more than one criterion in the evaluation process.

SURFACE 4: This surface was ranked the third most complex surface. The residual maps show that all three algorithms have "pockets" of relatively large errors, but CISS gives the best results. Part of the patterns in CISS and LISS are the same and generally LIXY has a different pattern. None of the residual maps resemble the original synthetic surface - an indication of the absence of systematic error.

SURFACE 5: This surface is ranked as the least complex of the six synthetic surfaces. One would expect linear interpolation to perform well. This is confirmed by an examination of the LISS and LIXY residual maps. These maps illustrate the random nature of the errors and the low values of the errors. On the basis of the three residual maps for this surface one can see that both LIXY and LISS give better results than CISS. But it is not possible to tell which of the two linear interpolation algorithms is the better. The numerical values given in Table 5 show that LISS is slightly better when considering the standard deviation.

SURFACE 6: This surface was ranked as the next least complex surface after surface 5. The residual maps show the CISS and LIXY algorithms as having better fits than the LISS algorithm. Here, as in surface 5, we notice that the least sophisticated algorithm (LIXY) performs well in terrain of low complexity.

The residual maps have not indicated the existence of any systematic error in the interpolation procedures (if the residual maps resembled the original surfaces or exhibited "topographic shapes," then one would suspect the existence of systematic error). Attention was drawn to the manner in which blunders could be discovered. The actual blunders apparent in the residual maps were corrected so that the remaining random errors could be statistically analyzed. In an evaluation procedure, one may need to investigate the cause of the blunders. In the three algorithms being used for this project, the blunders were due to a bad determination of the contours by the raster processing. For these small data sets they were easily corrected.

Figure 20

Surface 1 - CISS Residuals
Scale 1:20,000 C.I. = 2 m

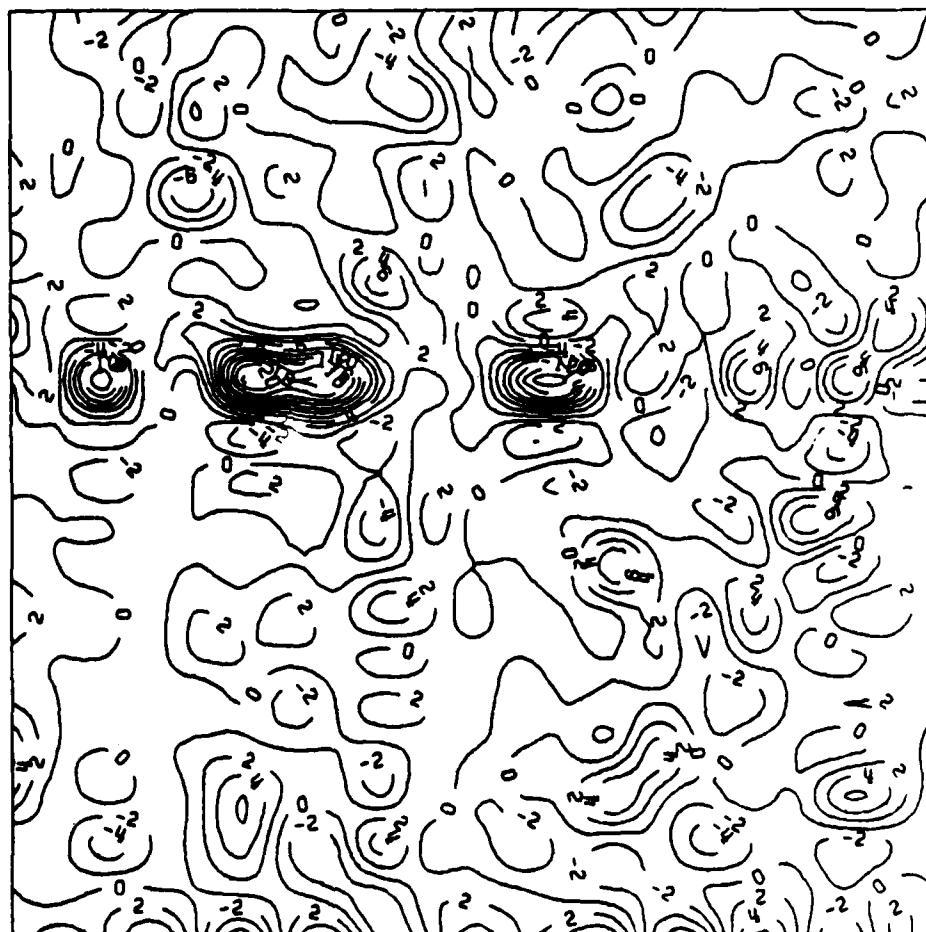


Figure 21

Surface 1 - LISS Residuals
Scale 1:20,000 C.I. = 2 m

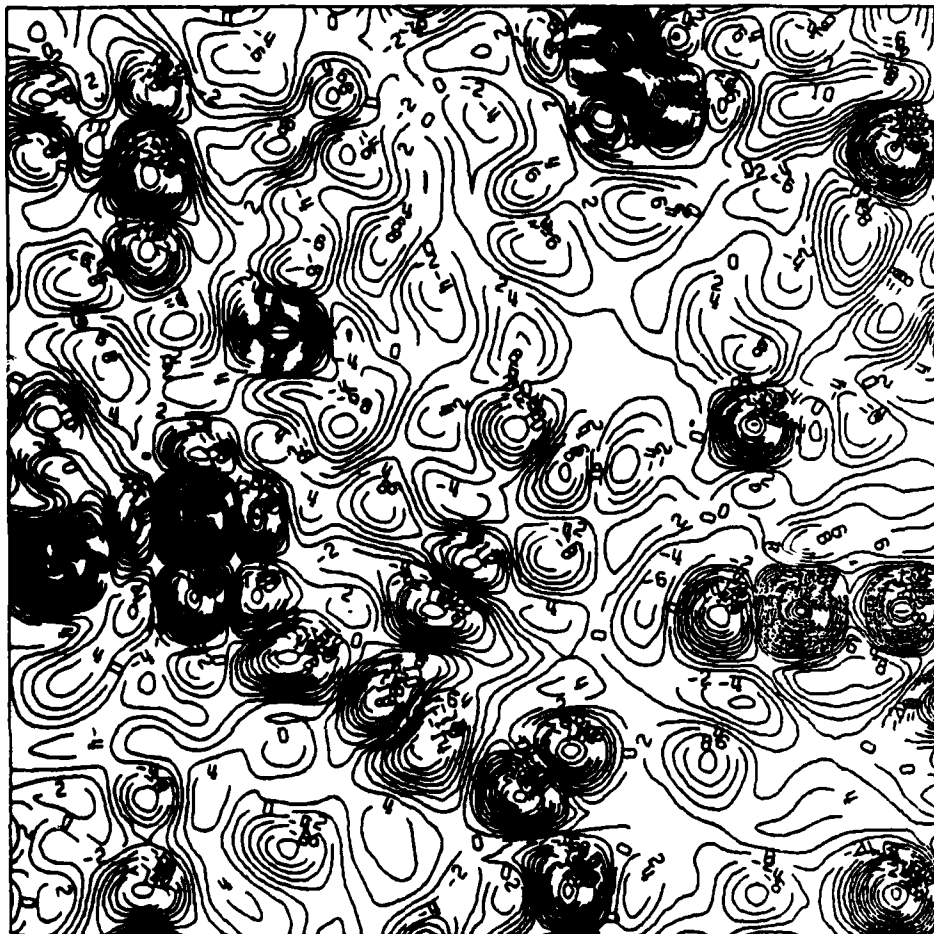


Figure 22

Surface 1 - LIXY Residuals
Scale 1:20,000 C.I. = 2 m

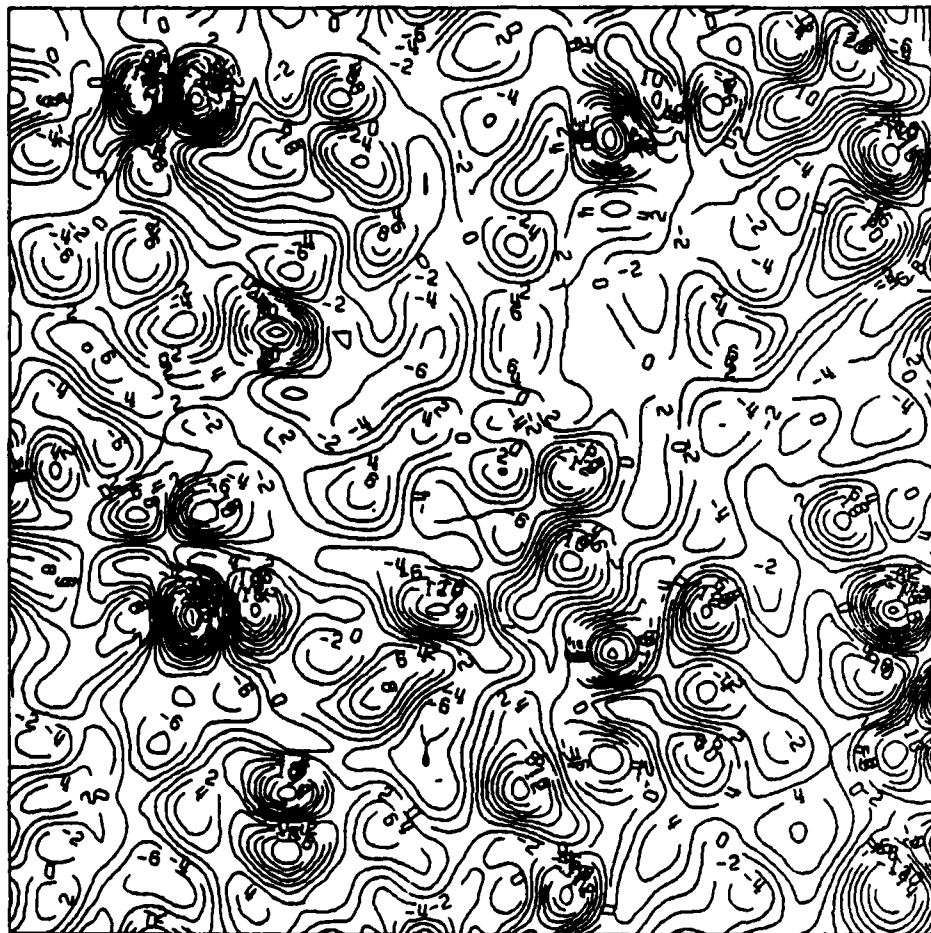


Figure 23

Surface 2 - CISS Residuals
Scale 1:20,000 C.I. = 10 m

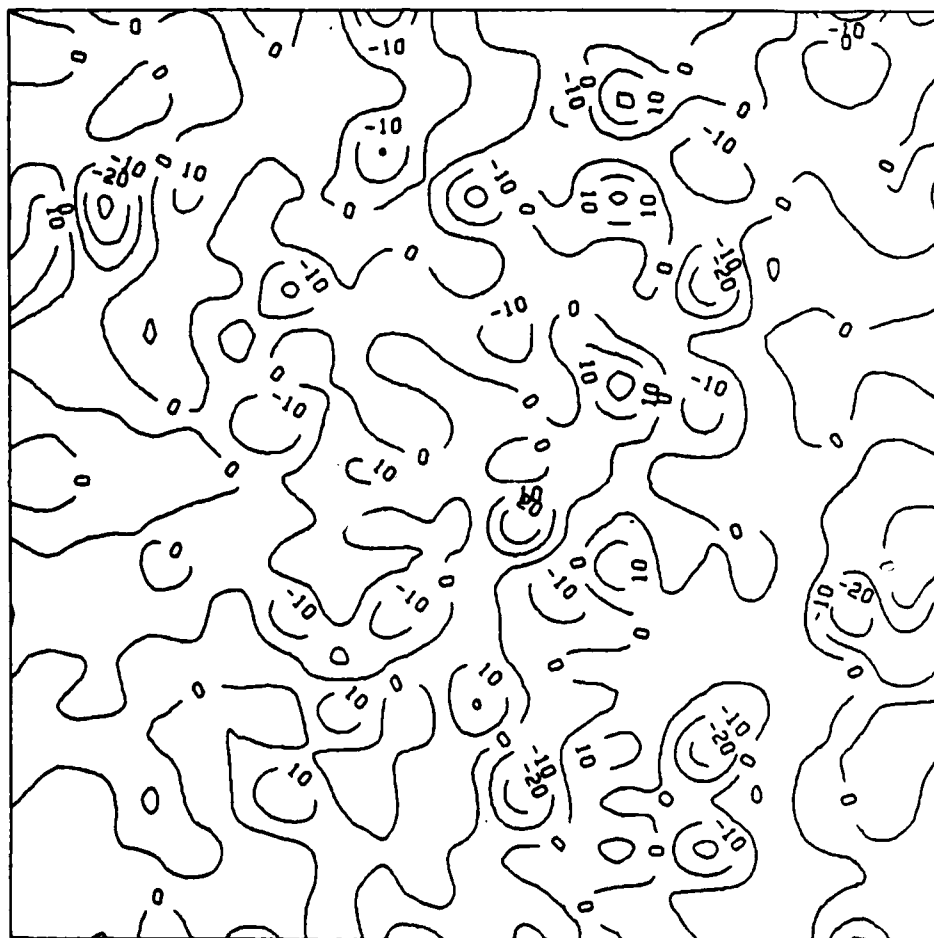


Figure 24

Surface 2 - LISS Residuals
Scale 1:20,000 C.I. = 10 m

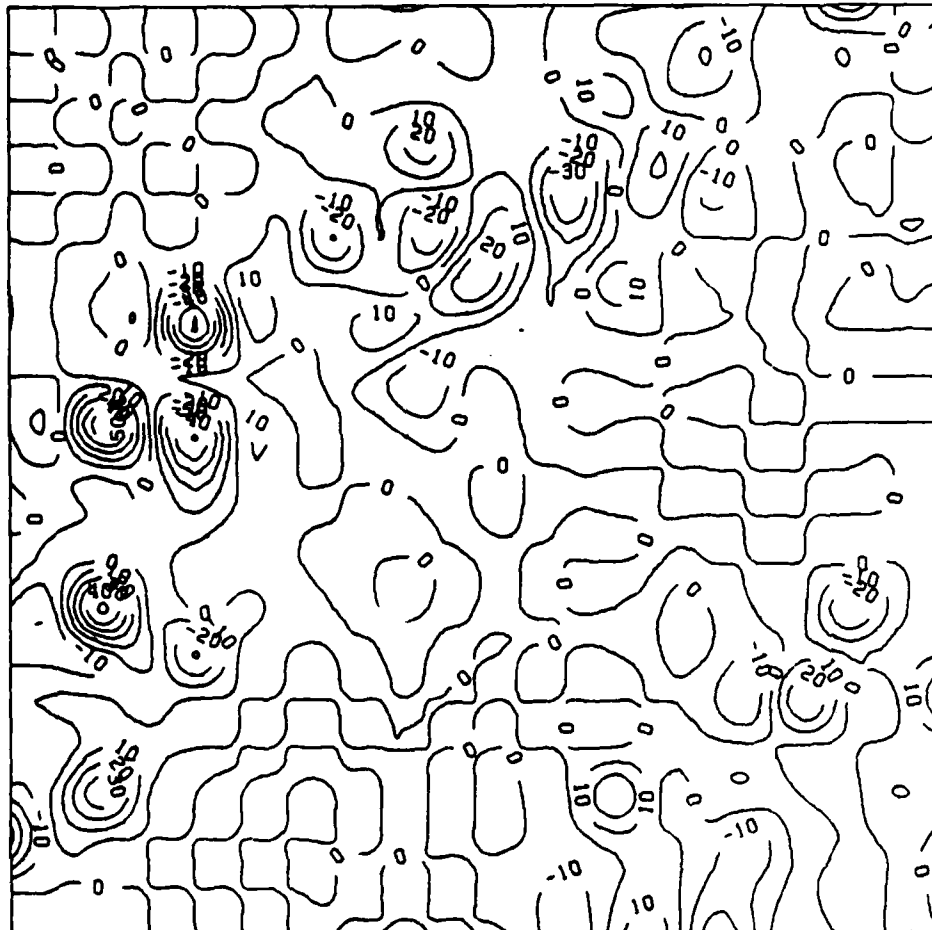


Figure 25

Surface 2 - LIXY Residuals
Scale 1:20,000 C.I. = 10 m

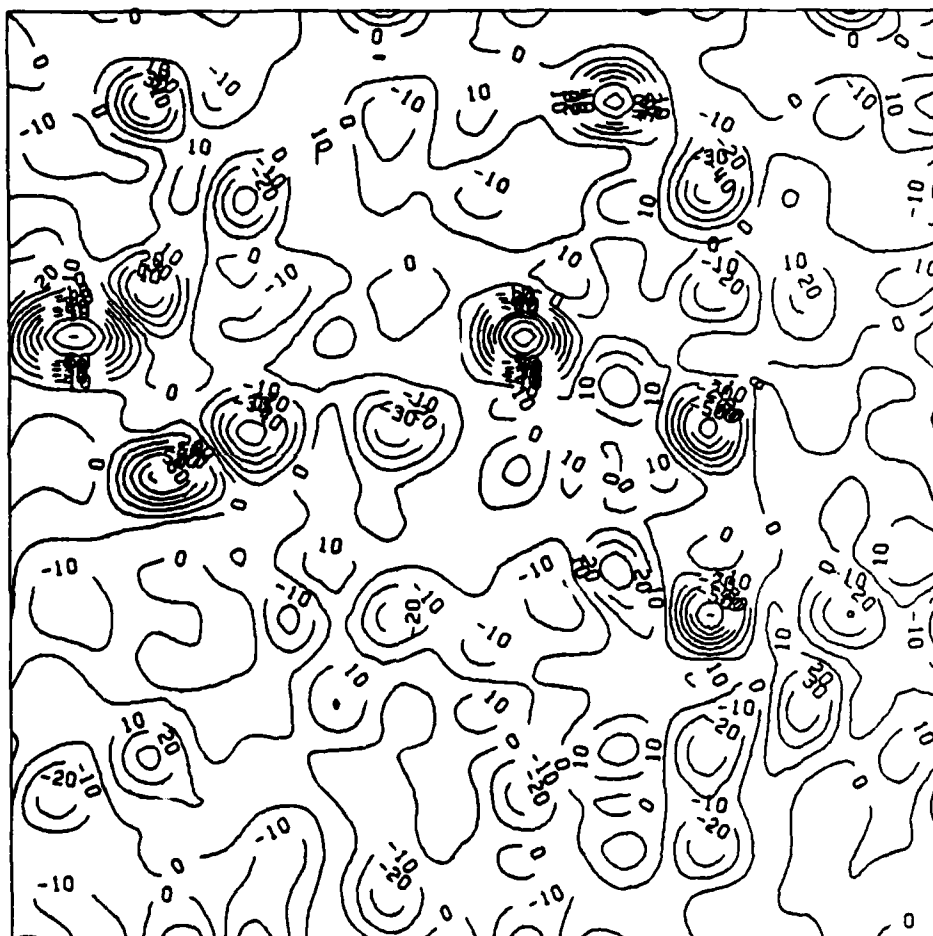


Figure 26

Surface 3 - CISS Residuals
Scale 1:20,000 C.I. = 2 m

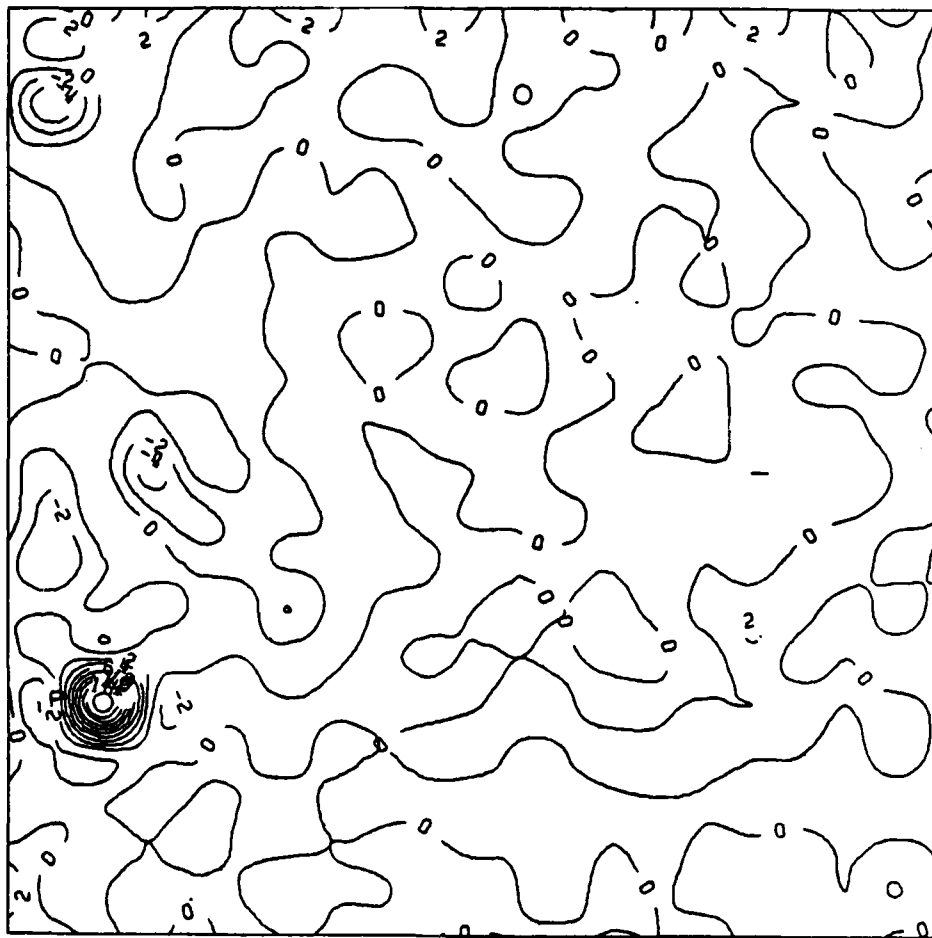


Figure 27

Surface 3 - LISS Residuals
Scale 1:20,000 C.I. = 2 m

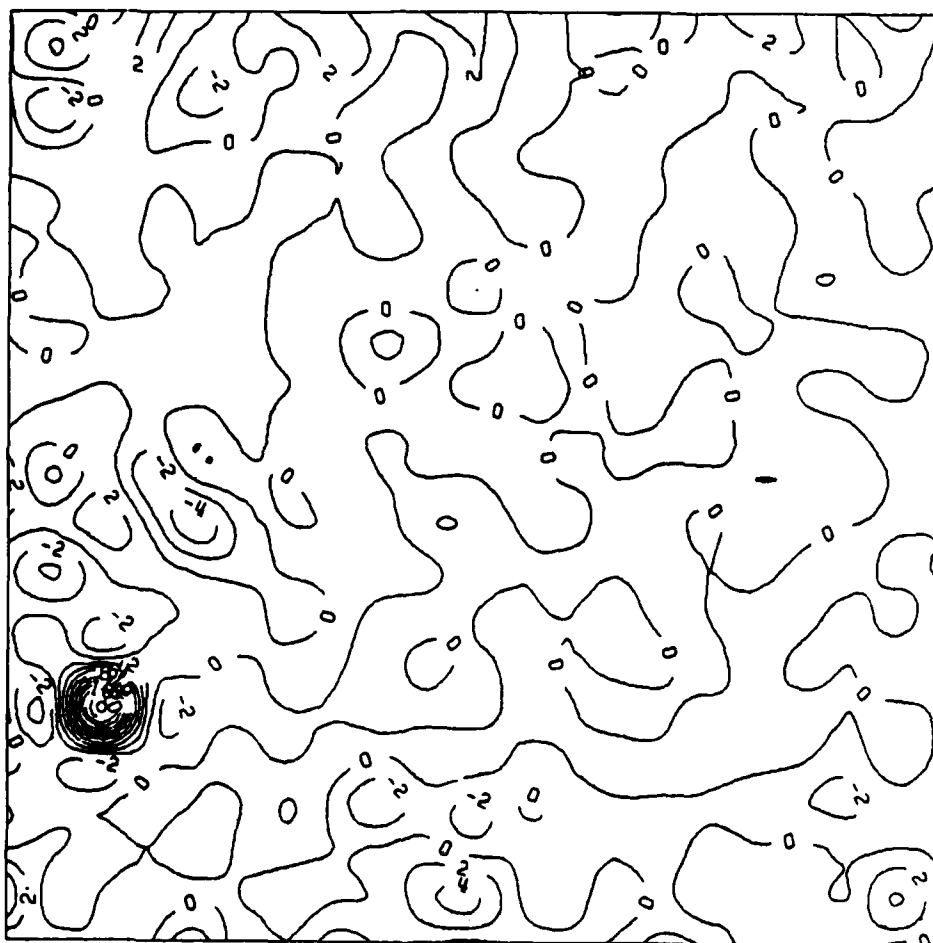


Figure 28

Surface 3 - LIXY Residuals
Scale 1:20,000 C.I. = 2 m

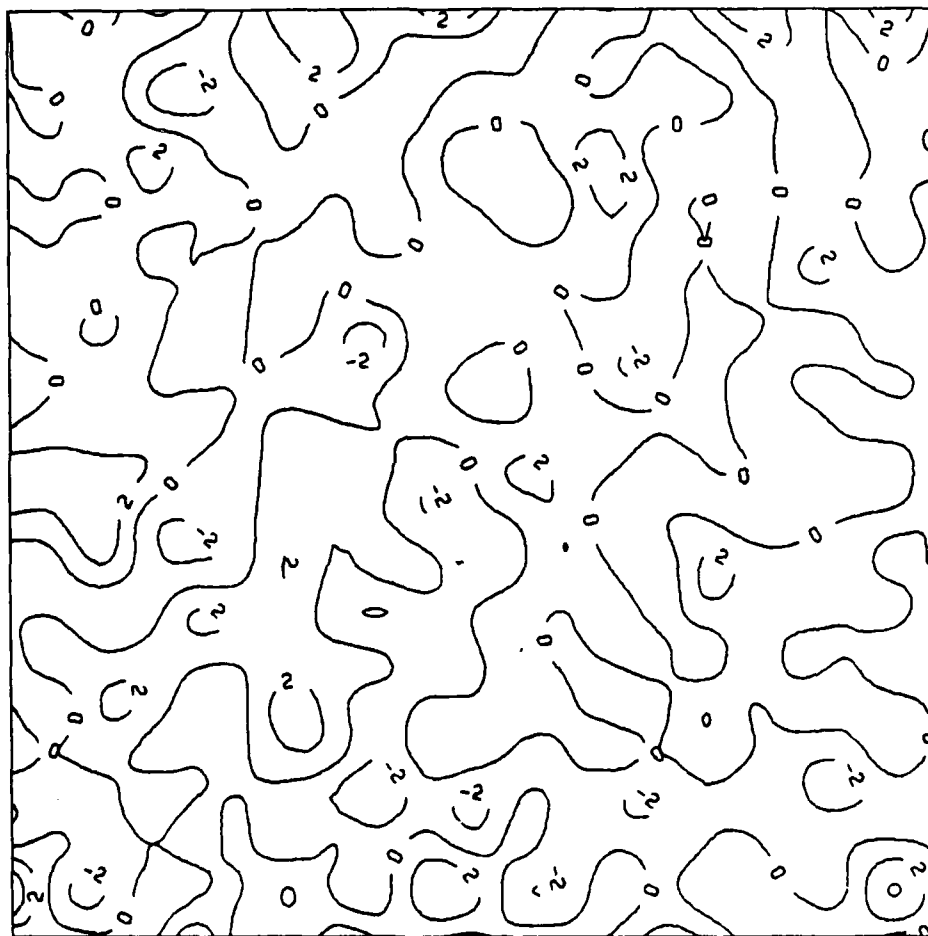


Figure 29

Surface 4 - CISS Residuals
Scale 1:20,000 C.I. = 20 m

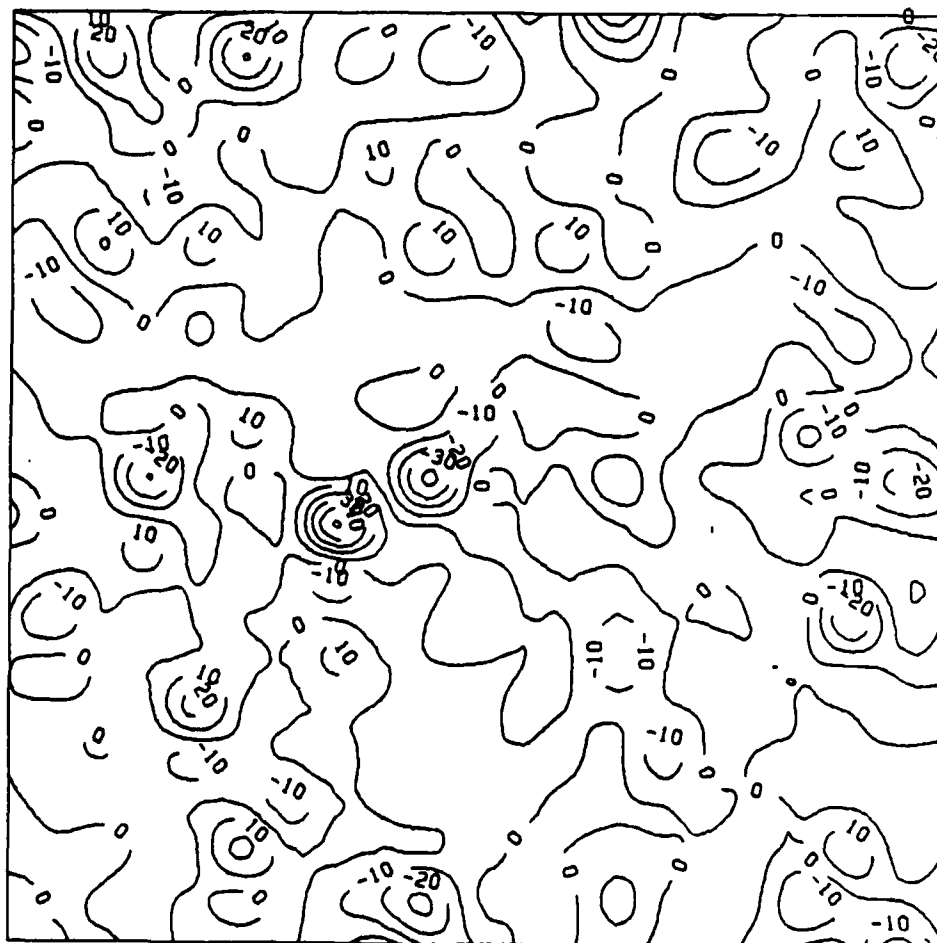


Figure 30

Surface 4 - LISS Residuals
Scale 1:20,000 C.I. = 10 m

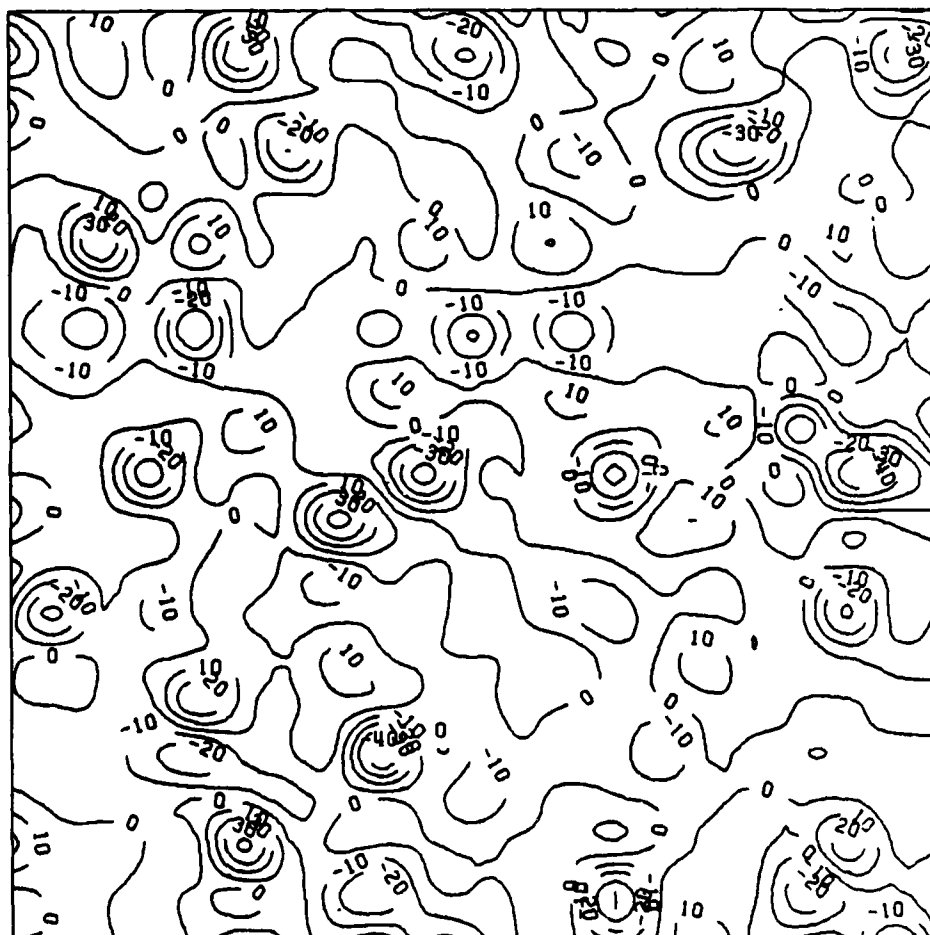


Figure 31

Surface 4 - LIXY Residuals
Scale 1:20,000 C.I. = 10 m

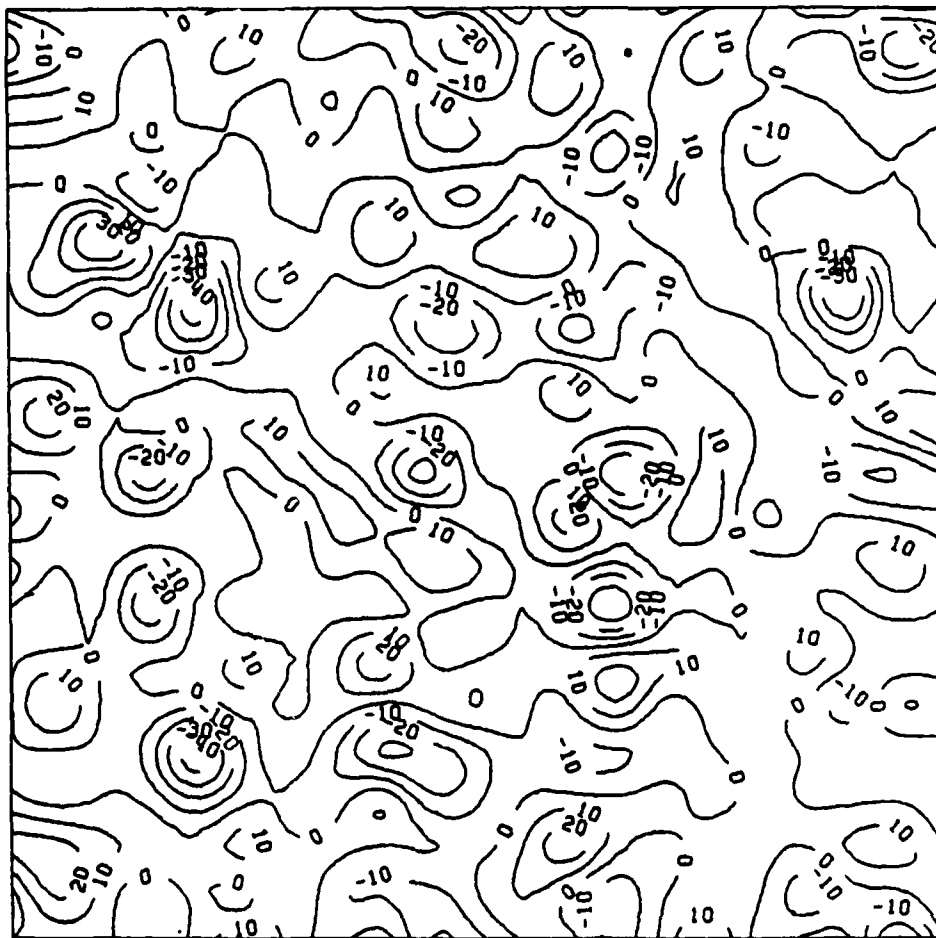


Figure 32

Surface 5 - CISS Residuals
Scale 1:20,000 C.I. = 2 m

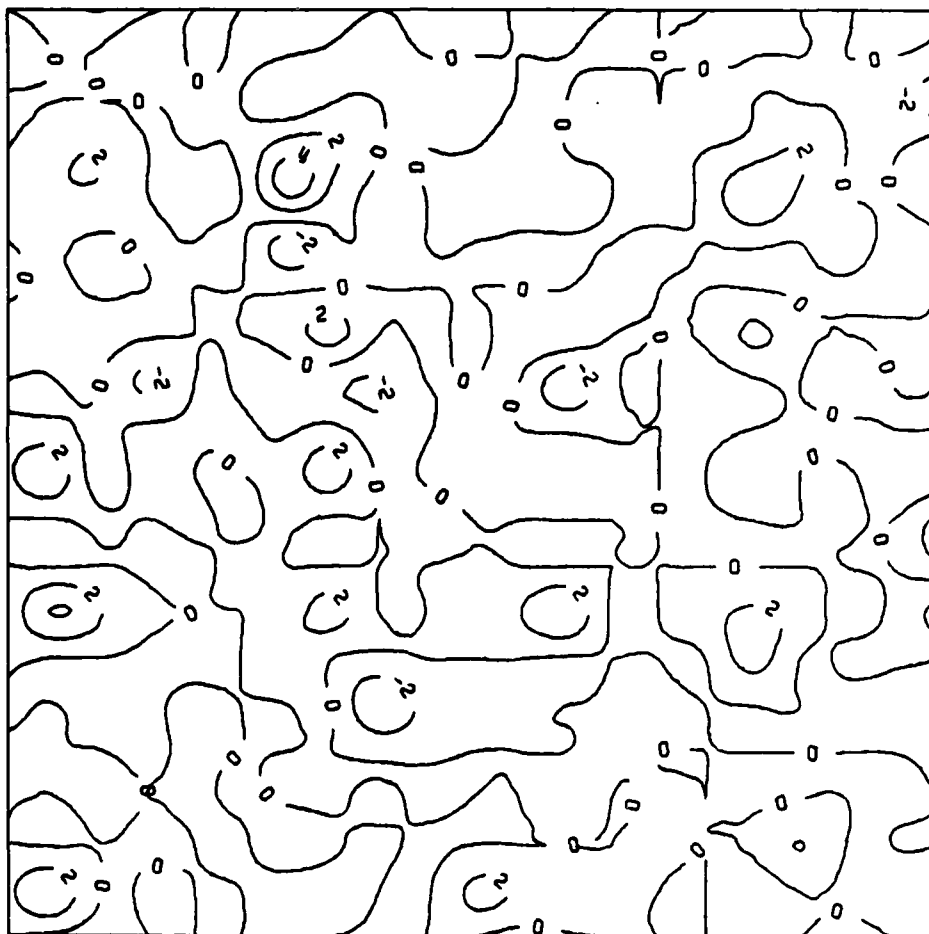


Figure 33

Surface 5 - LISS Residuals
Scale 1:20,000 C.I. = 2 m

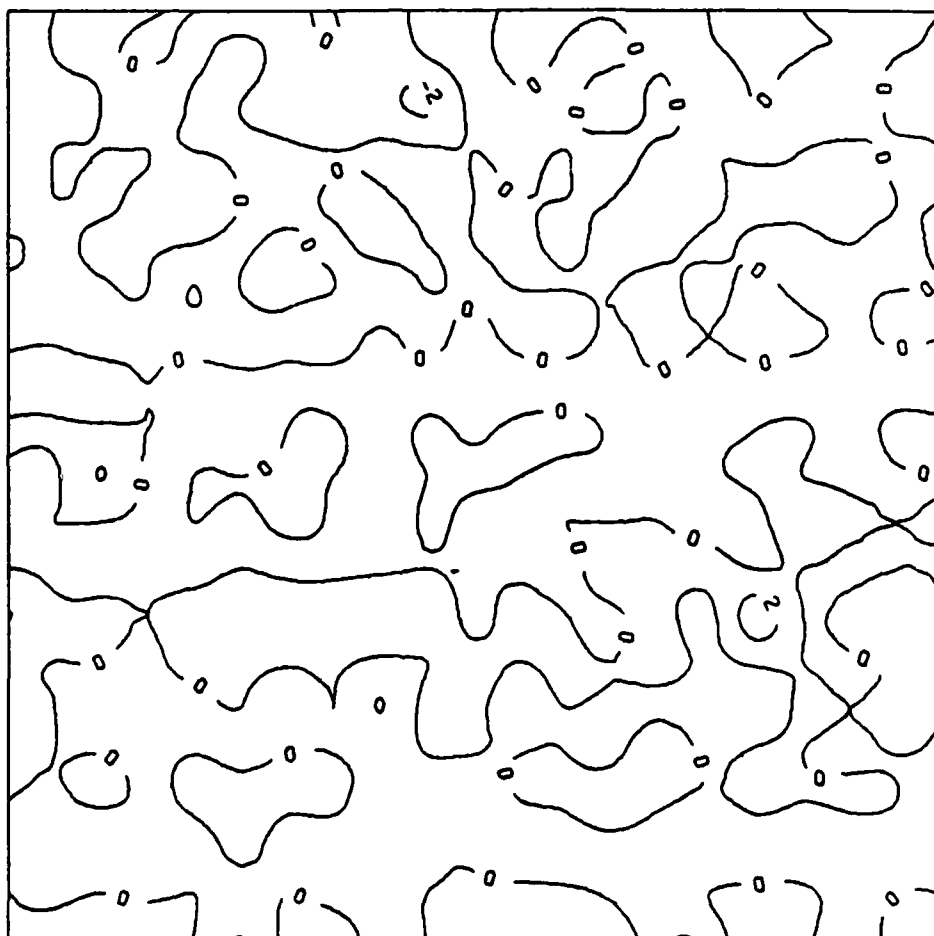


Figure 34

Surface 5 - LIXY Residuals
Scale 1:20,000 C.I. = 2 m

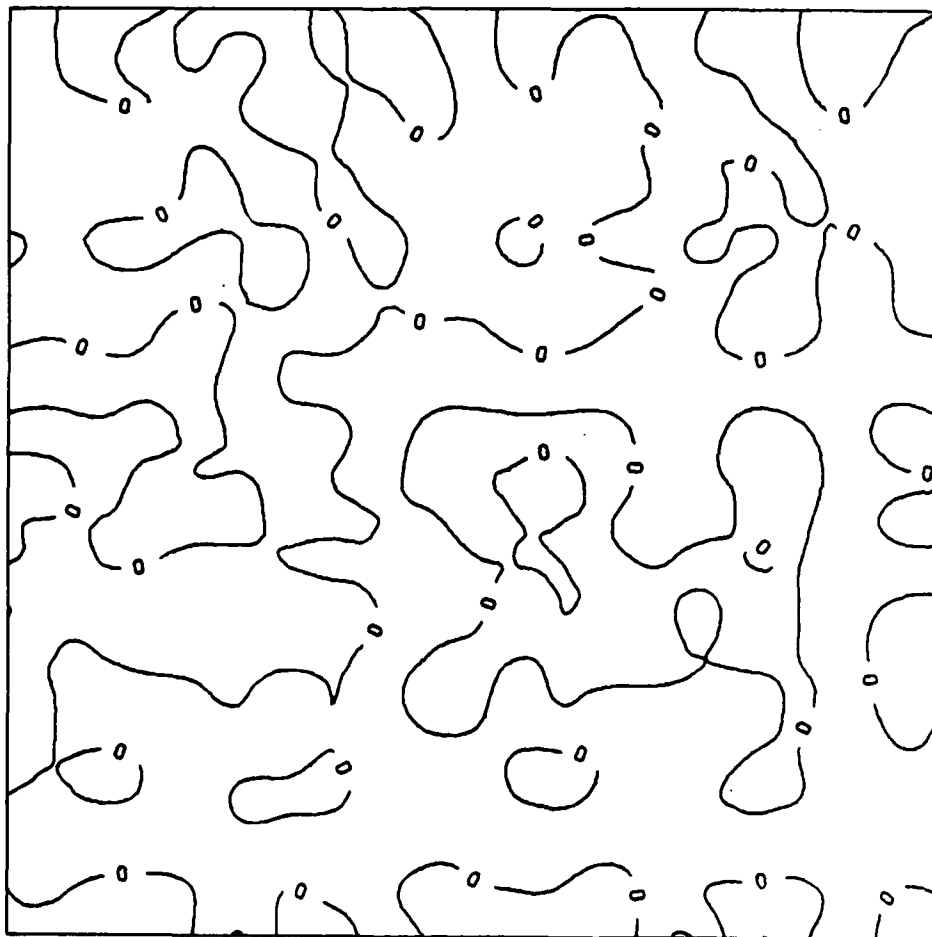


Figure 35

Surface 6 - CISS Residuals
Scale 1:20,000 C.I. = 2 m

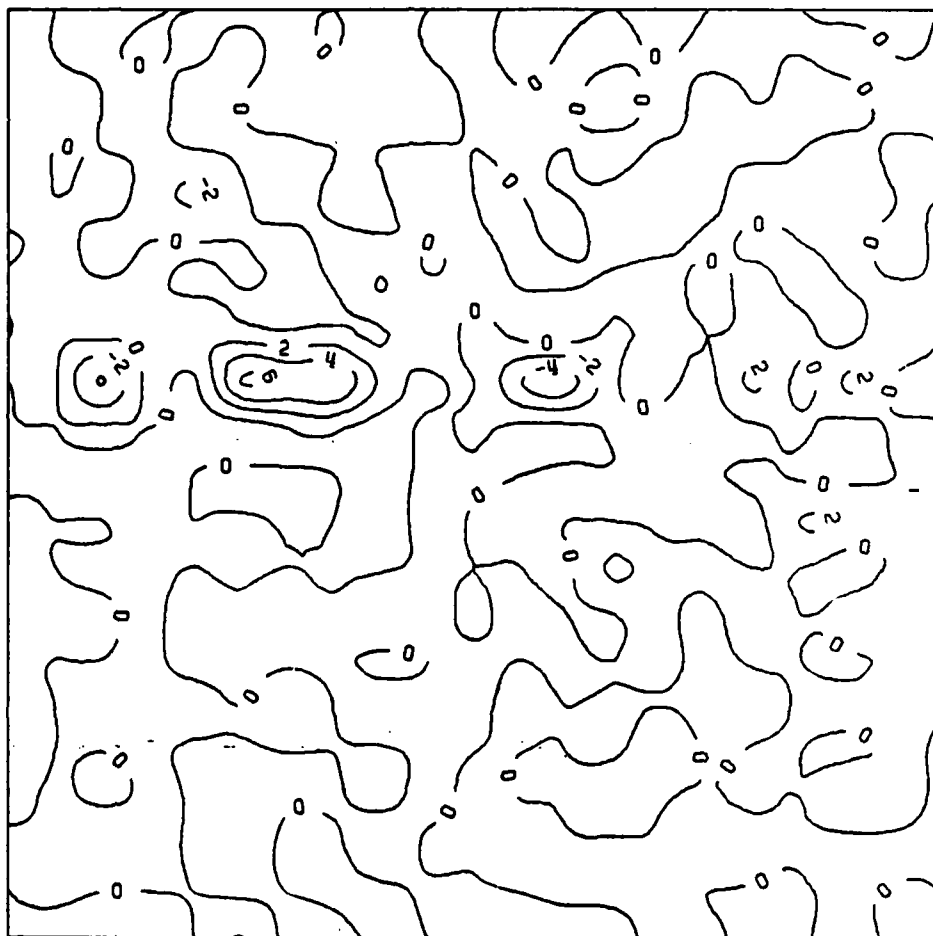


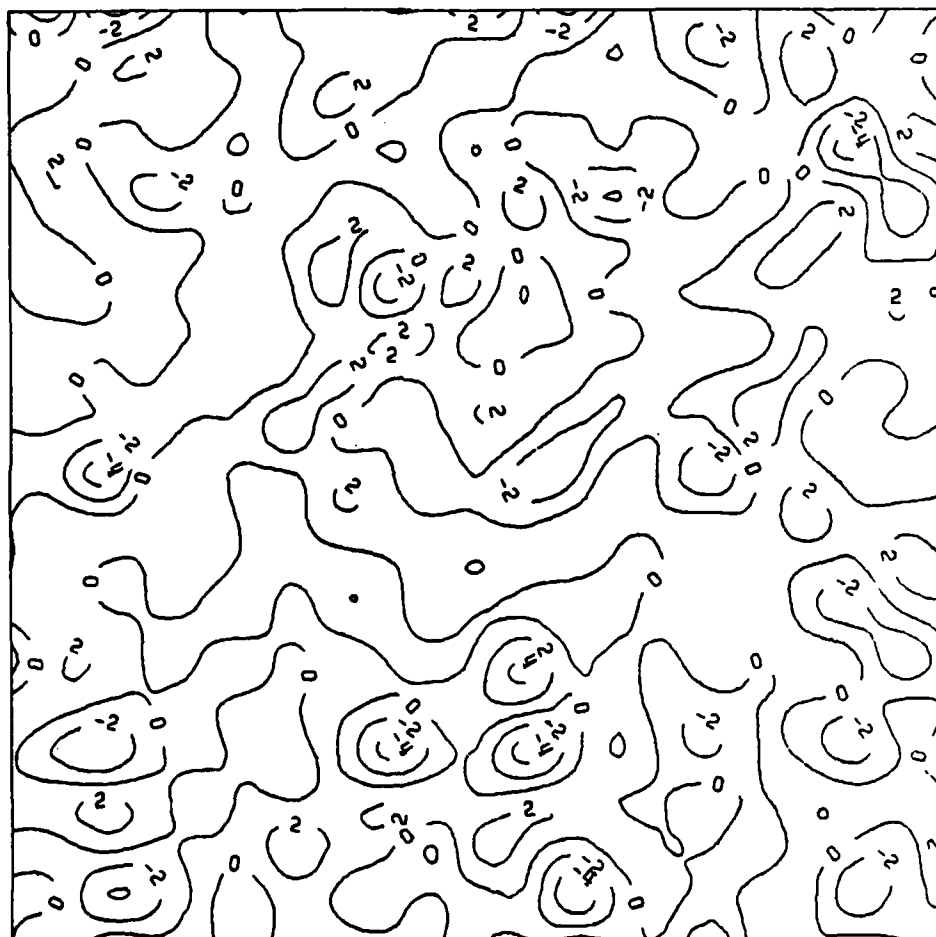
Figure 36

Surface 6 - LISS Residuals
Scale 1:20,000 C.I. = 2 m



Figure 37

Surface 6 - LIXY Residuals
Scale 1:20,000 C.I. = 2 m



In the following figures, we have shown, for each surface and for each interpolation method, the true contours (obtained through the synthetic surface equation) and the contours obtained from the interpolated grid values. These figures therefore illustrate the practical significance of the error statistics discussed previously.

As mentioned before, the contouring algorithm was the GSPP package (Sunkel 1982). The accuracy of the contouring algorithm will not affect the conclusions drawn from the contour maps because the same method of producing the contours is used for both the original surface and the interpolated surface. On the following maps, we illustrate the practical differences (on a scale of 1:20,000) between true contours (obtained from synthetic surfaces) and derived contours (obtained via an interpolation algorithm).

Our discussion of errors so far has dealt with vertical errors, that is, errors in height. The following maps translate these vertical errors to horizontal errors at map scale for each algorithm and for each type of interpolation surface.

Figure 38

Surface 1 - Original Contour and via CISS
Scale 1:20,000 C.I. = 40 ft.

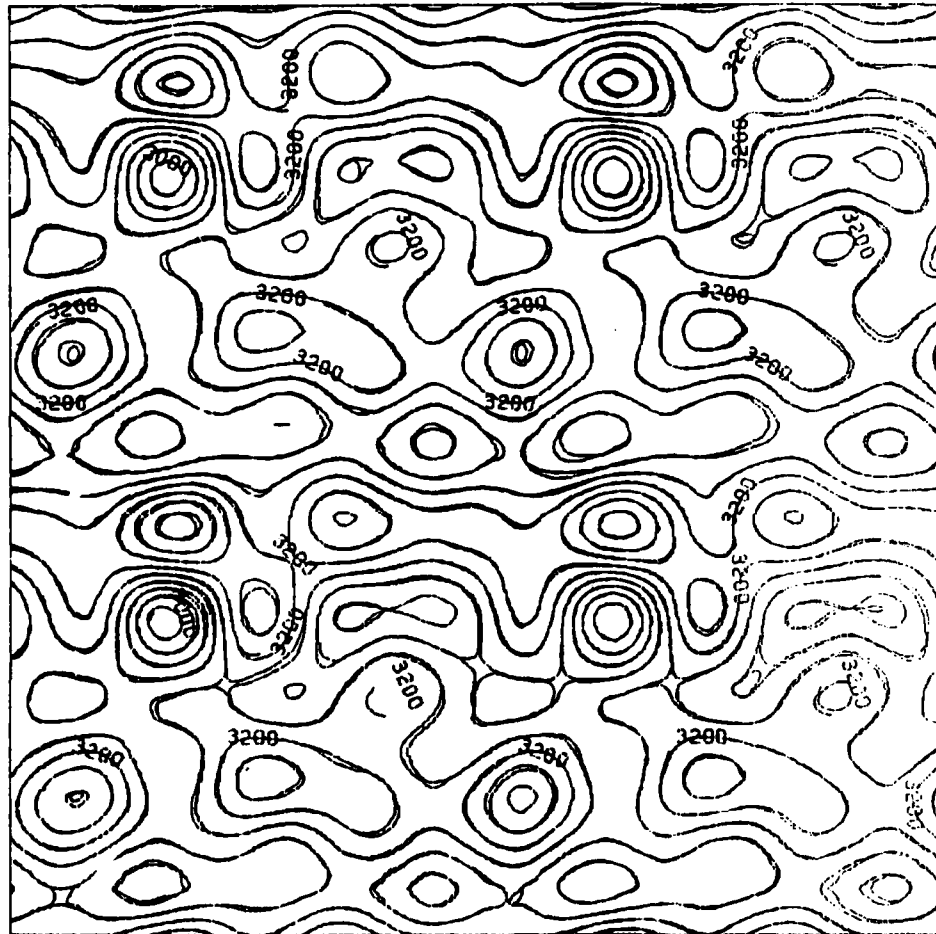


Figure 39

Surface 1 - Original Contour and via LISS
Scale 1:20,000 C.I. = 40 ft.

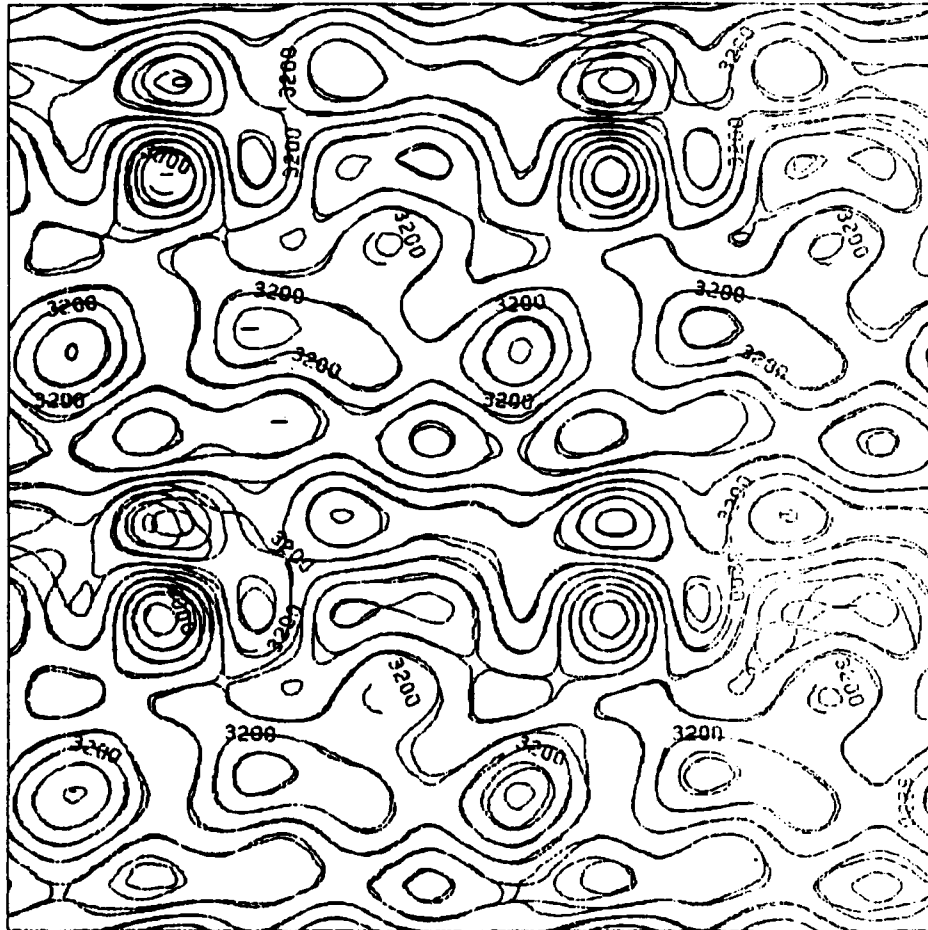


Figure 40

Surface 1 - Original Contour and via LIXY
Scale 1:20,000 C.I. = 40 ft.

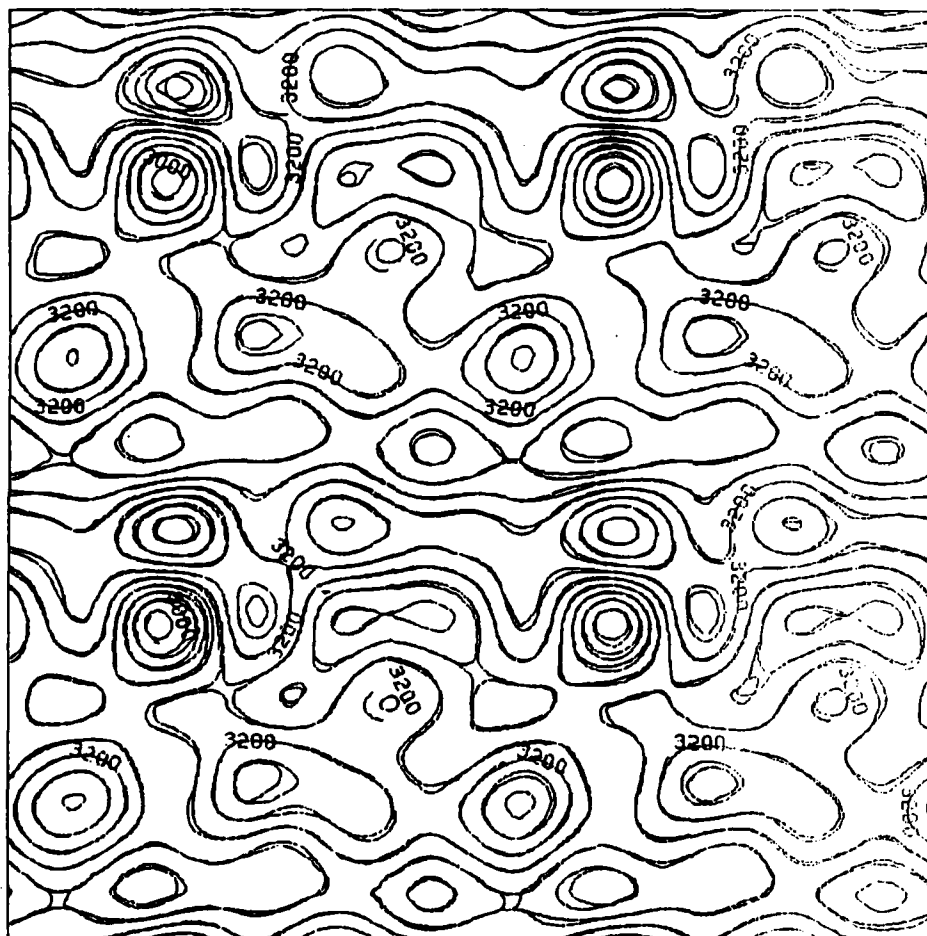


Figure 41

Surface 2 - Original Contour and via CISS
Scale 1:20,000 C.I. = 100 ft.

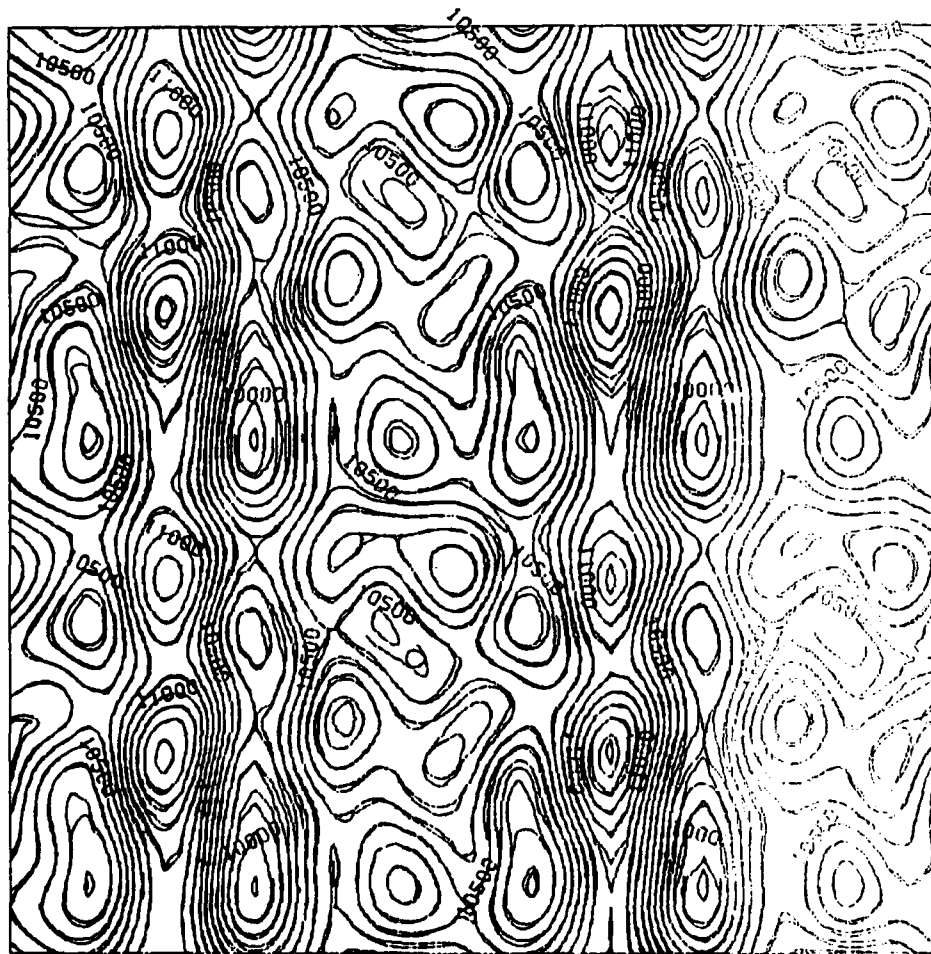


Figure 42

Surface 2 - Original Contour and via LISS

Scale 1:20,000 C.I. = 100 ft.

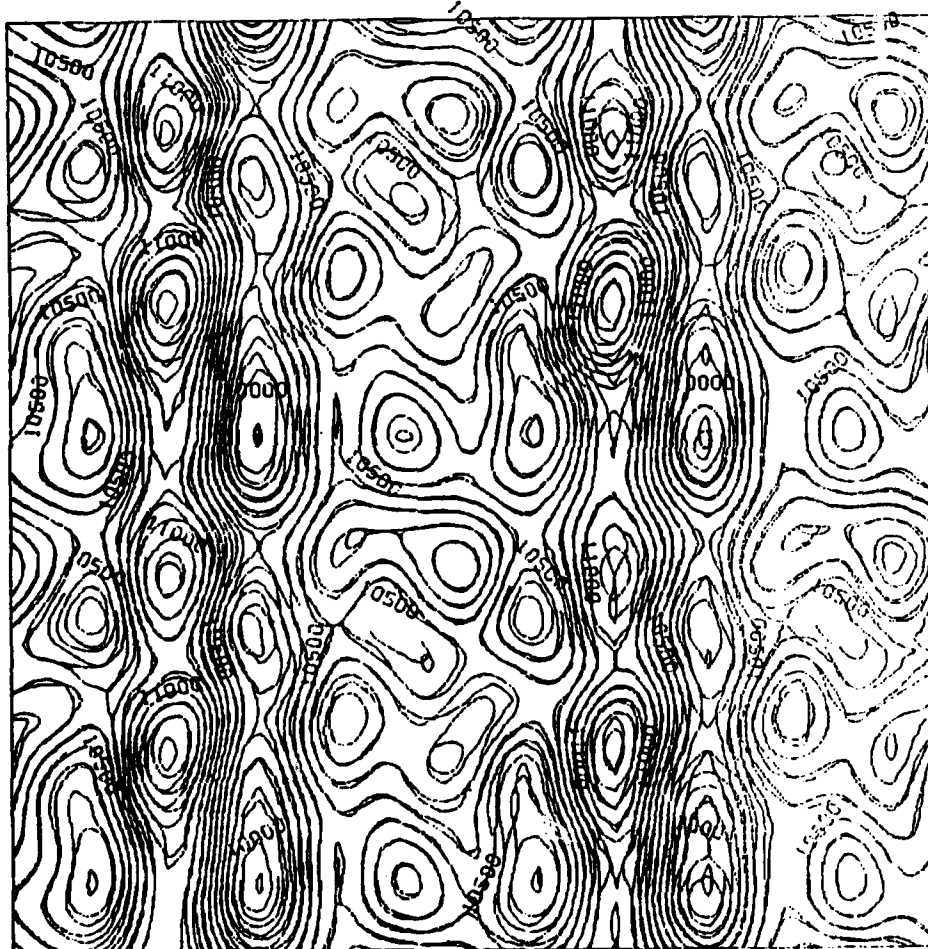


Figure 43

Surface 2 - Original Contours and via LIXY
Scale 1:20,000 C.I. = 100 ft.

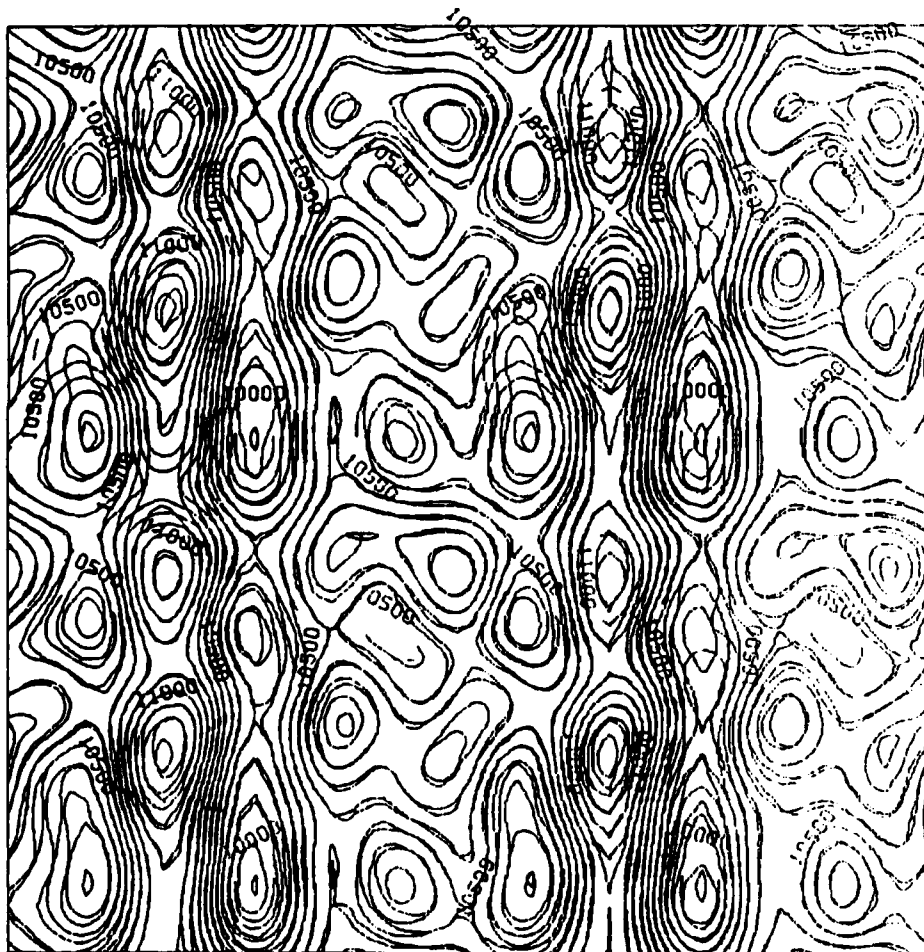


Figure 44

Surface 3 - Original Contour and via CISS
Scale 1:20,000 C.I. = 30 ft.

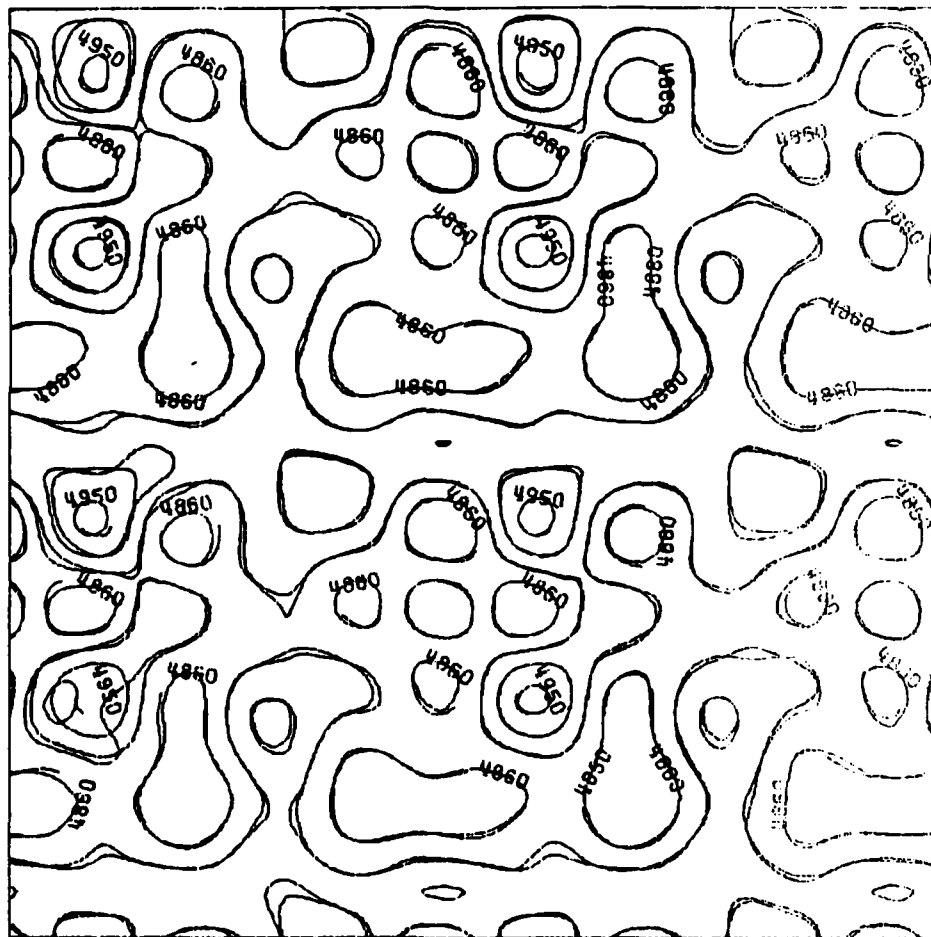


Figure 45

Surface 3 - Original Contour and via LISS

Scale 1:20,000 C.I. = 30 ft.

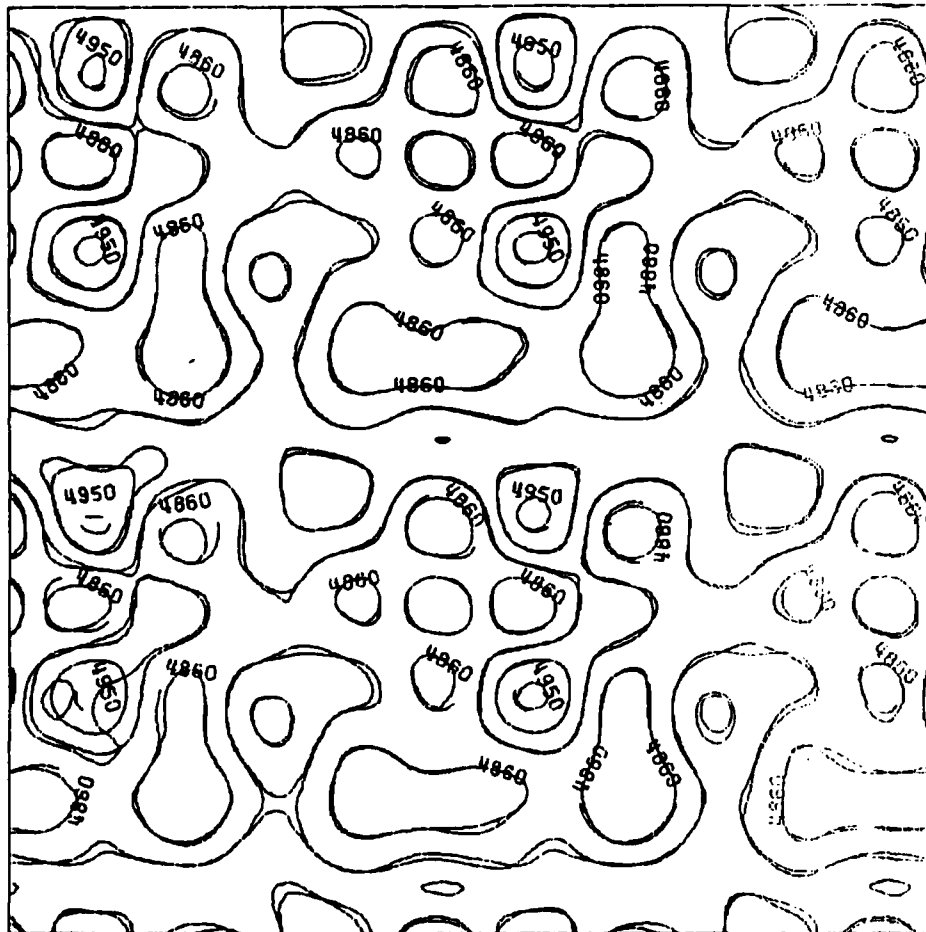


Figure 46

Surface 3 - Original Contour and via LIXY
Scale 1:20,000 C.I. = 30 ft.

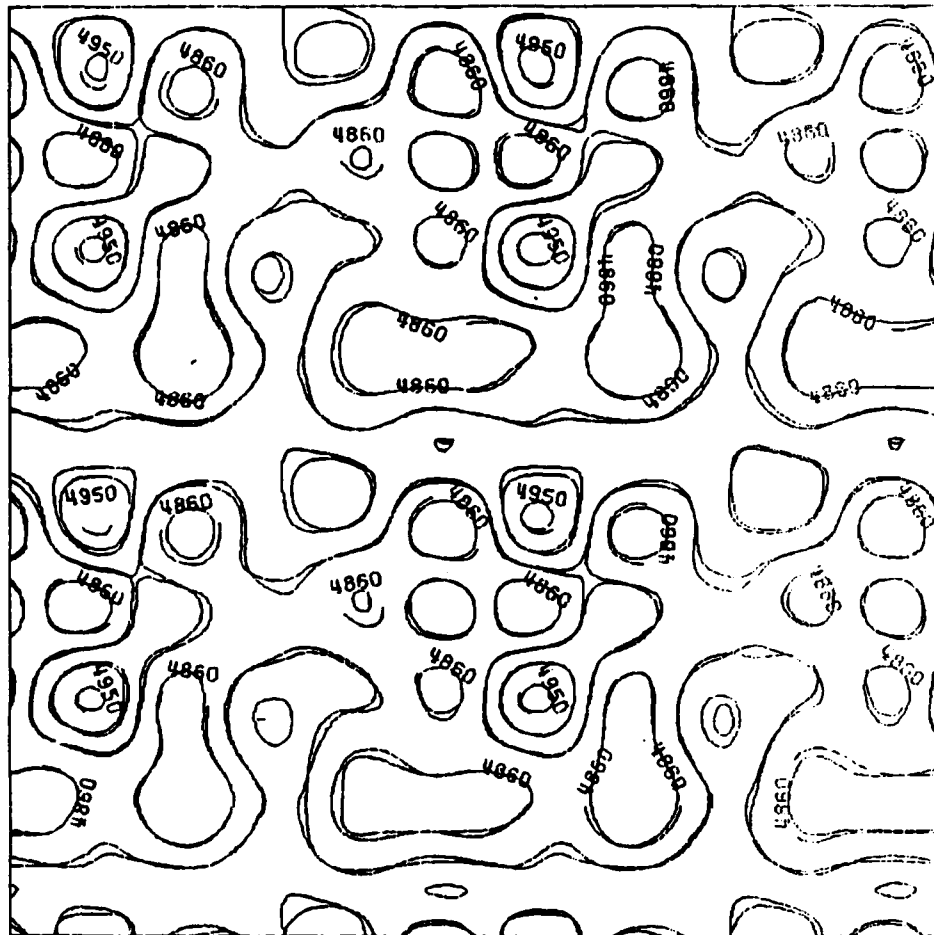


Figure 47

Surface 4 - Original Contour and via CISS

Scale 1:20,000 C.I. = 80 ft.

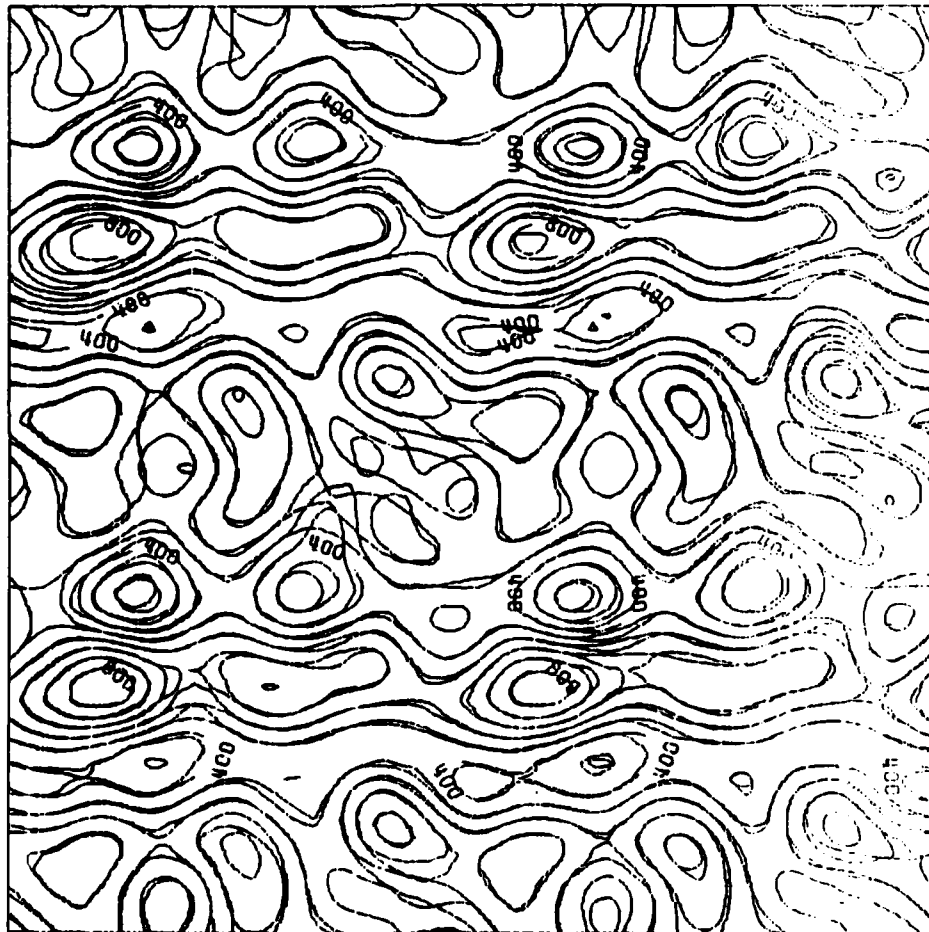


Figure 48

Surface 4 - Original Contour and via LISS
Scale 1:20,000 C.I. = 80 ft.

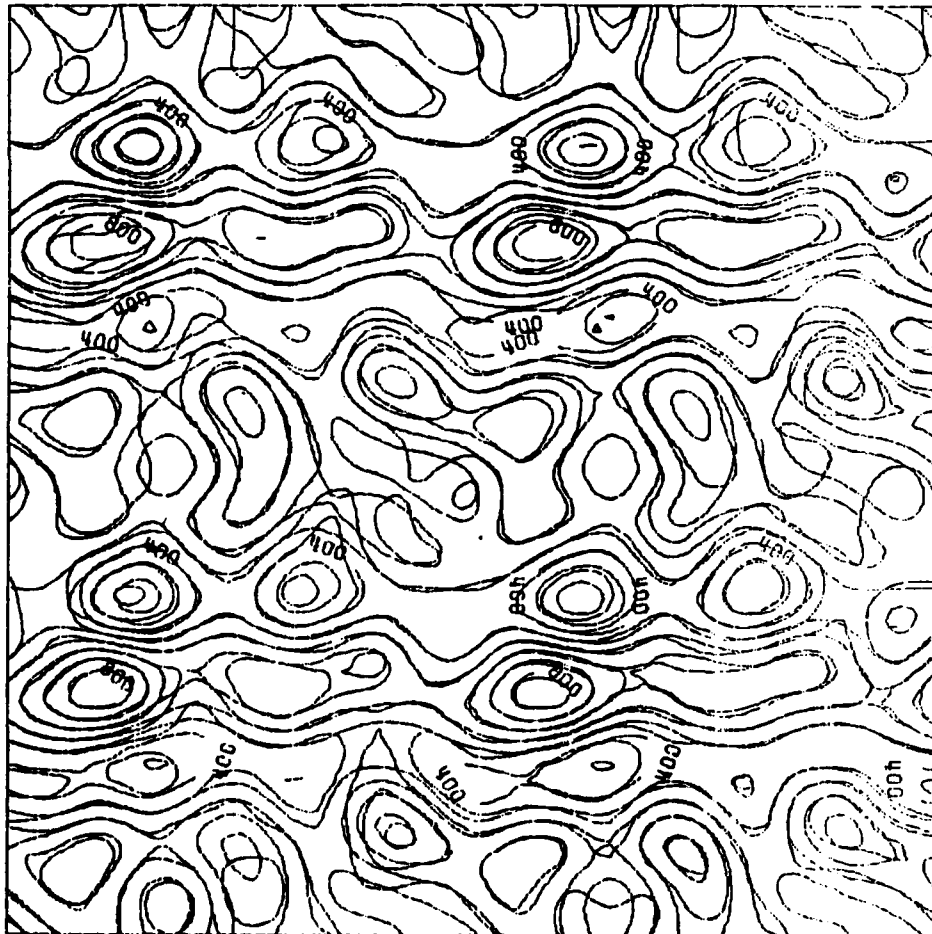


Figure 49

Surface 4 - Original Contour and via LIXY

Scale 1:20,000 C.I. = 80 ft.

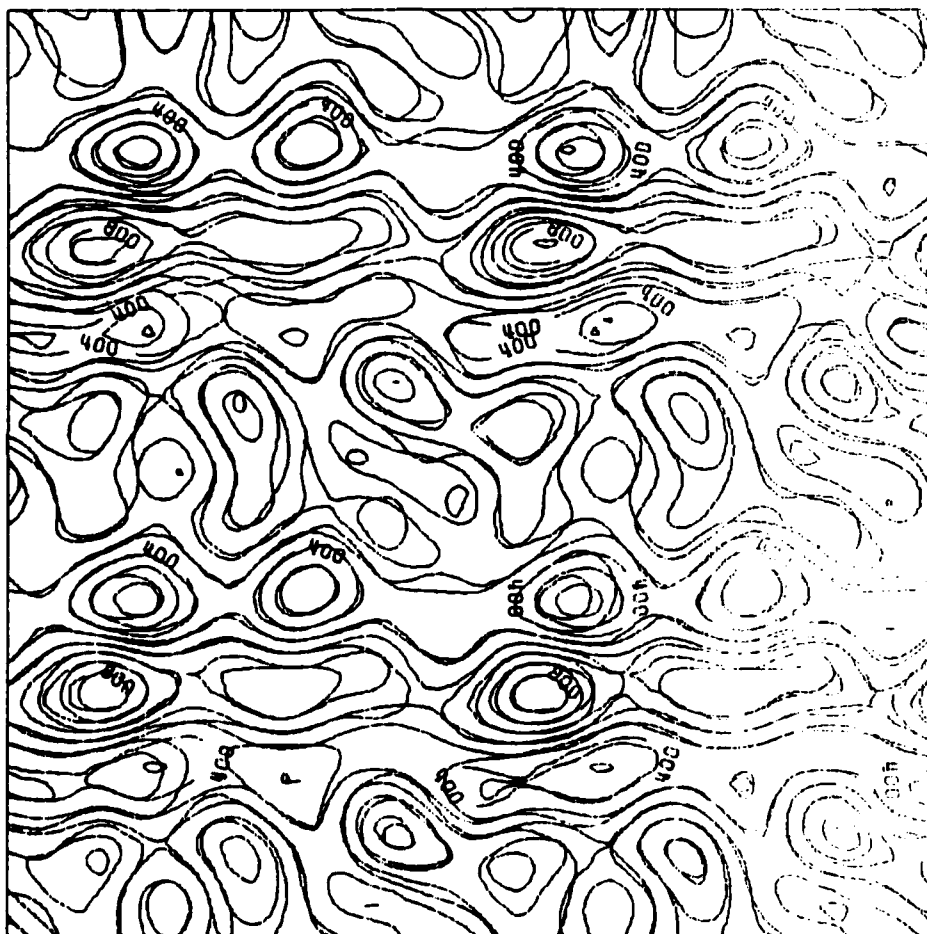


Figure 50

Surface 5 - Original Contour and via CISS
Scale 1:20,000 C.I. = 11 ft.

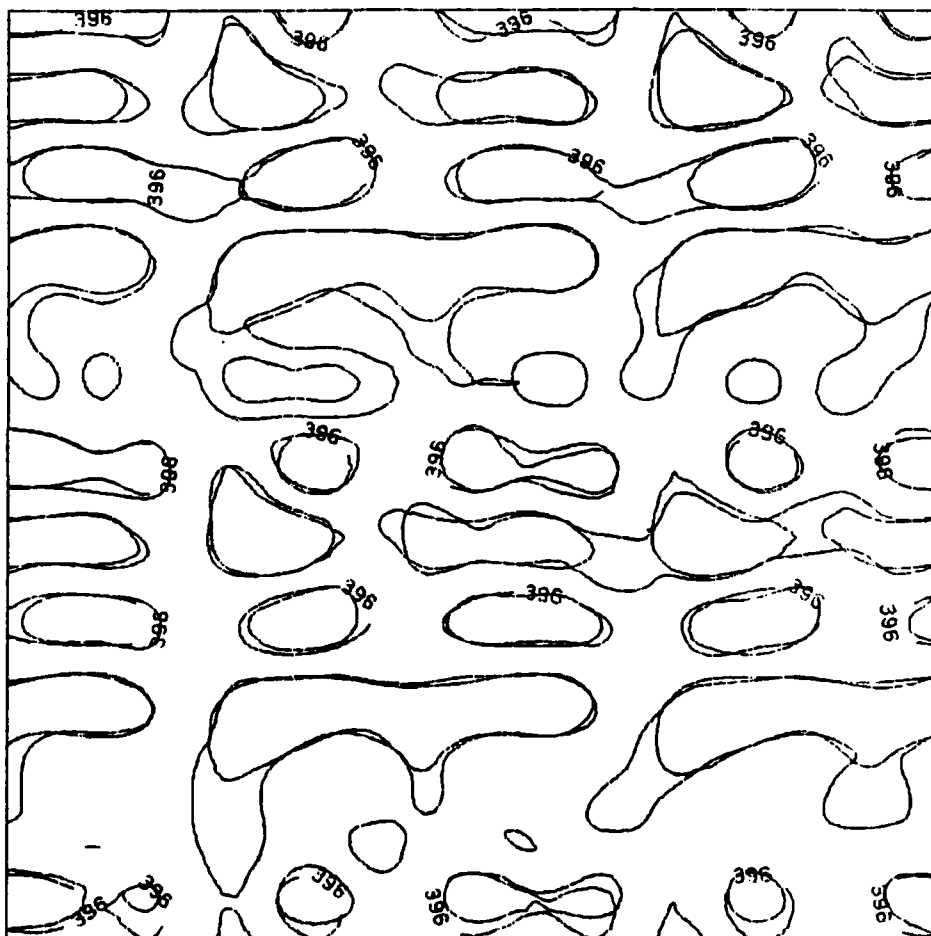


Figure 51

Surface 5 - Original Contour and via LISS
Scale 1:20,000 C.I. = 11 ft.

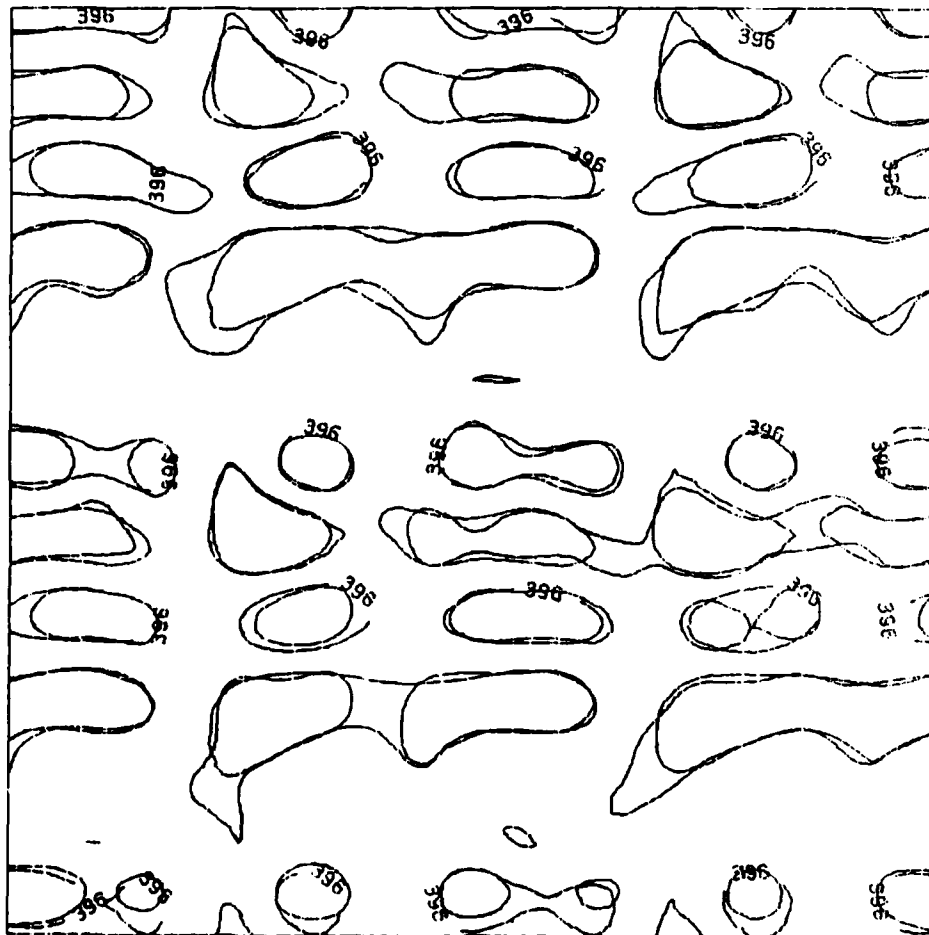


Figure 52

Surface 5 - Original Contour and via LIXY
Scale 1:20,000 C.I. = 11 ft.

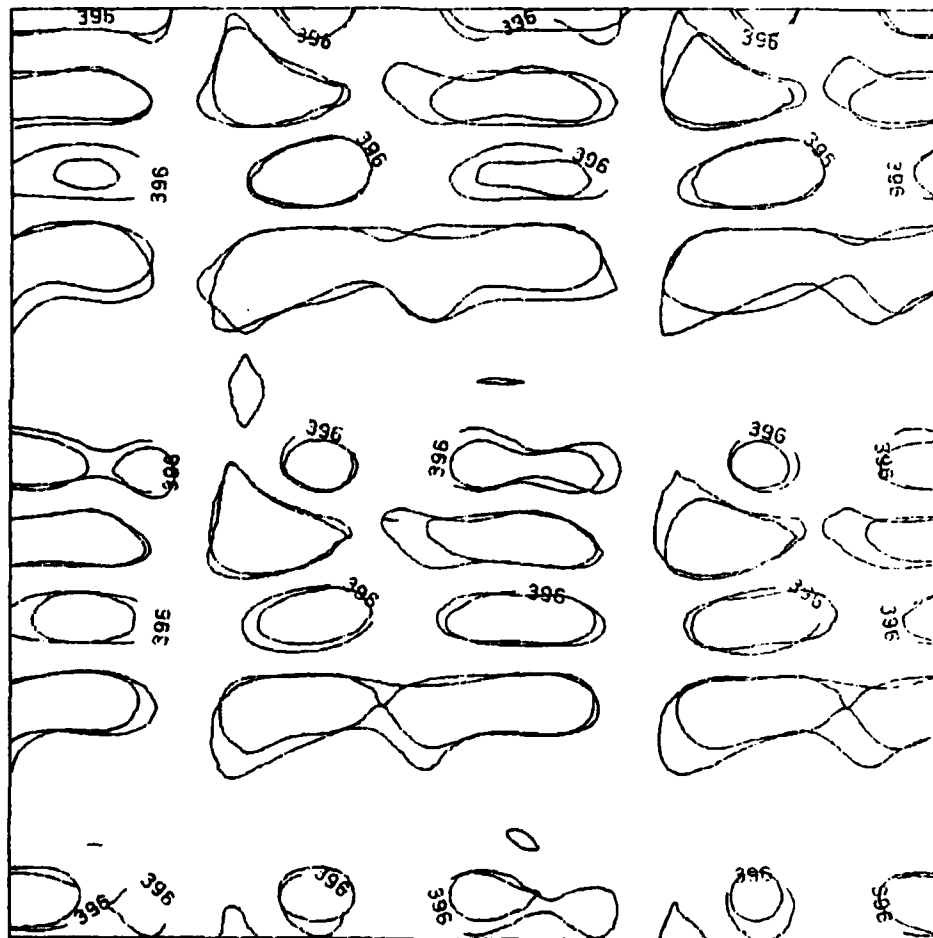


Figure 53

Surface 6 - Original Contour and via CISS
Scale 1:20,000 C.I. = 20 ft.



Figure 54

Surface 6 - Original Contour and via LISS
Scale 1:20,000 C.I. = 20 ft.

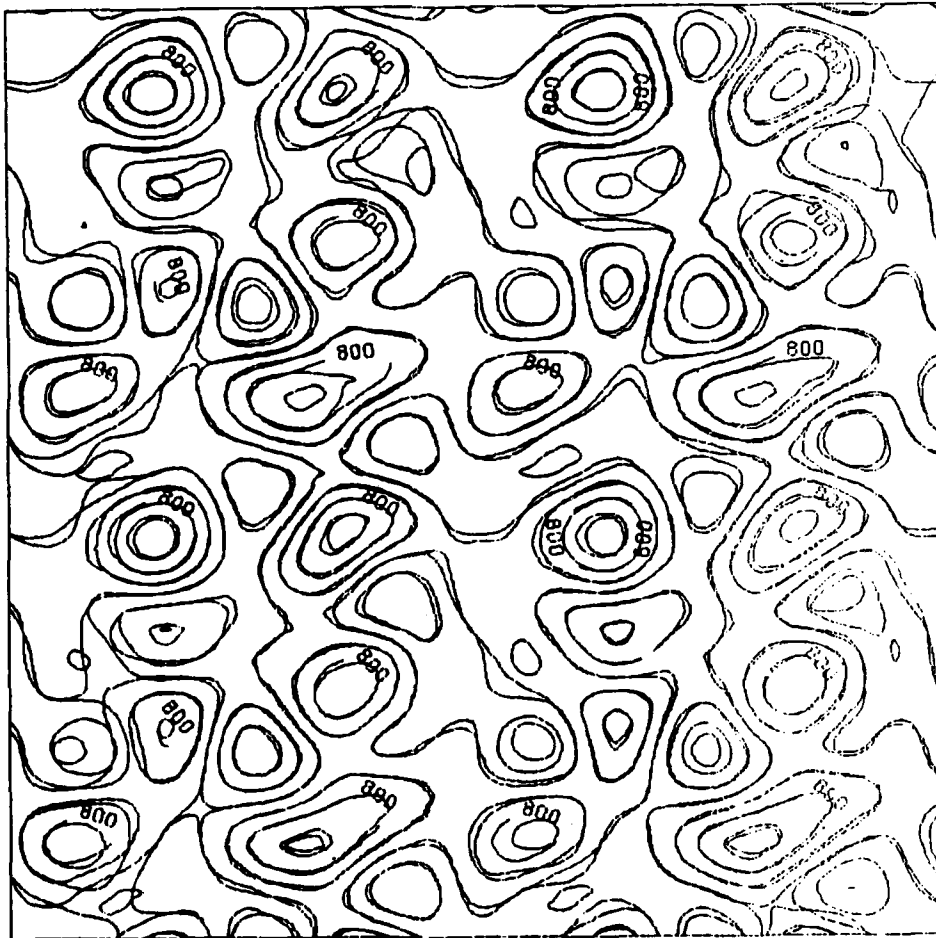
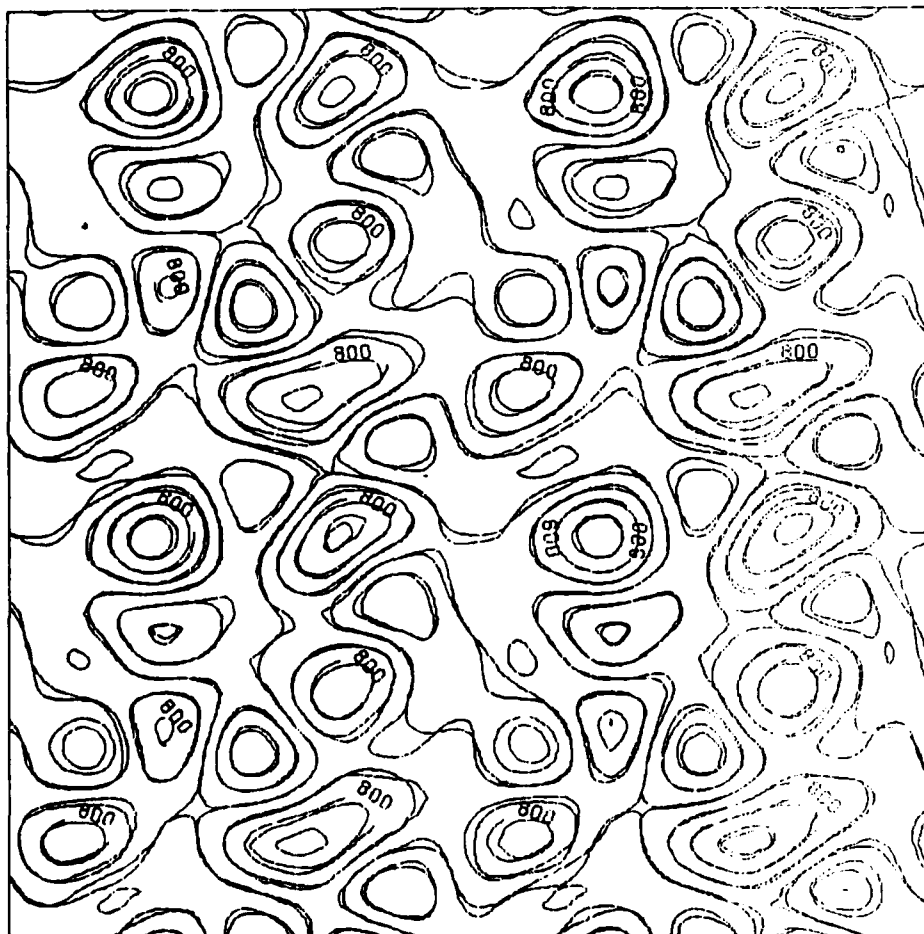


Figure 55

Surface 6 - Original Contour and via LIXY

Scale 1:20,000 C.I. = 20 ft.



7. Conclusions

7.1 Method for Evaluation

Our investigation as to methods for evaluation have shown that:

- A. Any particular algorithm performs differently in different types of interpolation regions.
- B. In the evaluation of an algorithm, one needs to look at more than one criterion. Each criterion gives us a different insight into the performance of an algorithm. That is, if a particular algorithm performs well for a certain interpolation region, it may not perform well for another type of interpolation region. Our investigations indicate that the important factor is the type of terrain where the interpolation takes place and not necessarily the method of interpolation.

At this stage, our proposals for a method of evaluating techniques (algorithms) for contour-to-grid interpolation would be as follows:

1. Select a set of synthetic surfaces representing different types of interpolation regions.
2. From the equations of these surfaces, generate "digitized" contours at suitable intervals. "Suitable intervals" would be contour intervals which are likely to be found on the base maps to be digitized.
3. Apply the technique (algorithm) to be tested to the "digitized" contours and obtain predicted grid elevations. The grid size chosen will be a function of the base map scale, the contour interval, and the user's requirements.
4. Generate, from the synthetic surface equation, true elevations at the grid intersections of the grid used in 3 above.
5. Using the results of 3 and 4 above, generate the following statistics and maps:
 - a. average error;
 - b. standard deviation of an error;
 - c. maximum absolute error;
 - d. a residual map;
 - e. a map (preferably in two colors) showing the true and the predicted contours. The true contours are those obtained from the elevations in 4 above using a contouring package and the predicted contours are those obtained from 3 above using the same contouring package. (The true contours should be the same as the contours in 2 above. Choose a contouring package that gives this condition. Time did not allow us to check GSPP - of more importance to us was the evaluation method).

To the above statistics, one may have to add others when using large data sets. For example:

- f. computer storage space required.
- g. time taken to perform interpolation.

The above statistics and maps must now be examined and a decision made on the performance of the interpolation technique (algorithm). One would be looking for evidence of systematic error, for large error, for blunders, for horizontal (mapped) error, etc. as described in Section 6 above. The final decision will depend on how one lists the following requirements in order of priority:

- accuracy
- speed of technique
- throughput speed (that is, including preparation time and time to achieve production of required output)
- storage space requirements

7.2 Future Work

- A. Our investigations described in the previous sections have shown that we do not have an essential tool for the evaluation of contour-to-grid algorithms. This tool is a set of representative synthetic surfaces - that is, a suite of synthetic surfaces which represent the types of interpolation regions one would encounter in practice. These synthetic surfaces should be capable of being defined, in such a manner, that any other sampled surface can be shown to be similar to one of the suites of surfaces mentioned above. Interpolation algorithms should be tested on the suite of representative synthetic surfaces (as described in 7 above). In this way, one could predict the behaviour of an interpolation algorithm on a particular sampled surface. We used a Fourier series for setting up our (admittedly not entirely satisfactory) synthetic surfaces. We indicated that there are other ways of generating synthetic surfaces. Before one can say that the Fourier Series method is not suitable, much more investigation is needed. With our time limitations, the Fourier series was used because it was available and it also supplied us with other information, like the power spectra. A high priority for future work should be the generation of suitable synthetic surfaces.
- B. In order to evaluate an interpolation technique, one also needs to compare the technique with other "standardized" techniques. Some of these standardized techniques could be the ones used in this study. For example, an interpolation technique being evaluated may give accurate results for a particular terrain type but a standardized technique, like linear interpolation, may give results within the accuracy requirements.
- C. This study has not considered large data sets, time and amount of storage space required. These factors should be considered in future work. Considering large data sets will bring up the question of breaklines and areas of homogeneity. That is, even though large data sets have to be

processed, the interpolation takes place only between breaklines in homogeneous areas.

- D. This study has only considered aspects of contour-to-grid interpolation. But one must eventually consider also grid-to-contour and grid-to-grid interpolation. The concepts used in this study may be found to be applicable in these cases.
- E. An investigation which is related to the above considerations, is the question of the density of the data collection. That is, if one wants to achieve a certain accuracy (of interpolated point values or of plotted contours) using a particular technique, at what intervals should the data be collected? Or, if the data is very dense, does one have to use all the data? The results of this study, indicate that one may be able to determine that, for a particular accuracy, only some of the data (for example, every fourth contour line) needs to be used.

APPENDIX A

BIBLIOGRAPHY OF SELECTED REFERENCES

Not all the following references have been cited. They provide a background to the research described in this report.

Bath, Markus (1974)

"Spectral analysis in Geophysics", Elsevier Sci. Publ. Co., Amsterdam 1974.

It is an extensive presentation of the mathematical background of the Fourier analysis, together with many applications in the geosciences. A discussion of topics like:

- power spectra/their computation
 - reliability and presentation of spectra
 - windows and filters etc.
- is also presented.

This book includes an extensive bibliography of applications of spectral analysis.

Boyle, A.R. (1980)

"Scan digitization of cartographic data", in H. Freeman and G. Pieroni, "Map Data Processing", Academic Press, 1980.

Deals with a method of scan digitization of existing maps in the light of recent advantages in software for line thinning and vectorization.

Clarke, A.L. (1982)

"Interpolation of grid digital elevation models from digitized contours", The Ohio State University, Department of Geodetic Science, M.Sc. thesis, August 1982.

The objectives of this study were to determine the best interpolation algorithm for generating high fidelity DEM's, and to determine the effect on DEM fidelity of the inclusion of supplementary non-contour data. A new contour - specific algorithm (using cubic spline interpolation in the direction of the steepest slope) is derived from an optimum fidelity conceptual model.

Clarke, A.L., Gruen, A. and Loon, J.C. (1982)

"The application of contour data for generating high fidelity grid digital elevation models", Auto-Carto 5 Proceedings, August 1982, pp. 213-222.

The special characteristics of contours as a DEM data source, and some published contour-specific interpolation algorithms, are reviewed in this paper. Test results of these algorithms are presented, employing both synthetic and real surface data.

Clerici, E. and Kubik, K. (1974)

"The theoretical accuracy of point interpolation on topographic surfaces", Intr. Soc. of Photogrammetry, Commission III, Munchen 1974, Proceedings of the symposium, pp. 179-187.

This report documents an investigation into the theoretical accuracy of point interpolation and volume computation for topographic surfaces. For this purpose the type and roughness of the terrain are described by a covariance function of exponential type. Based on this model, the accuracy of interpolated points and of volumes is derived by the application of the law of propagation of errors.

Crochiere, R.E. and Rabiner, L.R. (1981)

"Interpolation and Decimation of Digital Signals - A tutorial review", Proceedings of the IEEE, Vol. 69, No. 3, March 1981, pp. 300-331. ;

A tutorial overview of multirate digital signal processing as applied to systems for decimation and interpolation. Design techniques for the linear-time-invariant components of these systems (the digital filter) are discussed.

Cruz, Jaime (1983)

"Experiences with altimeter data gridding", The Ohio State University, Department of Geodetic Science and Surveying, Report #347, June 1983.

The effect of grid spacing, number of configuration of data points is used to predict a grid value, and prediction method used is illustrated. The prediction methods tested include least squares collocation, Bjerhammar's inverse distance weighting method, Hardy's multiquadratic method using a hyperboloid kernel, a general harmonic kernel method using Krarup's kernel, and a piecewise biquadratic surface fitting method.

Dahlquist, G. and Bjorck, A. (1974)

(translated by Ned Anderson), "Numerical methods", Prentice-Hall, Inc., New Jersey 1974.

Basic numerical methods include the following: basic concepts in approximation; approximation of functions by Least Squares; use of polynomials; use of orthogonal polynomials; use of spline functions.

Davis, D.M., Downing, J.A. and Zoraster, S. (1982)

"Algorithms for digital terrain data modeling". U.S. Army Engineer Topographic Laboratories Report number ETC-0302, July 1982.

Author's abstract: "Algorithms and test results are described for three different general operations used in computerized modeling and mapping. The algorithms are used for transforming strings of contour data into digital elevation models (DEM), transforming DEM's into a set of contour strings for

display, and smoothing DEM's using several filtering and convolution techniques. The use of DEM smoothing operations for the simplification of contour lines is examined and two methods of controlling filter effects for this applications are presented. As a separate research effort two interpolation algorithms which can be used for resampling DEM's are compared. Visual and statistical measures of performance are presented."

Davis, John C. (1973)

"Statistics and data analysis in Geology", J. Wiley & Sons, Inc., New York 1973.

In addition to basic statistics, matrix algebra there is a description of interpolation, Least squares regression analysis, autocorrelation and cross-correlation analysis, double Fourier series, moving averages and Kriging, and statistical tests of Geological data. An extensive list of FORTRAN programs is also given.

Davis, Phillip J. (1975)

"Interpolation and approximation", Dover Publ. Inc., New York 1975.

A description of the theories of interpolation and approximation, Hilbert spaces, orthogonal functions, orthogonal polynomials, measures of degree of approximation are presented in extent.

DMA (1979)

Defense Mapping Agency, Product Specifications for digitized elevation data for Firefinder. Hydrographic/Topographic Center, Washington D.C., First Edition, April 1979.

Ebner, H. (1980)

"HiFi - a minicomputer program package for height interpolation by finite elements", 14th Congress of ISP, Hamburg 1980, pp. 202-215.

A general minicomputer program package for height interpolation is presented. It is written in FORTRAN and interpolates a digital height model from arbitrarily disturbed reference points and breaklines, using the Finite Element method.

Ebner, H. and Reiss, P. (1981)

"Experiences with height interpolation by finite elements", ASP-ACSM Fall Technical Meeting, 1981.

After a brief description of the HiFi package the paper gives a review of the experiences gained with height interpolation by finite elements. Reference is made to the accuracy of DEM interpolation and to the operational use of HiFi.

Engelis, Theo (1983)

"Analysis of sea surface topography using Seasat altimeter data", The Ohio State University, Department of Geodetic Science and Surveying, Report #343, March 1983.

A summary of Fourier transform and low pass digital filters in two dimensions is given. A geoid corresponding to sea surface heights (derived from adjusted Seasat altimeter data) is computed up to a minimum wavelength of 2000 km, using the GEM1 gravity model. A comparison of filtering the spherical harmonics and use of digital filters is given.

Eren, Kamil (1980)

"Spectral analysis of GEOS-3 altimeter data and frequency domain collocation", The Ohio State University, Department of Geodetic Science and Surveying, Report #297, February 1980.

The mathematical background in spectral analysis is applied to geodetic applications is summarized. Frequency domain least-squares collocation techniques are also introduced and applied to estimating gravity anomalies from GEOS-3 altimeter data. Power of each frequency for discrete and non-periodic data is computed.

Fernando, K.V. and Nicholson, H. (1982)

"Two-dimensional curve fitting and prediction using spectral analysis", IEEE Proceedings, vol. 129, Part D., No. 5, September 1982, pp. 145-150.

A curve-fitting or prediction problem for two-dimensional or cyclic processes is defined and solved using spectral analysis. The assumed statistical model is structurally similar to the Karhunen-Loere expansion, and the technique can be implemented using the singular-value decomposition.

Franke, Richard (1979)

"A critical comparison of some methods for interpolation of scattered data." Report number NPS-53-79-003, Naval Postgraduate School, Monterey, California, 1979.

A comparison of 29 methods for the solution of the scattered data interpolation problem. The test surfaces used were very smooth - when compared with topographic terrain encountered in practice. The given (reference) points were randomly scattered.

Frederiksen, P. (1980)

"Terrain analysis and accuracy prediction by means of the Fourier transformation", 14th Congress of ISP, Hamburg 1980, Com. IV, pp. 284-293.

In this study, profiles are measured in different geological terrain types, and their power spectra are used for a statistical description of the different landscapes. By means of the spectrum, the standard deviation between the

terrain surface and a digital terrain model is estimated.

Frederiksen, P., Jacobi, O. and Kubik, K. (1984)

"Modelling and Classifying Terrain", invited paper, Commission III, XVth Congress of the International Society for Photogrammetry and Remote Sensing, Rio de Janeiro, 1984.

Author's abstract: "Different methods for terrain description and classification are presented. Descriptive classifications are known from geology. These descriptions have also been formalized using the concept of stochastic processes. Other classification methods are based on Fourier-transformation, classifying the terrain types according to their frequencies of undulation. Recent approaches are based on the concept of self similarity, observing the presence of lack of similarity of micro- and macro-structures in the terrain. A comparison of these classification models is given and the applicability of these models for interpolation and other deductions is discussed."

Hamilton, Walter C. (1964)

"Statistics in physical science", The Ronald Press Co., New York 1964.

A book on estimation theory, hypothesis testing and least squares methods as applied to data of physical sciences.

Hannah, M.J. (1981)

"Error detection and correction in Digital Terrain Models", Photogram. Eng. & Remote Sensing, Vol. 47, No. 1, pp. 63-69, 1981.

In this paper algorithms have been developed to detect and correct errors in digital terrain models. These algorithms focus on the use of constraints on both the allowable slope and the allowable change in slope in local areas around each point. Relaxation-like techniques are employed in the iteration of the detection and correction phases to obtain best results.

Hardy, R.L. (1977)

"Least squares prediction", Photogr. Eng. & Remote Sensing, Vol. 3, No. 4, April 1977, pp. 475-492.

The basic principles of least squares prediction using both multiquadratic functions and covariance functions are covered. Multiquadratic kernels are based on geometric and physical considerations, rather than stochastic processes as in the case of covariance kernels.

Jacobi, O. (1980)

"Digital Terrain model, point density, accuracy of measurements, type of terrain, and surveying expenses", 14th Congress of ISP, Hamburg 1980, Com. IV, pp. 361-366.

An attempt to calculate the connection between the accuracy of the digital terrain model, the terrain, and the surveying strategy, by means of a stochastic model of the terrain and an economic model of the surveying expense.

Jacobi, Ole and Kubic, Kurt (1982)

"New concepts for digital terrain models", Intern. Society of Photogrammetry Commission III, Proceedings of the symposium, Helsinki 1982, pp. 247-265.

A conceptual model for the topographic surface is presented. A generalization of the above model including fractional noise is attempted, together with a small discussion on the concept of fractional noise.

Jancaitis, J.R. and Junkins, J.L. (1983)

"Modelling irregular surfaces", Photogrammetric Engineering, Vol. 39, No. 4, April 1973.

A two-independent variable interpolation has been developed for modelling irregular functions of two variables. This method represents the surface as a family of locally valid mathematical functions which join together continuously.

Kay, S.M. and Marple, S.L. (1981)

"Spectrum Analysis - A modern perspective", Proceedings of the IEEE, Vol. 69, No. 11, November 1981, pp. 1380-1419.

A summary of many of the new techniques developed in the last two decades for spectrum analysis of discrete time series is presented in this tutorial. Techniques discussed include the classical periodogram, classical Blackman-Tukey, autoregressive (maximum entropy), moving average, maximum likelihood, Prony, and Pisarenko methods.

Kearsley, W. (1977)

"The prediction and mapping of geoid undulations from GEOS-3 altimetry", The Ohio State University, Department of Geodetic Science, Report #267, December 1977.

Geoid heights are obtained for grid points in the region to be mapped, and two of the parameters critical to the production of an accurate map are investigated. These are:

- (i) The spacing of the grid, which must be related to the half-wavelength of the altimeter signal whose amplitude is the desired accuracy of the contour, and
- (ii) the method adopted to predict the grid values.

Katsambalos, Kostas (1980)

"Comparison of some undulation prediction techniques from altimeter data", The Ohio State University, Department of Geodetic Science and Surveying, Report #303, July 1980.

Adjusted GEOS-3 altimeter data are used to predict and compare geoid undulations derived from two collocation models, the Bjerhammar estimator, and Hardy's multiquadratic formula.

Kratky, V. (1977)

"Grid-structured reflexive prediction and digital terrain modelling", Amer. Soc. of Phot., Fall Convention, Little Rock 1977, pp. 447-454.

If the prediction process is based on a covariance function separable in coordinates, conditions are set for an effective use of Rauhala's array algebra. Its advantages are demonstrated for the "reflexive" type of prediction implemented with or without least squares filtering.

Kratky, V. (1978)

"DTM interpolation with gliding vectors", Symposium of Digital Terrain Models, St. Louis, May 1978.

Expanding the size of the data grid, the central part of the matrix which is inverted in the process, eventually becomes stabilized at certain numerical values, regardless of any further size increase. One can derive a table of band limited vectors to serve as interpolation or smoothing operators.

Kratky, V. (1980)

"Spectral analysis of interpolation", 14th Congress of the International Society of Photogrammetry, Commission, III Hamburg 1980, pp. 389-397.

Basic concepts of spectral analysis are applied to interpret interpolation, smoothing and parametric transformation based on uniform sampling as different types of discrete convolution. Spectral properties of interpolation are then discussed with the main emphasis on its linear least squares version.

Lanczos, Cornelius (1966)

"Discourse on Fourier series", Oliver and Boyd Co., Edinburgh 1966.

A presentation of the development of the Fourier series as well as the application in approximation problems.

Leberl, F, Kropatsch, W. and Lipp, V. (1980)

"Interpolation of raster heights from digitized contour lines", XIV Congress of the International Society of Photogrammetry, Commission III, Hamburg 1980, International Archives of Photogrammetry Part B3, pp. 458-468.

An algorithm for converting contour information to digital Elevation Models is given here. Examples show that overall interpolation results compare well with manual interpolation.

Loon, J.C. (1982)

"An introduction to Digital Surface Models", unpublished manuscript, Department of Geodetic Science and Surveying, The Ohio State University, Columbus, Ohio, 1982.

An introduction to DEMs including:

- Data acquisition
- Terrain types
- Point distribution and density
- Interpolation procedures
- Overview of existing Digital Terrain Models
- Applications of Digital Surface Models

Moritz, H. (1978)

"Introduction to interpolation and approximation", in H. Moritz and H. Sunkel eds., "Approximation methods in Geodesy", H. Wichmann Verlag, Karlsruhe, 1978.

The following topics are treated:

- Polynomial interpolation (formulas of Newton and Lagrange)
- Least Squares approximation
- Polynomial approximation (Weierstrass and Chebyshev theorems)
- Finite elements
- Spline functions
- Least squares interpolation and collocation

Morrison, J.L. (1971)

"Method-produced error in Isarithmic Mapping", ACSM Technical Monograph, No. CA-5.

This paper deals with errors introduced by isarithm algorithms. In order to evaluate them the author constructs four synthetic surfaces formulated by logarithmic functions, trigonometric series or equations for a parabola. Since these surfaces are mathematically defined, an absolute error measure can be defined.

Rhind, D. (1975)

"A skeletal overview of spatial interpolation techniques", Computer Applications, Vol. 2, No. 384, pp. 293-309, 1975.

A critical review of the literature concerning interpolation methods.

Roberts, P.A. (1980)

"Computer based technique for converting a contour map into an equispaced grid of points", U.S. Dept. of Commerce, National Technical Information Service, September 1980.

This report describes a technique for converting a contour map into an equispaced grid of points. Included are discussions of the problems associated

with the digitization of a contour map and those of interpolation in general. Listings of all programs, which are written in computer independent ANSI FORTRAN V, are given.

Schultz, H.E. (1973)

"Spline analysis", Prentice-Hall, Inc., Englewood Cliffs, N.J., 1973.

This paper is an abbreviated version of lectures on the principle and methods of approximating functions of one and two variables.

Shut, G.H. (1974)

"Evaluation of some interpolation methods", Proceedings of the symposium of the International Society for Photogrammetry, Commission III, Munchen 1974, pp. 160-170.

Different interpolation methods are discussed. For example,

- Kraus's linear least squares interpolation.
- Arthur's interpolation of a function of many variables.
- Hardy's interpolation with multiquadratic equations
- Pointwise interpolation
- and so on.

Interpolation methods are divided into six groups.

Shut, G.H. (1976)

"Review of interpolation methods for Digital Terrain Models", the Canadian Surveyor, Vol. 30, No. 5, December 1976, pp. 389-411.

A review of the methods of height interpolation for digital terrain models that have been published in photogrammetric and related journals. These methods are classified into six groups, according to the type of surface representation that they produce, and a short comparative evaluation is made. In addition, the construction of profiles and of contour lines is reviewed.

Sunkel, H. (1980)

"A general surface representation module designed for Geodesy", Report No. 292, Department of Geodetic Science and Surveying, The Ohio State University, Columbus, Ohio, 1980.

The theoretical background and the manual for the GSPP package designed for interpolation, least squares collocation, generation of profiles and contours from irregular or equally spaced reference points.

Tempfli, K., and Macarovic, B. (1978)

"Transfer function of interpolation methods", the ITC Journal 1978-1, pp. 50-79.

The objective of this investigation is to judge the performance of interpolation methods in general. No assumptions are made with regard to the type of terrain relief, but sampling is assumed to be homogeneous. For this purpose a special analytical approach is formulated and applied for the computation of Transfer Functions.

Tempfli, K. (1980)

"Spectral analysis of terrain relief for the accuracy estimation of digital terrain models", ITC journal special issue, (ITC papers presented at the XIVth ISP Congress, Hamburg), 1980-3, pp. 478-510.

Deals with estimation of errors introduced in profiles, due to sampling interval, interpolation method, aliasing effect etc. The theoretical background of spectral analysis used, is also given. Included is an application with graphs in logarithmic scale.

Werner, H. (1980)

"Numerical algorithms for interpolation and smoothing", in H. Freeman and G. Pieroni, "Map Data Processing", Academic Press, 1980.

Wild, E. (1980)

"Interpolation with weight-functions. A general interpolation method", XIV Congress of the International Society for Photogrammetry, Hamburg 1980, International Archives of Photogrammetry, part B3, pp. 780-793.

A discussion on the use of weight functions in interpolation. It includes:

- the deduction of weight functions of known interpolation methods.
- the characteristics of weight functions and their effects on interpolation surfaces.
- weight functions as a linear combination of base functions.
- consideration of additional information, i.e. curvature lines, lines of steepest slope, highs, lows, etc.

APPENDIX B

DESCRIPTION OF SELECTED PROGRAMS USED IN THIS STUDY

AD-A164 305

DIGITAL TERRAIN ELEVATION MODEL ANALYSIS(US OHIO STATE
UNIV RESEARCH FOUNDATION COLUMBUS J C LOOM ET AL.
JUL 83 OSURF-716042 ETL-0393 DAAG29-81-D-0100

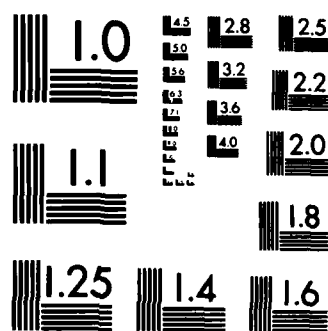
272

UNCLASSIFIED

F/G 8/6

NL





MICROCOPY RESOLUTION TEST CHART
NBS 1963-A

C I S S ANDREW L. CLARKE
CUBIC INTERPOLATION / STEEPEST SLOPE /
/ BREAKLINE DATA MAY BE INCLUDED / SPRING 1982

THIS PROGRAM USES A RASTER IMAGE OF CONTOUR LINES
TO INTERPOLATE A REGULAR DEM. THE ALGORITHM IS:

**"HEIGHT AT A POINT IS FOUND BY CUBIC POLYNOMIAL
INTERPOLATION WITHIN FOUR KNOWN POINTS ON THE LINE
OF STEEPEST SLOPE PASSING THROUGH THE UNKNOWN POINT"**

STEEPEST SLOPE:

FOUR DIRECTIONS. ARE TESTED FOR STEEPEST SLOPE :-

1. WEST-EAST, 2. NW-SE, 3. NORTH-SOUTH, 4. NE-SW. THE SLOPE IS COMPUTED FROM THE FIRST CONTOUR FOUND AT EACH END OF THE DIRECTION LINE. IF THE STEEPEST SLOPE VALUE OCCURS IN MORE THAN ONE DIRECTION LINE, THE DIRECTION HAVING THE SHORTEST DISTANCE BETWEEN CONTOURS IS USED.

INTERPOLATION:

AFTER FINDING THE DIRECTION OF STEEPEST SLOPE, THE LINE IS EXTENDED TO THE NEXT CONTOUR AT EACH END.

THE UNKNOWN HEIGHT IS THEN FOUND BY FITTING A CUBIC POLYNOMIAL TO THE 4 POINTS, WITH THE INTERPOLATION

POINT IN THE CENTRAL SEGMENT: C1--C2--INT--C3--C4.

IN CASES WHERE EITHER C1 OR C4 CANNOT BE FOUND, AS

AT BREAK LINES OR THE MAP EDGE, ONE OF TWO INTERPOLATION METHODS MAY BE USED (3 POINT CASES):

1. FIND C0 OR C3 AND INTERPOLATE BY CUBIC SPLINE.

2. FIND C0 OR C5, THEN CREATE AN EXTRA POINT AT EACH END BY LINEAR EXTRAPOLATION. INTERPOLATE BY CUBIC SPLINE, AS IN TYPE 1.

EDGE POINTS:

INTERPOLATION AT THE EDGE POINTS IS BY CUBIC POLYNOMIAL OR SPLINE, AS ABOVE, BUT IS LIMITED TO THE DIRECTION OF THE EDGE.

MASTER DATA:

THE RASTER IMAGE IS STORED ON DISK (UNIT #1), WITH EACH COLUMN AN UNFORMATTED LOGICAL RECORD. EACH CORNER HAS A HEIGHT VALUE, AND THERE ARE NO GAPS IN THE CONTOURS IN THE FOUR TEST DIRECTIONS. IF SPOT HEIGHT DATA ARE INCLUDED, THE PIXELS ALONG THE LINE OF STEEPEST SLOPE THROUGH THE SPOT SHOULD CONTAIN INTERPOLATED HEIGHTS.

BREAK LINE DATA:

IF BREAK LINES ARE INCLUDED, THEY SHOULD BE FLAGGED BY HAVING THE CONSTANT "BFLAG" ADDED TO THE HEIGHT VALUE AT EACH BREAK LINE PIXEL. DATA POINTS ON THE OPPOSITE SIDE OF A BREAKLINE TO A DEM POINT WILL NOT BE USED DURING INTERPOLATION AT THAT DEM POINT.

OUTPUT DEM:

THE INTERPOLATED DEM IS STORED ON DISK UNIT 2, WITH EACH COLUMN AN UNFORMATTED LOGICAL RECORD.

```

INPUT VARIABLES:
THE FOLLOWING VARIABLES MUST BE SET BY THE USER IN
THE MAIN PROGRAM. DIMENSION VARIABLES MUST AGREE
WITH THE ACTUAL DIMENSIONS IN THE MAIN PROGRAM.
M,N      = DIMENSIONS OF THE INPUT RASTER
CI       = CONTOUR INTERVAL OF THE INPUT DATA
RES      = MAP RESOLUTION OF THE RASTER DATA (MM)
BASE     = CONTOUR VALUE CORRESPONDING TO MENU NAV=1
RCD      = GROUND RESOLUTION OF THE RASTER (UNITS=CI)
IBREAK   = FLAG FOR BREAKLINE DATA: 0 = NO, 1 = YES
BFLAG    = CONSTANT ADDED TO BREAK LINE HEIGHTS
K,L      = DIMENSIONS OF THE OUTPUT DEM
ISM      = INTERPOLATION MODEL FOR 3 POINT CASE
TITLE    = 60 CHARACTER TITLE READ FROM UNIT 5

SUBROUTINES:
EDGE     - CONTROL ROUTINE FOR EDGE INTERPOLATION
INSIDE   - CONTROL ROUTINE FOR INSIDE INTERPOLATION
DATA     - FINDS INTERPOLATION CASE AND DATA POINTS
POLY     - INTERPOLATES WITH CUBIC POLYNOMIAL
SPLINE   - INTERPOLATES WITH NATURAL CUBIC SPLINE
LINEAR   - PERFORMS LINEAR INTERPOLATION
TEST     - COMPARES INTERPOLATED HEIGHT WITH CONTOURS
PRINT    - PRODUCE A LINE PRINTER MAP OF THE RASTER
READ     - READ A RASTER OR DEM COLUMN FROM DISK
WRITE    - WRITE A RASTER OR DEM COLUMN TO DISK

NOTES :
-----
1. THE VALUE IGRID=(M-1)/(K-1) SHOULD BE AN INTEGER
   NUMBER. THIS IS A RESTRICTION TO THE DIMENSIONS
   OF THE PRODUCED DEM, GIVEN THE DIMENSION OF THE
   RASTER.
2. THE CORNERS OF THE INPUT RASTER SHOULD HAVE AT
   LEAST APPROXIMATE VALUES (IE. OTHER THAN ZERO).
   TO MODIFY THEREFORE THE RASTER VALUES AT THE
   CORNERS YOU SHOULD EITHER INPUT THESE VALUES IN
   THE PROGRAM BEFORE THEY WILL BE USED, OR BETTER
   YOU CAN USE THE PROGRAM "RASEDIT" FOR THIS PURPOSE.
=====

```

L I S S ANDREW L. CLARKE
LINEAR INTERPOLATION / STEEPEST SLOPE WINTER 1982

THIS PROGRAM USES A RASTER IMAGE OF CONTOUR LINES TO INTERPOLATE A REGULAR DEM. THE ALGORITHM USED IS: HEIGHT AT A POINT IS FOUND BY LINEAR INTERPOLATION ALONG THE LINE OF STEEPEST SLOPE PASSING THROUGH THE POINT. FOUR DIRECTIONS ARE TESTED FOR STEEPEST SLOPE: WEST - EAST, NW - SE, NORTH - SOUTH, NE - SW. THE END POINTS OF THE SLOPE LINE ARE THE FIRST CONTOUR OR EDGE FOUND IN THE TEST DIRECTION.

RASTER DATA:

THE RASTER IS STORED ON DISK UNIT 1,
WITH EACH COLUMN AN UNFORMATTED LOGICAL RECORD.
EACH CORNER HAS A HEIGHT VALUE, AND THERE ARE NO
GAPS IN THE CONTOURS IN THE FOUR TEST DIRECTIONS.

OUTPUT DEM:

THE INTERPOLATED DEM IS STORED ON DISK UNIT 2, WITH EACH COLUMN AN UNFORMATTED LOGICAL RECORD.

INPUT VARIABLES:

```

THE FOLLOWING VARI ABLES MUST BE SET IN THE MAIN
PROGRAM.  DIMENSIONS MUST BE CONSISTENT.
K,L  = DIMENSIONS OF THE INTERPOLATED DEM
M,N  = DIMENSIONS OF THE INPUT RASTER
RES  = RESOLUTION (PIXEL SIZE) OF RASTER IN MM.
CI   = CONTOUR INTERVAL
BASE = CONTOUR VALUE ASSOCIATED WITH MENU NAV = 1
BFLAG = CONSTANT ADDED TO BREAK LINES (IF USED)
TITLE = 60 CHARACTER TITLE READ FROM UNIT 5

```

SUBROUTINES:

READ - READ A RASTER COLUMN FROM DISK
WRITE - WRITE A DEM COLUMN TO DISK
EDGE - INTERPOLATE EDGE DEM HEIGHTS
INSIDE - INTERPOLATE INTERIOR DEM HEIGHTS
PRINT - PRODUCE A LINE PRINTER MAP OF THE RASTER

NOTES :

1. THE VALUE $(M-1)/(K-1)$ SHOULD BE AN INTEGER NUMBER. THIS IS A RESTRICTION ON THE DIMENSIONS OF THE PRODUCED DEM, GIVEN THE DIMENSIONS OF THE RASTER.
2. THE CORNERS OF THE INPUT RASTER SHOULD HAVE AT LEAST APPROXIMATE VALUES (IE. OTHER THAN ZERO). TO MODIFY THEREFORE THE RASTER VALUES AT THE CORNERS YOU SHOULD EITHER INPUT THESE VALUES IN THE PROGRAM BEFORE THEY WILL BE USED, OR BETTER YOU CAN USE THE PROGRAM "RASEDIT" FOR THIS PURPOSE.

```

*****
L I X Y                                ANDREW L. CLARKE
LINEAR INTERPOLATION / X,Y MEAN        WINTER 1982

```

```

THIS PROGRAM USES A RASTER IMAGE OF CONTOUR LINES
TO INTERPOLATE A REGULAR DEM. THE ALGORITHM USED IS:
HEIGHT AT A POINT MAY BE APPROXIMATED BY THE MEAN
OF THE VALUES FOUND BY LINEAR INTERPOLATION BETWEEN
THE NEAREST CONTOURS IN THE X AND Y DIRECTION.

```

```

RASTER DATA:
THE RASTER IS STORED ON DISK UNIT 1,
WITH EACH COLUMN AN UNFORMATTED LOGICAL RECORD.
EACH CORNER HAS A HEIGHT VALUE, AND THERE ARE NO
CAPS IN THE X OR Y DIRECTION THROUGH A CONTOUR.

```

```

OUTPUT DEM:
THE INTERPOLATED DEM IS STORED ON DISK UNIT 2, WITH
EACH COLUMN AN UNFORMATTED LOGICAL RECORD.

```

```

INPUT VARIABLES:
THE FOLLOWING VARIABLES MUST BE SET IN THE MAIN
PROGRAM. DIMENSIONS MUST BE CONSISTENT.
K,L   = DIMENSIONS OF THE INTERPOLATED DEM
M,N   = DIMENSIONS OF THE INPUT RASTER
RES   = RESOLUTION (PIXEL SIZE) OF RASTER IN MM.
CI    = CONTOUR INTERVAL
BASE  = CONTOUR VALUE ASSOCIATED WITH MENU NAV = 1
BFLAG = CONSTANT ADDED TO BREAK LINES (IF USED)
TITLE = 60 CHARACTER TITLE READ FROM UNIT 5

```

```

SUBROUTINES:
READ   - READ A RASTER COLUMN FROM DISK
WRITE  - WRITE A DEM COLUMN TO DISK
EDGE   - CONTROL ROUTINE FOR DEM EDGE INTERPOLATION
INSIDE - CONTROL ROUTINE FOR INTERIOR INTERPOLATION
LINT   - LINEAR INTERPOLATION WITHIN A ROW OR COLUMN
PRINT  - PRODUCE A LINE PRINTER MAP OF THE RASTER

```

```

NOTES :
1. THE VALUE IGRID=(M-1)/(K-1) SHOULD BE AN INTEGER
   NUMBER. THIS IS A RESTRICTION ON THE DIMENSIONS
   OF THE PRODUCED DEM, GIVEN THE DIMENSIONS OF THE
   RASTER.
2. THE CORNERS OF THE INPUT RASTER SHOULD HAVE AT
   LEAST APPROXIMATE VALUES (IE. OTHER THAN ZERO).
   TO MODIFY THEREFORE THE RASTER VALUES AT THE
   CORNERS YOU SHOULD EITHER INPUT THESE VALUES IN
   THE PROGRAM BEFORE THEY WILL BE USED, OR BETTER
   YOU CAN USE THE PROGRAM 'RASEDIT' FOR THIS
   PURPOSE.

```


F F T A N A L

PURPOSE : GIVEN A DATA MATRIX OF MXN IT COMPUTES :

1. MEAN & VARIANCE OF THE DATA
2. AVERAGE POWER
3. POWER PER FREQUENCY AND ITS % CONTRIBUTION TO THE OVERALL POWER
4. POWER PER HARMONIC SURFACE
5. APPLIES A T-TEST WITH A% SIGNIFICANCE LEVEL AND DELETES THE INSIGNIFICANT FREQUENCIES
6. CALCULATES (2), (3) & (4) FOR THE FILTERED SURFACE
7. GIVES BACK THE FILTERED DATA

DIMENSIONS : Z(M,N), ZI(M,N), ZSTAR(M,N), X(M,N)
P(M1,N1), C(M1,N1), PF(M1,N1), CF(M1,N1)
IWK(I), RWK(I), I=6*MAX(M,N)+150

NOTE 1 : THE USER SHOULD ALSO CHANGE THE DIMENSIONS OF :
X(M,N), CWK(M,N) (COMPLEX MATRICES) IN THE ROUTINES
"SPECTR" & "SPECT1"

PARAMETERS : M = NUMBER OF ROWS IN DATA MATRIX
N = " " COLS " " "
M1= NYQUIST FREQUENCY IN X-AXIS
N1= " " " " " "
THE NYQUIST FREQUENCIES ARE CALCULATED BY :
M1=M/2 : IF M=EVEN NUMBER
M1=(M+1)/2 : IF M=ODD NUMBER
A = SIGNIFICANCE LEVEL OF T-TEST (EG. 0.05)

AUTHOR : P.C. PATIAS
DATE : MAY 25, 1984

SUBROUTINES USED : UTIL, SPECTR, SPECT1, FTEST, HARM
FFT3D, MDFD (FROM IMSL LIBRARY)

FOURIER

PURPOSE : TO CALCULATE THE FOURIER COEFFICIENTS IN THE TRIGONOMETRIC FOURIER SERIES EXPANSION OF A SURFACE GIVEN BY A MATRIX OF GRID VALUES. THE COEFFICIENTS WILL COVER ONLY UP TO 3RD HARMONIC SURFACE

ALGORITHM : LEAST SQUARES ADJUSTMENT

AUTHOR : P.C.PATIAS

DATE : MAY 6, 1984

DIMENSIONS: THE USER NEED ONLY TO CHANGE THE DIMENSIONS OF :
A(NN,67), AT(49,NN), Z(NN), XX(NN), YY(NN), AP(NN,49)
WHERE : NN = TOTAL NUMBER OF POINTS OF THE SURFACE

PARAMETERS: THE USER SHOULD CHANGE THE NEXT PARAMETERS :
NN = TOTAL NUMBER OF POINTS OF THE SURFACE
X0 = X-COORD. OF THE UPPER LEFT CORNER OF THE GRID
Y0 = Y-COORD. OF THE UPPER LEFT CORNER OF THE GRID
D = INCREMENT DISTANCE BETWEEN THE GRID NODES ON
X & Y AXIS.

OUTPUT : THE EQUATION FOR THE SURFACE UP TO 3RD HARMONIC SURFACE WILL BE GIVEN

ROUTINES REQUIRED : THE MATRIX ROUTINES OF THE
SCFODSCI.WYLEXEC*CSWMR LIBRARY

TERRAIN

THIS PROGRAM CALCULATES THE Z-VALUES, GIVEN THE FOURIER COEFFICIENTS (UP TO 3RD HARMONIC POWER) AS THEY ARE CONSTRUCTED BY THE PROGRAM "FOURIER".
IF OPTION=1 IS CHOSEN IT ALSO GIVES A PRINTER CONTOUR MAP

DIMENSIONS : THE USER NEEDS ONLY TO CHANGE THE DIMENSIONS OF Z(M,N), W(M,N)

OPTIONS : 0 = GENERATION OF FULL MATRIX
IF OPTION=0 IS CHOSEN SET THE UNNECESSARY PARAMETERS TO ZERO.
1 = GENERATION OF SPARSE RASTER CONTAINING ONLY CONTOUR POINTS

PARAMETERS : M = NUMBER OF ROWS OF THE DESIRED OUTPUT MATRIX
N = " " COLUMNS " "

X0= X-COORD. OF THE LOWER LEFT CORNER

Y0= Y- " " " "

IOPT = OPTION USED (IE. 0, 1)

XX= DISTANCE INTERVAL ON X-AXIS

YY= " " " " Y " "

CI= CONTOUR INTERVAL

BASE = Z-VALUE OF FIRST CONTOUR

TOL = TOLERANCE VALUE FOR OBTAINING THE CONTOUR PIXELS

FORMAT : THE USER SHOULD ALSO CHANGE THE FORMAT "I" FOR THE PROPER READING OF THE INPUT COEFFICIENTS, AND THE FORMAT "II" FOR THE PRINTING OF THE RASTER MATRIX

AUTHOR : P.C. PATIAS

DATE : MAY 22, 1984

SUBROUTINES USED : PRINT

APPENDIX C

EQUATIONS FOR THE SIX SYNTHETIC SURFACES

For all the following equations:

$$0 < X < 1000$$

$$0 < Y < 1000$$

$$K = \frac{2\pi}{1200}$$

Surface 1

$$Z = 10377.716$$

$$\begin{aligned} &+ 27.314 * \cos(KY) + 9.689 * \sin(KY) + \\ &-144.006 * \cos(2KY) + 78.367 * \sin(2KY) + \\ &-96.210 * \cos(3KY) + 8.106 * \sin(3KY) + \\ &-19.391 * \cos(KX) + -24.610 * \sin(KX) + \\ &15.350 * \cos(KX) * \cos(KY) + -45.900 * \cos(KX) * \sin(KY) + \\ &24.897 * \sin(KX) * \cos(KY) + 20.210 * \sin(KX) * \sin(KY) + \\ &27.870 * \cos(KX) * \cos(2KY) + -37.742 * \cos(KX) * \sin(2KY) + \\ &-40.409 * \sin(KX) * \cos(2KY) + -12.417 * \sin(KX) * \sin(2KY) + \\ &-34.540 * \cos(KX) * \cos(3KY) + -13.399 * \cos(KX) * \sin(3KY) + \\ &-16.007 * \sin(KX) * \cos(3KY) + -22.004 * \sin(KX) * \sin(3KY) + \\ &-10.200 * \cos(2KX) + 43.699 * \sin(2KX) + \\ &-39.250 * \cos(2KX) * \cos(KY) + 10.537 * \cos(2KX) * \sin(KY) + \\ &-38.625 * \sin(2KX) * \cos(KY) + -10.503 * \sin(2KX) * \sin(KY) + \\ &14.397 * \cos(2KX) * \cos(2KY) + -30.372 * \cos(2KX) * \sin(2KY) + \\ &-37.590 * \sin(2KX) * \cos(2KY) + -117.541 * \sin(2KX) * \sin(2KY) + \\ &11.400 * \cos(2KX) * \cos(3KY) + 2.370 * \cos(2KX) * \sin(3KY) + \\ &38.604 * \sin(2KX) * \cos(3KY) + 77.697 * \sin(2KX) * \sin(3KY) + \\ &-58.975 * \cos(3KX) + 5.764 * \sin(3KX) + \\ &30.090 * \cos(3KX) * \cos(KY) + 25.505 * \cos(3KX) * \sin(KY) + \\ &71.077 * \sin(3KX) * \cos(KY) + 4.310 * \sin(3KX) * \sin(KY) + \\ &-1.151 * \cos(3KX) * \cos(2KY) + 65.695 * \cos(3KX) * \sin(2KY) + \\ &-2.616 * \sin(3KX) * \cos(2KY) + 49.067 * \sin(3KX) * \sin(2KY) + \\ &-21.069 * \cos(3KX) * \cos(3KY) + -13.294 * \cos(3KX) * \sin(3KY) + \\ &-26.096 * \sin(3KX) * \cos(3KY) + -29.041 * \sin(3KX) * \sin(3KY) \end{aligned}$$

Surface 2

$$Z = 10594.618$$

$$\begin{aligned}
 &+ -96.139 * \cos(KY) + 34.713 * \sin(KY) + \\
 &-53.703 * \cos(2KY) + 118.403 * \sin(2KY) + \\
 &-34.055 * \cos(3KY) + -37.226 * \sin(3KY) + \\
 &33.936 * \cos(KX) + 32.523 * \sin(KX) + \\
 &7.519 * \cos(KX) * \cos(KY) + 12.635 * \cos(KX) * \sin(KY) + \\
 &-3.440 * \sin(KX) * \cos(KY) + -13.169 * \sin(KX) * \sin(KY) + \\
 &-3.444 * \cos(KX) * \cos(2KY) + 5.630 * \cos(KX) * \sin(2KY) + \\
 &-4.491 * \sin(KX) * \cos(2KY) + -3.193 * \sin(KX) * \sin(2KY) + \\
 &-14.616 * \cos(KX) * \cos(3KY) + 4.256 * \cos(KX) * \sin(3KY) + \\
 &0.511 * \sin(KX) * \cos(3KY) + -3.764 * \sin(KX) * \sin(3KY) + \\
 &-60.513 * \cos(2KX) + -205.447 * \sin(2KX) + \\
 &-4.706 * \cos(2KX) * \cos(KY) + 23.211 * \cos(2KX) * \sin(KY) + \\
 &-2.036 * \sin(2KX) * \cos(KY) + 47.317 * \sin(2KX) * \sin(KY) + \\
 &-37.214 * \cos(2KX) * \cos(2KY) + -9.047 * \cos(2KX) * \sin(2KY) + \\
 &36.352 * \sin(2KX) * \cos(2KY) + -22.190 * \sin(2KX) * \sin(2KY) + \\
 &-7.707 * \cos(2KX) * \cos(3KY) + -7.233 * \cos(2KX) * \sin(3KY) + \\
 &-39.709 * \sin(2KX) * \cos(3KY) + -5.360 * \sin(2KX) * \sin(3KY) + \\
 &149.163 * \cos(3KX) + 149.975 * \sin(3KX) + \\
 &16.329 * \cos(3KX) * \cos(KY) + -21.027 * \cos(3KX) * \sin(KY) + \\
 &-16.219 * \sin(3KX) * \cos(KY) + -17.214 * \sin(3KX) * \sin(KY) + \\
 &-54.361 * \cos(3KX) * \cos(2KY) + -19.610 * \cos(3KX) * \sin(2KY) + \\
 &29.975 * \sin(3KX) * \cos(2KY) + -20.912 * \sin(3KX) * \sin(2KY) + \\
 &43.112 * \cos(3KX) * \cos(3KY) + -13.544 * \cos(3KX) * \sin(3KY) + \\
 &-1.637 * \sin(3KX) * \cos(3KY) + -40.640 * \sin(3KX) * \sin(3KY)
 \end{aligned}$$

Surface 3

$$Z = .4885.711$$

$$\begin{aligned} &+ 6.637 * \cos(KY) + 8.616 * \sin(KY) + \\ &15.610 * \cos(2KY) + 10.024 * \sin(2KY) + \\ &5.197 * \cos(3KY) + -2.637 * \sin(3KY) + \\ &-3.995 * \cos(KX) + -0.042 * \sin(KX) + \\ &0.593 * \cos(KX) * \cos(KY) + 1.181 * \cos(KX) * \sin(KY) + \\ &-4.018 * \sin(KX) * \cos(KY) + 1.940 * \sin(KX) * \sin(KY) + \\ &3.993 * \cos(KX) * \cos(2KY) + 2.363 * \cos(KX) * \sin(2KY) + \\ &2.031 * \sin(KX) * \cos(2KY) + 0.340 * \sin(KX) * \sin(2KY) + \\ &0.957 * \cos(KX) * \cos(3KY) + -1.085 * \cos(KX) * \sin(3KY) + \\ &-1.428 * \sin(KX) * \cos(3KY) + -1.169 * \sin(KX) * \sin(3KY) + \\ &-9.139 * \cos(2KX) + 13.311 * \sin(2KX) + \\ &-1.603 * \cos(2KX) * \cos(KY) + -4.366 * \cos(2KX) * \sin(KY) + \\ &-1.046 * \sin(2KX) * \cos(KY) + -6.639 * \sin(2KX) * \sin(KY) + \\ &-1.109 * \cos(2KX) * \cos(2KY) + -15.239 * \cos(2KX) * \sin(2KY) + \\ &-2.332 * \sin(2KX) * \cos(2KY) + 13.767 * \sin(2KX) * \sin(2KY) + \\ &16.642 * \cos(2KX) * \cos(3KY) + 0.183 * \cos(2KX) * \sin(3KY) + \\ &-9.931 * \sin(2KX) * \cos(3KY) + -3.259 * \sin(2KX) * \sin(3KY) + \\ &0.025 * \cos(3KX) + -3.053 * \sin(3KX) + \\ &-0.297 * \cos(3KX) * \cos(KY) + 0.498 * \cos(3KX) * \sin(KY) + \\ &1.744 * \sin(3KX) * \cos(KY) + 4.817 * \sin(3KX) * \sin(KY) + \\ &-2.349 * \cos(3KX) * \cos(2KY) + -11.637 * \cos(3KX) * \sin(2KY) + \\ &4.835 * \sin(3KX) * \cos(2KY) + -1.696 * \sin(3KX) * \sin(2KY) + \\ &9.639 * \cos(3KX) * \cos(3KY) + 5.055 * \cos(3KX) * \sin(3KY) + \\ &1.822 * \sin(3KX) * \cos(3KY) + 4.210 * \sin(3KX) * \sin(3KY) \end{aligned}$$

Surface 4

Z = 528.873

$$\begin{aligned} &+ 16.513 * \cos(KY) + -26.522 * \sin(KY) + \\ &84.037 * \cos(2KY) + 17.811 * \sin(2KY) + \\ &-77.004 * \cos(3KY) + -48.115 * \sin(3KY) + \\ &1.424 * \cos(KX) + -3.278 * \sin(KX) + \\ &-11.140 * \cos(KX) * \cos(KY) + 0.215 * \cos(KX) * \sin(KY) + \\ &-6.516 * \sin(KX) * \cos(KY) + -0.111 * \sin(KX) * \sin(KY) + \\ &-31.641 * \cos(KX) * \cos(2KY) + -11.728 * \cos(KX) * \sin(2KY) + \\ &31.422 * \sin(KX) * \cos(2KY) + 16.233 * \sin(KX) * \sin(2KY) + \\ &17.250 * \cos(KX) * \cos(3KY) + -20.872 * \cos(KX) * \sin(3KY) + \\ &-0.317 * \sin(KX) * \cos(3KY) + -34.470 * \sin(KX) * \sin(3KY) + \\ &13.369 * \cos(2KX) + 20.835 * \sin(2KX) + \\ &24.209 * \cos(2KX) * \cos(KY) + 21.262 * \cos(2KX) * \sin(KY) + \\ &3.992 * \sin(2KX) * \cos(KY) + 0.931 * \sin(2KX) * \sin(KY) + \\ &-32.397 * \cos(2KX) * \cos(2KY) + -34.015 * \cos(2KX) * \sin(2KY) + \\ &44.598 * \sin(2KX) * \cos(2KY) + 34.224 * \sin(2KX) * \sin(2KY) + \\ &25.222 * \cos(2KX) * \cos(3KY) + -18.340 * \cos(2KX) * \sin(3KY) + \\ &33.155 * \sin(2KX) * \cos(3KY) + -11.538 * \sin(2KX) * \sin(3KY) + \\ &-46.120 * \cos(3KX) + -17.337 * \sin(3KX) + \\ &-6.823 * \cos(3KX) * \cos(KY) + -10.069 * \cos(3KX) * \sin(KY) + \\ &-18.734 * \sin(3KX) * \cos(KY) + 14.239 * \sin(3KX) * \sin(KY) + \\ &7.297 * \cos(3KX) * \cos(2KY) + 16.001 * \cos(3KX) * \sin(2KY) + \\ &-7.650 * \sin(3KX) * \cos(2KY) + -2.567 * \sin(3KX) * \sin(2KY) + \\ &15.364 * \cos(3KX) * \cos(3KY) + -3.995 * \cos(3KX) * \sin(3KY) + \\ &11.695 * \sin(3KX) * \cos(3KY) + 11.934 * \sin(3KX) * \sin(3KY) \end{aligned}$$

Surface 5

$$Z = 388.865$$

$$\begin{aligned}
 &+ 0.796 * \cos(KY) + 1.748 * \sin(KY) + \\
 &1.726 * \cos(2KY) + -3.577 * \sin(2KY) + \\
 &3.622 * \cos(3KY) + 3.876 * \sin(3KY) + \\
 &0.427 * \cos(KX) + 0.444 * \sin(KX) + \\
 &1.042 * \cos(KX) * \cos(KY) + 0.237 * \cos(KX) * \sin(KY) + \\
 &0.194 * \sin(KX) * \cos(KY) + -0.253 * \sin(KX) * \sin(KY) + \\
 &0.112 * \cos(KX) * \cos(2KY) + 0.234 * \cos(KX) * \sin(2KY) + \\
 &0.525 * \sin(KX) * \cos(2KY) + 1.057 * \sin(KX) * \sin(2KY) + \\
 &1.037 * \cos(KX) * \cos(3KY) + -0.030 * \cos(KX) * \sin(3KY) + \\
 &0.190 * \sin(KX) * \cos(3KY) + -0.005 * \sin(KX) * \sin(3KY) + \\
 &-1.421 * \cos(2KX) + 0.273 * \sin(2KX) + \\
 &-0.522 * \cos(2KX) * \cos(KY) + -0.268 * \cos(2KX) * \sin(KY) + \\
 &0.656 * \sin(2KX) * \cos(KY) + 0.066 * \sin(2KX) * \sin(KY) + \\
 &0.799 * \cos(2KX) * \cos(2KY) + 0.032 * \cos(2KX) * \sin(2KY) + \\
 &0.397 * \sin(2KX) * \cos(2KY) + -1.966 * \sin(2KX) * \sin(2KY) + \\
 &-1.497 * \cos(2KX) * \cos(3KY) + -1.329 * \cos(2KX) * \sin(3KY) + \\
 &1.933 * \sin(2KX) * \cos(3KY) + 1.911 * \sin(2KX) * \sin(3KY) + \\
 &1.216 * \cos(3KX) + 1.138 * \sin(3KX) + \\
 &1.460 * \cos(3KX) * \cos(KY) + 0.376 * \cos(3KX) * \sin(KY) + \\
 &0.223 * \sin(3KX) * \cos(KY) + 0.417 * \sin(3KX) * \sin(KY) + \\
 &1.375 * \cos(3KX) * \cos(2KY) + -0.018 * \cos(3KX) * \sin(2KY) + \\
 &0.156 * \sin(3KX) * \cos(2KY) + 1.019 * \sin(3KX) * \sin(2KY) + \\
 &0.616 * \cos(3KX) * \cos(3KY) + 0.735 * \cos(3KX) * \sin(3KY) + \\
 &0.332 * \sin(3KX) * \cos(3KY) + -0.467 * \sin(3KX) * \sin(3KY)
 \end{aligned}$$

Surface 6

Z = 766.565

$$\begin{aligned}
 &+ 4.562 * \cos(KY) + -1.442 * \sin(KY) + \\
 &-6.592 * \cos(2KY) + -1.257 * \sin(2KY) + \\
 &-15.870 * \cos(3KY) + -9.214 * \sin(3KY) + \\
 &0.755 * \cos(KX) + -3.615 * \sin(KX) + \\
 &-2.592 * \cos(KX) * \cos(KY) + -3.029 * \cos(KX) * \sin(KY) + \\
 &1.375 * \sin(KX) * \cos(KY) + 3.747 * \sin(KX) * \sin(KY) + \\
 &-2.079 * \cos(KX) * \cos(2KY) + -1.416 * \cos(KX) * \sin(2KY) + \\
 &-4.570 * \sin(KX) * \cos(2KY) + 2.792 * \sin(KX) * \sin(2KY) + \\
 &-0.415 * \cos(KX) * \cos(3KY) + 7.567 * \cos(KX) * \sin(3KY) + \\
 &5.124 * \sin(KX) * \cos(3KY) + -0.331 * \sin(KX) * \sin(3KY) + \\
 &-12.614 * \cos(2KX) + -0.365 * \sin(2KX) + \\
 &0.458 * \cos(2KX) * \cos(KY) + -2.973 * \cos(2KX) * \sin(KY) + \\
 &2.422 * \sin(2KX) * \cos(KY) + 1.130 * \sin(2KX) * \sin(KY) + \\
 &2.271 * \cos(2KX) * \cos(2KY) + -4.490 * \cos(2KX) * \sin(2KY) + \\
 &3.013 * \sin(2KX) * \cos(2KY) + -24.557 * \sin(2KX) * \sin(2KY) + \\
 &10.230 * \cos(2KX) * \cos(3KY) + 2.659 * \cos(2KX) * \sin(3KY) + \\
 &2.334 * \sin(2KX) * \cos(3KY) + -5.447 * \sin(2KX) * \sin(3KY) + \\
 &3.767 * \cos(3KX) + 8.413 * \sin(3KX) + \\
 &0.492 * \cos(3KX) * \cos(KY) + 1.267 * \cos(3KX) * \sin(KY) + \\
 &-1.115 * \sin(3KX) * \cos(KY) + 0.465 * \sin(3KX) * \sin(KY) + \\
 &-6.194 * \cos(3KX) * \cos(2KY) + 6.732 * \cos(3KX) * \sin(2KY) + \\
 &0.250 * \sin(3KX) * \cos(2KY) + 5.958 * \sin(3KX) * \sin(2KY) + \\
 &7.659 * \cos(3KX) * \cos(3KY) + -4.528 * \cos(3KX) * \sin(3KY) + \\
 &3.579 * \sin(3KX) * \cos(3KY) + -2.302 * \sin(3KX) * \sin(3KY)
 \end{aligned}$$

END

FILMED

3

-86

DTIC